1986

Nonphotochemical hole burning of laser dyes, rare earth ions and photosynthetic pigments in polymer films

Thomas P. Carter
Iowa State University

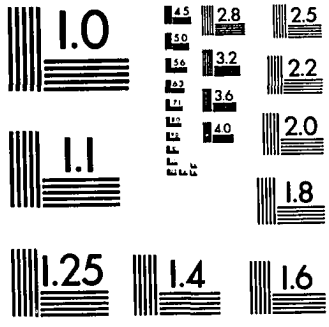

MICROCOPY RESOLUTION TEST CHART
NATIONAL BUREAU OF STANDARDS
STANDARD REFERENCE MATERIAL 1010a
(ANSI and ISO TEST CHART No. 2)

INFORMATION TO USERS

This reproduction was made from a copy of a manuscript sent to us for publication and microfilming. While the most advanced technology has been used to photograph and reproduce this manuscript, the quality of the reproduction is heavily dependent upon the quality of the material submitted. Pages in any manuscript may have indistinct print. In all cases the best available copy has been filmed.

The following explanation of techniques is provided to help clarify notations which may appear on this reproduction.

1. Manuscripts may not always be complete. When it is not possible to obtain missing pages, a note appears to indicate this.

2. When copyrighted materials are removed from the manuscript, a note appears to indicate this.

3. Oversize materials (maps, drawings, and charts) are photographed by sectioning the original, beginning at the upper left hand corner and continuing from left to right in equal sections with small overlaps. Each oversize page is also filmed as one exposure and is available, for an additional charge, as a standard 35mm slide or in black and white paper format.*

4. Most photographs reproduce acceptably on positive microfilm or microfiche but lack clarity on xerographic copies made from the microfilm. For an additional charge, all photographs are available in black and white standard 35mm slide format.*

***For more information about black and white slides or enlarged paper reproductions, please contact the Dissertations Customer Services Department.**

Carter, Thomas P.

NONPHOTOCHEMICAL HOLE BURNING OF LASER DYES, RARE EARTH IONS AND PHOTOSYNTHETIC PIGMENTS IN POLYMER FILMS

Iowa State University PH.D. 1986

PLEASE NOTE:

In all cases this material has been filmed in the best possible way from the available copy. Problems encountered with this document have been identified here with a check mark __√__.

1. Glossy photographs or pages _____
2. Colored illustrations, paper or print _____
3. Photographs with dark background _____
4. Illustrations are poor copy _____
5. Pages with black marks, not original copy _____
6. Print shows through as there is text on both sides of page _____
7. Indistinct, broken or small print on several pages __√__
8. Print exceeds margin requirements _____
9. Tightly bound copy with print lost in spine _____
10. Computer printout pages with indistinct print _____
11. Page(s) _____ lacking when material received, and not available from school or author.
12. Page(s) _____ seem to be missing in numbering only as text follows.
13. Two pages numbered _____. Text follows.
14. Curling and wrinkled pages _____
15. Dissertation contains pages with print at a slant, filmed as received _____
16. Other _____

_____

_____

University
Microfilms
International

Nonphotochemical hole burning of laser dyes, rare earth ions and photosynthetic pigments in polymer films

by

Thomas P. Carter

A Dissertation Submitted to the
Graduate Faculty in Partial Fulfillment of the
Requirements for the Degree of
DOCTOR OF PHILOSOPHY

Department: Chemistry
Major: Physical Chemistry

Approved:

Signature was redacted for privacy.
In Charge of Major Work

Signature was redacted for privacy.
For the Major Department

Signature was redacted for privacy.
For the Graduate College

Iowa State University
Ames, Iowa

1986

TABLE OF CONTENTS

EXPLANATION OF DISSERTATION FORMAT

THIS DISSERTATION IS A COMPILATION OF FIVE PUBLICATIONS WHICH DESCRIBE THE RESULTS OF EXPERIMENTS PERFORMED BY THE CANDIDATE IN COLLABORATION WITH THE VARIOUS CO-WORKERS LISTED ON THE TITLE PAGE FOR EACH PUBLICATION. THE CANDIDATE WAS INVOLVED IN EVERY ASPECT OF THE EXPERIMENTATION AND DATA ANALYSIS AS WELL AS ORIGINAL MANUSCRIPT PREPARATIONS.

THE DISSERTATION IS ARRANGED IN TWO SECTIONS, EACH OF WHICH CONTAINS AN ORIGINAL INTRODUCTION, DETAILED EXPERIMENTAL SECTION, AN ADDITIONAL RESULTS AND DISCUSSION AND REFERENCES. SECTION I CONTAINS THREE PUBLICATIONS PRIMARILY CONCERNING THE RESULTS FOR THE LASER DYES AND RARE EARTH IONS. SECTION II PRESENTS TWO PUBLICATIONS CONTAINING THE RESULTS OBTAINED IN THE NPHB EXPERIMENTS ON THE CHLOROPHYLLS.

GENERAL INTRODUCTION

When a molecule is placed as an impurity into a host environment in which it may occupy a number of inequivalent orientations with respect to the surrounding media, each type of local environment interacts uniquely with the molecule, and therefore the energy levels of the molecule are perturbed differently by each local environment. This type of interaction occurs in ordinary liquid solutions and in solid solutions where the host does not have a large degree of ordering in its structure (as do, for example, mixed crystals). These types of systems may be described as having (in various degrees perhaps) disorder, and are sometimes termed amorphous. The term applied to the distribution of impurity energy levels which occurs as a result of the disorder is the inhomogeneous distribution, which gives rise to the spectral broadening observed in these systems, termed inhomogeneous broadening. The intrinsic linewidth for spectral transitions of a set of non-interacting molecules in equivalent environments is termed the homogeneous linewidth and is determined by the dephasing of the molecule(s). Thus, inhomogeneously broadened spectral transitions of non-interacting molecules in a rigid system may be viewed as being due to a closely spaced quasi-continuous distribution of homogeneous transitions.

Dephasing or T_2 processes are separated into two categories: pure dephasing or T_2^* processes [1] and ordinary depopulation or T_1 processes. Pure dephasing may be thought of qualitatively as a process whereby a coherent set of excited state molecules loses phase coherence without depopulating the excited state. If a homogeneous set of

molecules is excited with a coherent source, then the ensemble of molecules will be induced into oscillating in phase with themselves and with the radiation field. This sets up a macroscopic polarization **P** which is defined as the vector sum of all the molecular transition dipole moments of the ensemble. If the radiation field is then turned off, each molecule of the ensemble may interact with the thermal motions of the host lattice and be perturbed slightly from its initial transition energy. Because of this change in oscillation frequency, it begins to lose phase coherence with the original ensemble and has thus "dephased". Since the thermal motion of the host lattice is a stochastic process, the energy spreading of the original ensemble due to pure dephasing follows a statistical distribution which, in turn, leads to the characteristic T_2^* relaxation time. It should be noted that this description is valid only if the host lattice fluctuations can be considered random, and that pure dephasing contributions should dissappear as the temperature goes to 0 K. The T_1 processes are those which lead to the depopulation of the initially prepared excited state and include, for electronic states, fluorescence, intersystem crossing and internal conversion; these processes occur even at 0 K. The overall dephasing time T_2 for a homogeneous transition is determined by both T_1 and T_2^* processes as governed by the equation:

$$\frac{1}{T_2} = \frac{1}{2T_1} + \frac{1}{T_2^*} \qquad (1)$$

which can then be related to the spectral line width using the equation:

$$\Delta\nu = \Delta\omega c = (\pi T_2)^{-1} \; . \qquad (2)$$

where $\Delta\nu$ is the full width (in Hz) of the transition at half of the maximum intensity (FWHM), $\Delta\omega$ is the FWHM in cm^{-1}, and c is the speed of light. If, as is the case in the experiments presented herein, the T_1 lifetime is known (from emission lifetime measurements, for example), and the measured homogeneous linewidth is broader than can be accounted for from this contribution, then rapid pure dephasing (T_2^* processes) can be inferred. Since pure dephasing is due to the interactions between the impurity and the host (usually **via** phonons), then information about the pure dephasing of the impurity yields information about the host as well.

Measuring the homogeneous linewidth (or, equivalently, the T_2 relaxation time) of a molecule in the presence of inhomogeneous broadening mechanisms is not an easy task. As a result, there are only a few ways of accomplishing this:

(1) The photon echo technique [2], which is directly analogous to methods used in pulsed NMR experiments, takes advantage of the fact that T_2^* relaxation can be reversed, yielding an optical echo whose intensity at various echo delay times depends on the dephasing time, T_2.

(2) The free induction decay method [3,4] in which the total dephasing of the macroscopic polarization of the sample induced by coherent excitation leads to a decay of the "beating" between this polarization and the laser frequency. The beating is induced by either rapid modulation of the laser frequency or by rapid modulation of the molecular energy levels (**via** Stark modulation, **e.g.**). Since the modulation must be fast relative to T_2, this technique is not easily applied to systems with very rapid dephasing.

(3) Fluorescence line narrowing [5], which takes advantage of the fact that the inhomogeneity is due to a distribution of non-interacting homogeneous "sites" which, with narrow band excitation, can be selectively excited to emit, and then the linewidth in emission is measured and analyzed to give the T_2 time.

(4) Spectral hole burning [6-8], which has two main types: transient (or population, or bottleneck) hole burning, and persistent hole burning. In transient hole burning, a homogeneous "site" within an inhomogeneous profile is excited to some state with a lifetime T_1, during which time the inhomogeneous absorption profile shows a depletion of absorbers at the original excitation frequency. The spectral width of the "hole" left by these absorbers is then governed by Equations 1 and 2. However, to use this technique, it is necessary to probe the absorption spectrum within a time which is on the order of the T_1 lifetime and as a result the technique is used mainly for metastable states and primarily to determine T_1 lifetimes. In persistent hole burning however, the originally excited site undergoes a transformation, while in the excited state, to some other configuration or state; there it relaxes to some new ground state configuration which no longer absorbs at the original excitation frequency and from which the original configuration for the absorber is not accessible. The nature of the excited state transformation may be one in which the molecules from the original site are "transformed" to another type of site within the original inhomogeneous distribution, a process which is termed nonphotochemical or photophysical hole burning. It is not known, in most cases, whether the actual transformation involves a rearrangment of

the guest or the host or some combination of the two; the important point is that some change occurs in the interaction between guest and host that shifts the transition energy of the guest. If the transformation involves some type of inter- or intramolecular chemical transformation, then the process is termed photochemical hole burning and the new entity thus produced will, in general, absorb at a frequency outside the original inhomogeneous profile. In either case, a hole is left in the inhomogeneous profile as in transient hole burning, but the hole does not recover or "fill in"; that is, the holes persist at least as long as conditions are such to prevent spontaneous site reorganizations from occurring (through thermal or phonon-assisted mechanisms or subsequent irradiations). It should be noted that persistent hole burning can only occur when site interconversion processes in the ground state are absent or very slow, otherwise the holes would spontaneously fill in completely. This process does occur in some systems (see Paper III, Section I), but usually is slow and incomplete; only a fraction of the hole (in units of integrated area) fills spontaneously.

It is the nonphotochemical hole burning technique and related phenomena as applied to the study of various impurities dissolved in several types of disordered polymeric systems, as well as to the study of the nature of the disordered state itself, which is the subject of this work.

SECTION I.

NONPHOTOCHEMICAL HOLE BURNING OF LASER DYES AND RARE EARTH IONS

INTRODUCTION

The first observations of nonphotochemical hole burning (NPHB) of organic molecules dissolved in glassy hosts were reported in 1974 [9-11]. The observed holes were persistent, that is, they do not "fill in" with time as do transient saturation holes due to a metastable state. Persistent holes remain in the spectrum as long as the sample is kept at or below the temperature at which they were burned, T_B, and as long as there are no subsequent irradiations which may cause additional site reorientations to occur.

In most cases of NPHB, the nonphotochemical nature of the process is inferred from the lack of known or reasonable photochemical transformations intrinsic to the impurity. If such processes do occur, then the photoproduct usually will absorb in a spectral region separate from the inhomogeneous absorption of the initial species. This reasonable assumption provides a rule of thumb which is widely used: if the photoproduct absorption (antihole) lies within the inhomogeneous band of the original impurity, then the hole burning process is likely NPHB. However, the range of processes which lead to hole burning sometimes makes hazy the appropriate application of the terms photochemical and nonphotochemical hole burning. Take for instance the example of quinizarin: 1,4 dihydroxyanthraquinone. This molecule has the capability of forming strong intramolecular hydrogen bonds between its hydroxyl protons and the keto oxygens. When placed in a hydrogen bonding glassy matrix at low temperatures, hole burning is observed and has been attributed to breaking these intramolecular hydrogen bonds and

forming intermolecular hydrogen bonds with nearby solvent molecules [12]. This process in no way changes the chemical nature of quinizarin, but by the rule of thumb presented above, it belongs in the photochemical hole burning category because of where the antihole appears. There are other similarly hard-to-categorize examples, and it has been suggested [8] that it is perhaps more meaningful (less confusing) to think in terms of a continuum of hole burning processes which proceed from intramolecular mechanisms where the chemical nature of the absorber is changed, to intermolecular processes where bonds between absorber and host are rearranged, to NPHB where only matrix rearrangements occur.

In general, a hole burned absorption spectrum (or the equivalent fluorescence excitation spectrum, either of which is hereafter referred to as the spectrum) will exhibit a hole in resonance with the burn frequency, ω_B (the zero-phonon line), together with a phonon side band hole at higher energy which is a result of the electron-phonon (e-p) coupling of the guest and host. When guest zero-phonon transitions are burned out, those molecules are no longer available at the original frequencies for absorption through their phonon side bands and thus a phonon hole is observed to higher energies. The shape of this phonon hole is governed by the e-p coupling and the phonon distribution of the host. Usually, however, a more "intense" (deeper) side hole is observed to lower energy from ω_B; this feature is known as the pseudo-phonon hole and is produced by a distribution of overlapping zero-phonon holes which are burned out as a result of molecules being excited through their phonon side bands. As a result, pseudo-phonon holes also have a shape

governed by the e-p coupling and the phonon distribution of the host. Also occurring, but with a usually negligible effect (in the short burn time limit and for small e-p coupling), is the secondary hole producing process due to the true phonon hole from those molecules responsible for the production of the pseudo-phonon hole; this hole occurs over a range of frequencies which overlaps the zero-phonon hole, and for systems with large e-p coupling or systems driven to saturation, distorts the zero-phonon line shape.

If, for molecular species, an ω_B is chosen in the region of the inhomogeneous profile corresponding to 0-0 transitions, then in addition to the above features which are in the near vicinity of the laser frequency, hole burned spectra often show zero-phonon holes (and associated side holes) to higher energy from ω_B and at frequency spacings corresponding to the optically allowed molecular vibrational frequencies of the excited state. These features are simply the result of the resonant hole; a certain subset of sites has shifted absorption frequencies and those molecules no longer absorb through their vibronic transitions at their original places and thus the additional holes [13]. Yet another type of hole sometimes occurs in the hole burning of molecular species when an ω_B is chosen higher up in the inhomogeneous profile. In this case the molecules may absorb the radiation through their vibronic transitions and then hole burn, leaving holes at the frequencies at which their 0-0 transitions occur (as well as a hole in resonance with ω_B), and those will be on the low energy side of ω_B. Thus, a characteristic set of nonresonant holes is produced as a result of burning many sites at once through the different molecular vibronic

frequencies [14]. Either one of these last two processes can provide detailed vibronic information about a molecule which is often unobtainable by other means [14].

One of the most poorly understood and least studied aspects of NPHB is the process known as laser-induced hole filling (LIHF) (see Paper III, Section I). Phenomenologically, this is a process where an initially prepared hole burned in a spectrum at some ω_{B1}, is partially or completely filled by subsequent irradiation at some new frequency, ω_{B2} [15]. This process is not identified as a thermal one resulting from local heating owing to the secondary irradiation, since no broadening of the initial hole is observed after filling, as is the case when the sample temperature is rapidly raised a few degrees and then lowered back to T_B. Nor is it identified as direct reversal of the original NPHB event. Even more provoking is the evidence that LIHF is not strongly related to the absorption of the impurity at ω_{B2}. Also, a pronounced change in the LIHF "efficiency" when ω_{B2} is moved from frequencies higher than ω_{B1} to those lower than ω_{B1} has been observed in several systems.

The following three Papers present some of the results of the research which has been performed by myself together with my collaborators while a student at Iowa State University. Paper I is a brief review of the important recent developments in NPHB theories and experiments and presents for the first time the results of some of our own experiments. Paper II presents the first report of NPHB in an important new class of systems: organic ionic dyes doped into hydrogen bonding polymer films. Paper III is an in-depth discussion together

with new results concerning the various phenomenological and mechanistic aspects of LIHF.

EXPERIMENTAL METHODS

Sample Preparation

The earliest hole burning experiments discussed here were performed on cresyl violet perchlorate (CV) in the low temperature glass forming mixture glycerol-water, and this system was the only one which did not make use of a polymer film as the host. The main reasons for studying this particular system were that it had previously been shown to undergo profound spectral changes upon laser irradiation [6], and its absorption spectrum was in the range accessible to the available dye laser. Initially the experiment was conducted as a test for the absorption spectrometer which I had constructed and which at that time was still in its earliest form. The results which were obtained were promising enough to warrant further study.

The mixture of glycerol-water (5:4 v/v) yields an excellent uncracked, clear, colorless glass with relative ease (compared to, say, ethanol-methanol) when cooled to liquid helium temperature. This glass is especially useful for polar solutes like CV; non-polar substances (e.g. aromatic hydrocarbons) have only limited solubility in this mixture. The solution was not plunged into the cryogen as this caused the glass to crack; rather, it was cooled fairly rapidly in the helium vapor, going from 300 K to 4.2 K in 10-15 minutes. Cooling too slowly, especially in the region from 120 K to 90 K, also caused problems, sometimes producing a cloudy semi-transparent solid which often cracked upon further cooling. The actual sample preparation was straightforward: crystals of CV (Exciton Chemical Company) were

dissolved directly in the prepared solvent mixture. The solution was then transferred to a cylindrical fused silica tube (1 cm i.d.) which was taped to a brass holder attached to the cryostat sample rod.

All of the remaining samples studied were in the form of doped polymer films which were solids at room temperature; the polymer film samples for the experiments reported in Section I were prepared by Bryan Fearey. These films were prepared by first dissolving the solid polymer powder (either poly(vinyl alcohol) or poly(acetic acid); Aldrich Chemical Company in all cases) in water while heating and stirring. It should be noted that both methanol and ethanol were tried as substitutes for water but were found unsuitable both because the polymers took too long to dissolve in these solvents and, when making films, the solvent evaporated too quickly and gave poor quality films. Even with water, several hours were required to fully dissolve the polymers. The amount of water was adjusted to produce a solution which was syrupy in consistency but not too viscous, because that made the dissolution of the dopant more difficult than necessary. When the consistency was right, crystals of the appropriate dopant (Exciton Chemical Company, except where noted) were added to the solution while heating and stirring were continued. After all the solids were apparently dissolved, the mixture was passed through a filter syringe to remove any remaining dopant or polymer solids which sometimes remain to produce a non-homogeneous film. If adjustment of the optical density of the sample was necessary, additional dopant crystals were added or the solution was diluted with undoped polymer solution, as appropriate. The prepared solution was then poured onto clean glass plates; originally,

2" x 2" x 1/8" plates were used but in later experiments 18 mm round microscope cover slips were found to be more convenient. The solution was allowed to completely cover the glass surface and enough was used so as to produce a "bubble" of liquid which remained on the glass solely by its surface tension. The solution was then allowed to evaporate uncovered and away from any drafts; if left in a fume hood, for example, the solution dried too quickly and the film acquired an irregular surface having thicker and thinner regions or even pronounced ridges. Depending on the amount of solution used, the resulting films ranged in thickness from about 50 μ to over 200 μ. The film could then, if desired, be removed from the glass plate. In most cases, especially when quantitative information was desired, pieces were cut from the film and individually taped over small (2-5 mm) holes bored through a thin (1/16") brass plate attached to the cryostat sample rod. In the interests of maximum uniformity, the pieces were cut from the same area of the original film. In this way, different experiments (irradiations) were performed on separate pieces of film, possible interferences between experiments were minimized. However, in some non-critical experiments a single piece of film was used to span several holes in the brass plate, and each hole then treated as a separate sample.

The samples containing rare earth ions (RE) (Pr^{3+} and Nd^{3+}, obtained as $PrCl_3$ and $NdCl_3$ from Dr. Frank Spedding, Ames Laboratory) were prepared in a similar manner except that they were not allowed to dry fully (drying was stopped when the film was slightly tacky but firm) and were not removed from the glass plate because attempting to do so caused it to stretch and lose its optical clarity. Allowing it to dry fully

gave rise to an absorption spectrum which was altered slightly from that observed in the liquid solution or "wet" film and such dry films did not exhibit NPHB. It is suggested here that the NPHB process for these ions depends critically upon their solvation state.

Having to leave the film on the the cover slip (the only glass substrate used for the RE samples) was not particularly a problem; however, this did mean that the film necessarily covered several of the holes in the brass plate, and having a separate piece of film for each hole in the plate was not possible. Also, the presence of the cover slip sometimes produced an artificial modulation of the absorbance signal (modulation of the absoprtion intensity with respect to wavelength) owing to an etalon effect caused by the parallel surfaces of the cover slip. This effect was also noted at times using demounted films (caused by the two surfaces of the film itself) and was easily reduced or eliminated simply by rotating the sample rod so that the film was at an angle (15-30°) to the absorption probe beam.

Cryogenic Equipment and Methods

All samples were cooled in a Janis Research model 8-DT Super Vari-Temp liquid helium immersion cryostat equipped with an optical access tail section. This device is capable of cooling samples to 4.2 K by itself and, when used with an auxiliary vacuum pump to reduce the pressure over the liquid helium in the sample chamber, it can achieve temperatures as low as about 1.7 K. Sample temperatures were measured using a silicon diode thermometer (Lake Shore Cryogenics model DT-500K) calibrated over the range from 1.4 K to 300 K. To utilize this

thermometer, a homemade device designed to provide a constant 10μA current (regardless of the load impedance) was used which allowed the diode resistance to be monitored simply by measuring the potential drop across it using a precision 5 digit digital microvoltmeter (Hickock model 3410).

The thermal cooldown procedure used for the glycerol-water glass has been described in the previous section. For the polymer samples (which were solids at room temperature) the following method was used in order to provide some reproducibility in their thermal treatment (it is not known whether this is important for polymer samples). The sample chamber of the cryostat was filled with liquid helium up to the top of the windows and then the sample was plunged into the liquid. The introduction of this thermal mass nearly instantly vaporized all the helium in the sample chamber down to a level just below the bottom of the sample. The level of the helium was then quickly raised until the sample was completely immersed. In order to obtain a homogeneous temperature throughout the sample and ameliorate radiational heating owing to the hole burning and probe beams and the large optical windows in the cryostat, the sample was kept immersed in pumped helium whenever possible. When temperatures above 4.2 K were needed, an attempt was made to keep the liquid level as constant as possible.

Hole Burning Equipment and Methods

With the exception of the NPHB experiments on CV in glycerol-water, all the holes reported here were produced using various cw (continuous wave) lasers. For the CV/glycerol-water experiment, a pulsed (repetition rate 10 Hz) Nd:YAG laser-pumped dye laser (Quantel YG-481B and TDL III) was used as a burning source. In general, it is not a good idea to use this type of laser for producing nonphotochemical holes since the high peak powers attained during the very short (5-10 nsec) pulses can easily saturate the absorption transition of the sample. This can lead to an artificially broadened hole owing to absorption and NPHB of molecules which are not exactly in resonance with the laser. Also, this process produces holes with a much lower apparent quantum yield than what would be observed with a cw source having the same total fluence and a lower power. Nevertheless, holes were observed in the CV spectrum using this source.

Many of the NPHB experiments on the laser dyes were performed using a simple low power (5 mW) cw He-Ne laser (Spectra-Physics 134) which oscillates simultaneously in three cavity modes having an intensity ratio of about 1:3:1 and a spacing of 440 MHz. Thus, the effective linewidth of this burn source is about 1 GHz or 0.03 cm^{-1}. However, none of the samples burned with this laser showed any sign of having been burned with a multi-mode source because of the broadness of their hole widths relative to the mode spacing. The holes were typically in the range from 0.2 to 1.0 cm^{-1} which is about 12 to 60 times larger than the laser mode separation.

The balance of the NPHB experiments were performed using a single frequency ring dye laser (Coherent 699-05) pumped by a 5 W argon ion laser (Coherent Innova 90-5). The dye laser was passively frequency stabilized by virtue of two low finesse intra-cavity etalons having free spectral ranges of 10 GHz and 200 GHz, together with a three plate birefringent filter with a 380 GHz bandpass. These three elements together were sufficient to select a single longitudinal cavity mode (cavity mode spacing ~ 185 MHz) for coherent gain. The linewidth of this laser was limited by rapid jitter (of unknown origin) to about 20 MHz.

Figure 1 shows the configuration of the apparatus used for producing holes. The output from the Ar^+ laser was sent directly into the dye laser using no intervening optics. A portion of the dye laser was extracted using a wedged quartz plate, BS I, (one surface uncoated, one surface anti-reflection coated, Newport Research Corporation 10Q20 NC.1-AR) and sent into a confocal spectrum analyzer (Spectra-Physics model 470-04, FSR = 8 GHz) to monitor the laser frequency stability. The output of the spectrum analyzer was displayed on an oscilloscope. The remainder of the laser output was then directed through a variable attenuator (Newport Research Corporation model 935-3) which was used to adjust the laser intensity to an appropriate value for the NPHB experiment. In order to measure the intensity after attenuation, part of the beam was split off by BS II (identical to BS I), modulated by a mechanical chopper (PAR model 125) and monitored using a photodiode detector PD (Molectron LP-141) and a lock-in amplifier LIA (PAR model 124 with a model 118 preamplifier). This detection arrangement was calibrated by setting the laser intensity to 50 or 100 mW (as measured

Figure 1. Hole burning and measuring apparatus

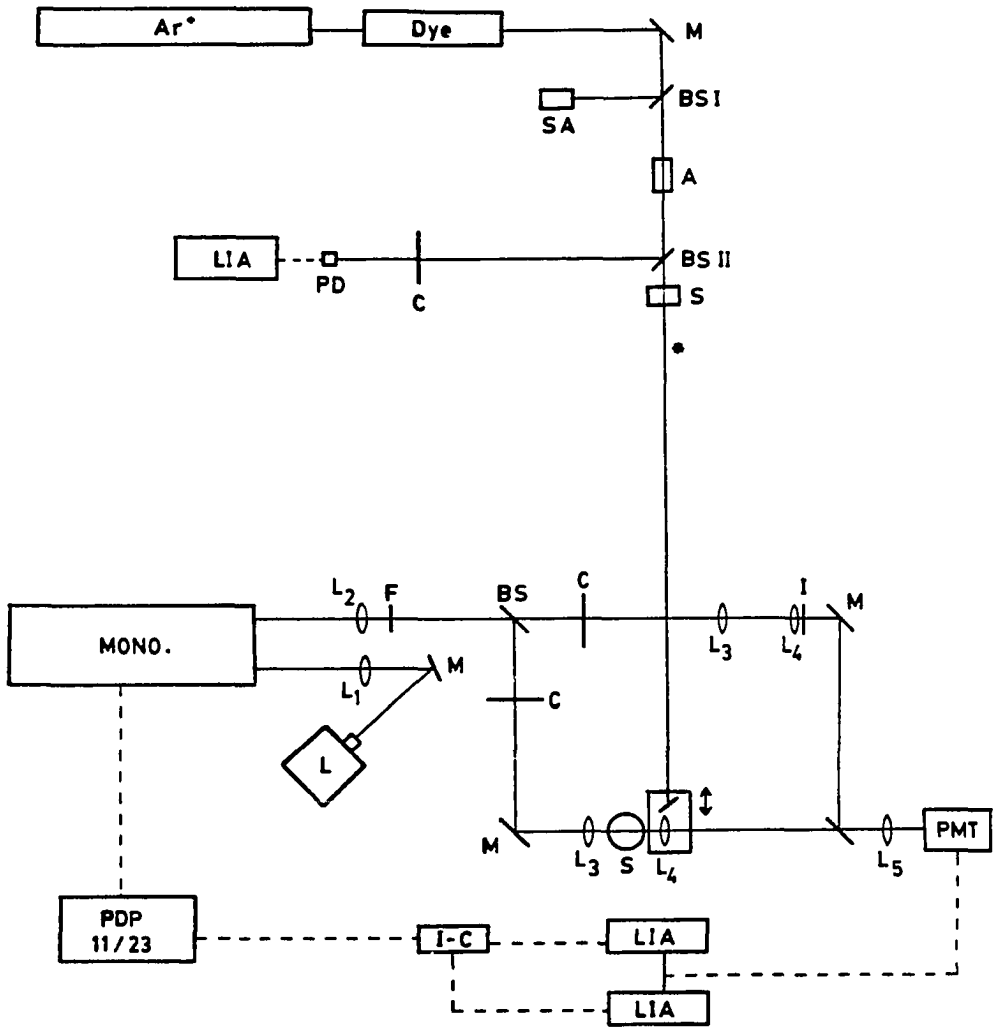
Ar°
Dye
M
SA
BS I
A
LIA
PD
C
BS II
S
L2
F
BS
C
I
M
MONO.
L1
M
L3
L4
C
L
M
L3
S
L4
L5
PMT
PDP
11/23
I-C
LIA
LIA

at the point marked with an asterisk, using a Coherent model 210 power meter) and taking a reading on the LIA; the beam was then adjusted to the desired intensity using the LIA as a monitor. Sample irradiation times were controlled using a digital timer-controlled mechanical shutter (Newport Research Corporation model 845), capable of producing exposure times from 10 msec upwards with an accuracy of $\pm$ 0.05%. The irises in the beam path were used to prevent back reflections from re-entering the dye laser and providing feedback mechanisms which destroy the laser frequency stability. It should be noted that when the He-Ne was used it was placed in a position equivalent to that occupied by the dye laser.

Hole Probing Equipment and Methods

Also shown in Figure 1 is the high resolution double-beam absorption spectrometer which was designed and constructed by myself for the express purpose of probing NPHB holes in samples contained in an optical cryostat. Although initially the instrument was manually operated, it has since been interfaced with a microcomputer which controls wavelength scanning, data acquisition, manipulation and storage, and real-time output to an intelligent chart recorder.

The heart of the instrument is a 1.5 m high resolution monochromator (Jobin-Yvon HR-1500) equipped with a stepping motor and controller which provides for up to 5000 data points per nm. The monochromator has a rated reciprocal linear dispersion of 0.19 nm/mm and has a measured bandpass of about 0.0045 nm using 20 μ slit widths. The spectrometer was designed so that the radiation from the source arc lamp AL (a 500 W

xenon d.c. short arc lamp, Canrad-Hanovia model 959C1980 in an Oriel housing) is dispersed prior to probing the sample, since the alternative (sending white or broadband radiation through the sample and then dispersing and measuring) would necessitate subjecting the hole burned sample to high intensities of white light thereby distorting or erasing the hole in the process of measuring it. In this way the sample sees only a very low intensity, highly monochromatized beam, resulting in minimal hole distortion. The particular arc lamp used was chosen because it has a very small arc size (0.3 mm x 0.3 mm) which provides a very compact image size when its output is focused on the monochromator's entrance slit, thereby maximizing the coupling of radiation into the monochromator. The lens L_1 was chosen to have an f-number the same as that of the monochromator to maximize the throughput through the monochromator and minimize the stray light level inside it. Lens L_2, on the output side of the monochromator, was identical to L_1 and collimates the diverging monochromatized beam. Next, the beam was passed through a 50% beam splitter BS (Corion BS-200-S) whose surface is a "dot matrix" of uncoated circular areas within a totally reflecting aluminum coating which works by totally reflecting 50% of the "area" of the beam and transmitting the other 50%. This design circumvents the problems which arise when trying to obtain a matched pair of the usual type of beam splitter, which has a partially reflecting metallic coating over its entire surface, and it also provides a substantially broader spectral operating range. This split the beam into sample and reference legs, each of which was modulated by a mechanical chopper (Laser Precision CTX-534). The chopping frequency for each beam was different

and was chosen so that they did not have any common harmonics or sub-harmonics. Each beam then was brought to a focus and subsequently recollimated by lenses L_3 and L_4, respectively. The sample S contained in the cryostat was placed at the focal point of one of the beams. In order to provide a convenient and reproducible method of burning holes in the same part of the sample probed by the spectrometer, L_4 was mounted on a translation stage together with a 90° prism situated so that the stage could be reproducibly positioned to allow the laser beam to be directed by the prism through the sample in precisely the opposite direction of the probe beam. The reference beam contained an iris diaphragm just after L_4 which allowed the reference beam to be attenuated to match the intensity of the sample beam to account for insertion loss due to scattering by the cryostat windows and the sample. The intensities of the two beams were matched when the monochromator was set to a wavelength at which there was no sample absorption. The beams, which were directed by the mirrors M, were recombined into a single beam by another beam splitter BS identical to the first one. Thus, each leg of the spectrometer was treated identically, each passing through identical lenses, undergoing two reflections, and transmitting once through a quartz plate. When appropriate, an order sorting filter F was placed in a position common to both beams. The recombined beam (now having two components modulated at different frequencies) was focused by lens L_5 into a photomultiplier tube PMT (RCA C31034 in a PFR PR-1400-RF thermoelectrically cooled housing) which was used to measure the beam intensities. The output from the PMT was provided to each of two identical lock-in amplifiers LIA (initially, Ithaco model 391A

generously loaned for nearly two years by Professor David Lynch, Physics Department, then when computer interfaced, Ithaco model 397EO) each referenced to one of the chopping frequencies. Thus, each LIA provided a signal proportional to the intensity of one of the spectrometer beams. Prior to computer interfacing, the outputs of the two LIA's were sent to a logarithmic ratiometer (Evans Associates model 4122) that provided an output proportional to the sample absorbance which was then recorded on a strip chart. Computer interfacing for data acquisition was accomplished by replacing the logarithmic ratiometer with an integrator/coupler I-C (Ithaco model 385EO-2) which simultaneously converts two analog voltages to digital values using a voltage-to-frequency conversion technique and integrates the signals for selectable multiples of 1/60 sec. The digitized values of the two LIA signals were then transmitted to a microcomputer (Digital Equipment Corporation Micro PDP-11/23+) through an IEEE-488 interface and the computer then performed ratio and logarithm functions to calculate the sample absorbance and stored the result. The computer was also capable of programming the LIA gain settings through the INT to provide optimal signal levels for digitization. A commented copy of the source code used to run the spectrometer may be found in the Appendix.

When probing a hole, it was determined that in order to strike an acceptable compromise between the signal to noise ratio and the resolution of the measurement (as determined by the monochromator's bandpass), a slit width of 20 μ was optimal. Actual measurement of the bandpass at this slit width yielded a value of 0.0045 nm which, at the He-Ne transition at 632.8 nm, corresponds to a 0.11 cm^{-1} read

resolution. This means that the narrowest holes were consequently distorted to some degree, although corrections were made to the data to take this into account when necessary [16].

PAPER I.

NONPHOTOCHEMICAL HOLE BURNING - VERSATILITY AND THEORETICAL STATUS

NONPHOTOCHEMICAL HOLE BURNING - VERSATILITY AND THEORETICAL STATUS

THOMAS P. CARTER, JOHN M. HAYES, BRYAN L. FEAREY and GERALD J. SMALL

Ames Laboratory-USDOE and Department of Chemistry
Iowa State University, Ames, Iowa 50011

Accepted for Publication in
International Reviews in Physical Chemistry

INTRODUCTION

A nonphotochemical mechanism for the production of holes in the inhomogeneously broadened absorption spectra of impurity molecules in organic glasses, originally observed by Kharlamov **et al.** [1,2], was first proposed by Hayes and Small [3,4]. According to this mechanism, illustrated schematically in Figure 1, two conditions are necessary for nonphotochemical hole burning (NPHB): (a) the presence of a distribution of nearly isoenergetic configurations of solvent molecules and (b) a coupling between the impurity and solvent such that electronic excitation of the impurity induces an orders of magnitude increase in the rate of interconversion of these configurations. The existence of such a distribution of low energy excitations had previously been proposed [5,6] to explain anomalies in the low temperature ($T \leq 1$ K) specific heat and ultrasonic attenuation of glasses and has since been used in numerous theories proposed to explain a variety of experiments which measure the dephasing of electronic excitation and energy transport in glasses. This distribution of configurations is commonly referred to as the two-level system (TLS) model and TLS are generally accepted as being a universal property of the amorphous state. For a full discussion of the NPHB mechanism and review of the theories of dephasing in glasses available through 1982, the reader is referred to the paper by Small [7]. In this paper, we focus on our more recent applications of NPHB as well as present a discussion of progress in the understanding of dephasing in glasses.

Figure 1. Potential energy diagrams for a two level system coupling to an impurity in its ground (TLS_G) and excited (TLS_E) electronic states. TLS are characterized by a distribution of barrier heights, V, zero-point energies, E and well separations. There may also be a variety of different TLS coordinates, q

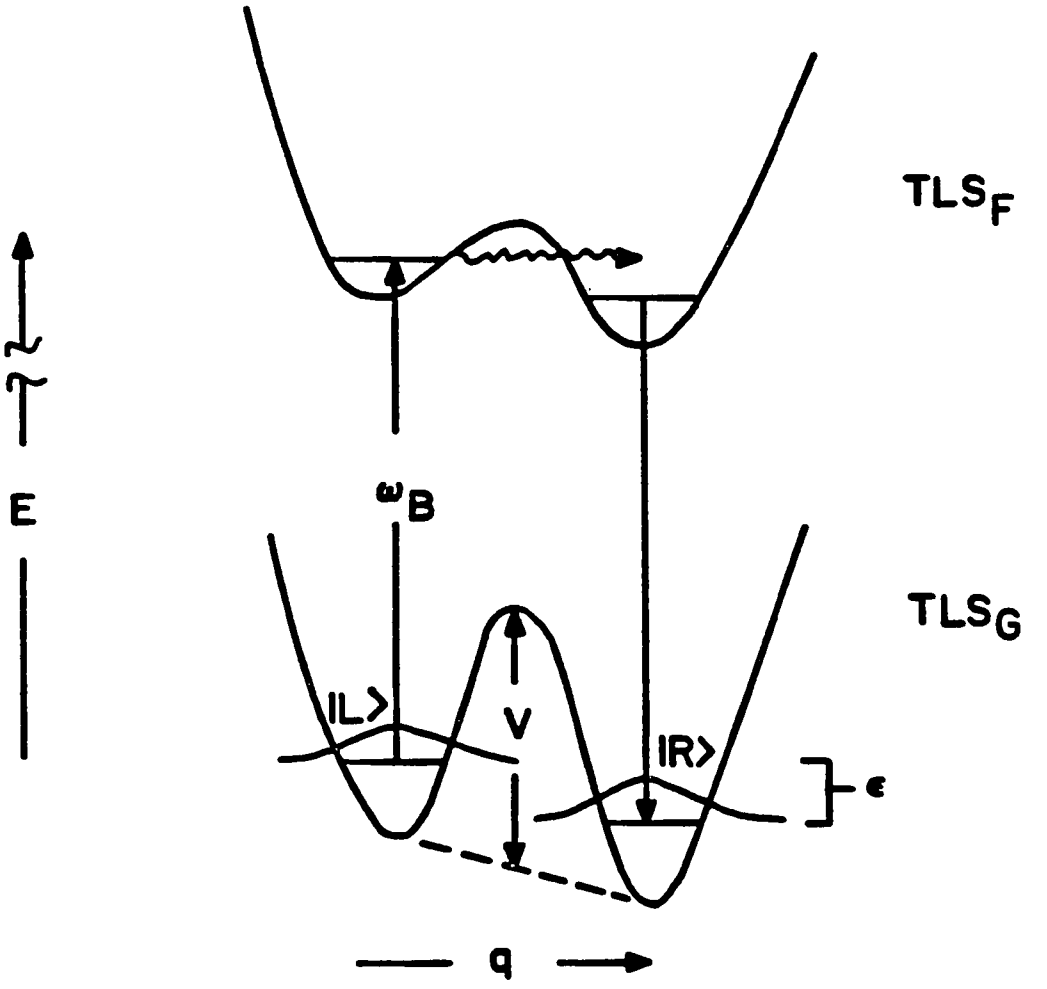
TLS$_F$
E
ω_B
TLS$_G$
|L>
V
|R>
ε
q

EXPERIMENTAL

Experimental and procedural methods used have been described previously [8]. However, for completeness, a brief summary of the experimental techniques shall be given. Holes were probed at low temperature in a Janis variable temperature helium cryostat by one of three methods: (1) by absorption **via** a home built high resolution low noise double beam absorption spectrometer (typically $\leq$ 0.005 nm), obtained by utilizing a J-Y HR-1500 monochromator (resolving power ~ 2.5 x 10^{-5}) and lock-in amplifiers, (2) by transmission using the same monochromator as above, or (3) by photoexcitation, **i.e.**, monitoring the total fluorescence while scanning a dye laser, thereby reproducing the absorption spectrum. Holes were burned by any of a plethora of lasers; a pulsed Quantel or Quanta-Ray Nd-YAG pumped dye laser, a pulsed Chromatix CMX-4 laser, a cw Control or Coherent argon ion laser, a Coherent cw ring dye laser or a cw Spectra-Physics helium-neon laser. The choice of burn laser generally depended upon availability, spectral range and limiting linewidth of the laser (1.5 cm^{-1} to 0.002 cm^{-1}) for each particular system of interest. Samples consisted of some impurity molecule or ion doped into a host. The dopants used were always of high purity and, when necessary, were purified by zone refining, recrystallization or vacuum sublimation. Impurity concentrations were typically adjusted such that an optical density of ~ 0.5 was obtained yielding concentrations ranging from 10^{-5} M to 1.5 M. Due to the high diversity of host materials (see Table I), a variety of cooling rates, from less than a minute to many hours for the touchiest glasses, were

Table I. Summary of hole burning systems

	←Hydrogen Bonding→					←Non-Hydrogen Bonding→								
	←Organic Glasses→					←Polymers→						←Organic glasses→		
	methanol/ethanol	glycerol/dimethyl-sulfoxide/dimethyl formamide	ethanol/methyl-tetrahydrofuran	glycerol/ethanol/water	ethyl ether/ethanol/water	poly(acrylic acid)	poly(vinyl alcohol)	poly(methyl methacrylate)	poly(vinyl carbazole)	polystyrene	decalin	pentane/methylpentane/methylcyclopentane	amorphous anthracene	silicate glass
Aromatic Hydrocarbons														
naphthalene	*													
anthracene	*													
tetracene	**	**			**			np	no	no	no	no	no	**[a]
pentacene								*[b]		no				
phenanthracene	**													
pyrene		**												
perylene	**[c]													
azulene			*											
phenylazaazulene				*										
Organic Dyes														
rhodamine 560							**							
rhodamine 640						***	***	**	no	no				
cresyl violet	***			***		***	***		*					
nile blue						***	***							
oxazine 720						***	***							
oxazine 725						***	***							
oxazine 750						*								
DCM									no					
Rare Earth Ions														
Pr^{3+}							**							**[d]
Nd^{3+}							**							*[d]
Biomolecules														
chlorophyll a					*[e]					***				
chlorophyll b					*[e]					***				

* hole burning facility is weak.
** hole burning facility is moderate.
*** hole burning facility is strong.

	methanol/ethan	glycerol/dimet sulfoxide/dim	ethanol/methy tetrahydrofur	glycerol/ ethanol/water	ethyl ether/ ethanol/water	poly(acrylic	poly(vinyl al	poly(methyl me	poly(vinyl ca	polystyrene	decalin	pentane/methy methylcyclope	amorphous an	silicate gla
Aromatic Hydrocarbons														
naphthalene	*													
anthracene	*													
tetracene	**	**			**			np	no	no	no	no	no	**[a]
pentacene								*		no				
phenanthracene	**													
pyrene		**												
perylene	**[c]													
azulene			*											
phenylazaazulene				*										
Organic Dyes														
rhodamine 560							**							
rhodamine 640						***	***	**	no	no				
cresyl violet	***			***		***	***		*					
nile blue						***	***							
oxazine 720						***	***							
oxazine 725						***	***							
oxazine 750						*								
DCM									no					
Rare Earth Ions														
Pr^{3+}							**							*[d]
Nd^{3+}							**							*[d]
Biomolecules														
chlorophyll a					*[e]					***				
chlorophyll b					*[e]					***				

* hole burning facility is weak.
** hole burning facility is moderate.
*** hole burning facility is strong.

a R. Jankowiak and H. Bassler, Chem. Phys. Lett. 95, 310 (1983).
b Mollenkamp and Wiersma [25].
c Kharlamov et al. [1,2].
d R. M. MacFarlane and R. M. Shelby, Opt. Commun. 45, 46 (1982).
e Avarmaa et al. [13].

required to cool the samples to liquid helium temperatures. To minimize thermal gradients, soft glasses were enclosed by a copper cylinder and the polymers were firmly attached to copper plates. Temperatures were accurately measured with a silicon diode sensor.

RESULTS AND DISCUSSION

Universality of NPHB

Given the universal nature of TLS in amorphous solids, one might expect based on the proposed mechanism [3,4] that NPHB would be a universal phenomenon, i.e. independent of the particular natures of the impurity or the matrix, only that the matrix be amorphous. Over the past few years, a large variety of systems have been surveyed for their propensity toward hole burning. Table I is a partial summary of those survey experiments. The table consists mainly of results obtained by the present authors but also contains other published reports in which a nonphotochemical nature can be ascribed to the holes. The table indicates, for the systems listed, if hole burning has been observed and, if it has, the hole burning facility. We hasten to add that the indicated facilities are meant to serve only as a rough guide. They are based on the time and burn flux required to burn a hole corresponding to an optical density change of ~ 10%. The hole burning facility is not necessarily correlated with the hole burning quantum efficiency.

From the table, it can be seen that there are systems in which hole burning has not been observed. This can be understood within the mechanism depicted in Figure 1, in the following way. NPHB requires a change of the potential energy surface for the TLS to be induced by electronic excitation of the impurity. Furthermore, the effect of this change must be to increase the interconversion rate between TLS wells from a time scale of hours to a time scale on the order of the lifetime of the excited state (i.e., ~ 10^{-8} sec.). The magnitude of the

electron-TLS coupling which induces this change will vary both with the nature of the impurity and with the nature of the TLS modes, **i.e.** with the particular atomic displacement coordinate, q. For most glasses, identification of the TLS modes has not been made. For example, NPHB experiments on tetracene show that the hole burning is more facile in hydrogen bonding glasses suggesting that the TLS responsible for hole burning may be hydroxyl groups. Indeed, it has been shown that the efficiency of hole production is dependent upon deuteration whereas dephasing is not [9]. In summary, for systems where hole burning has not been observed, it might be inferred that the electron-TLS coupling is not strong enough to induce the substantial TLS interconversion rate required in the excited state required for NPHB. However, another possibility is that TLS interconversion in the ground state is too rapid to permit the observation of a hole on the time scale of the experiment. Thus, one cannot say that hole burning is impossible in such a system, but only that under the conditions used it was not observed.

Vibrational Spectroscopy

In view of the diversity of materials which can form low temperature amorphous solids, the existence of systems in which hole burning facility is so low as to be not observable on a reasonable time scale does not limit the potential applications of NPHB. One area of application is in vibrational spectroscopy of large molecules and especially biologically important species (**vide infra**). For such molecules, NPHB can yield high resolution vibrational spectra. The presence of polar substituents on such molecules, which often leads to

Figure 2. Hole burning of cresyl violet perchlorate in PVOH. The sample was burned for 1 min. at 583 nm. Laser flux ~ 100 mW/cm^2, T = 4.2 K

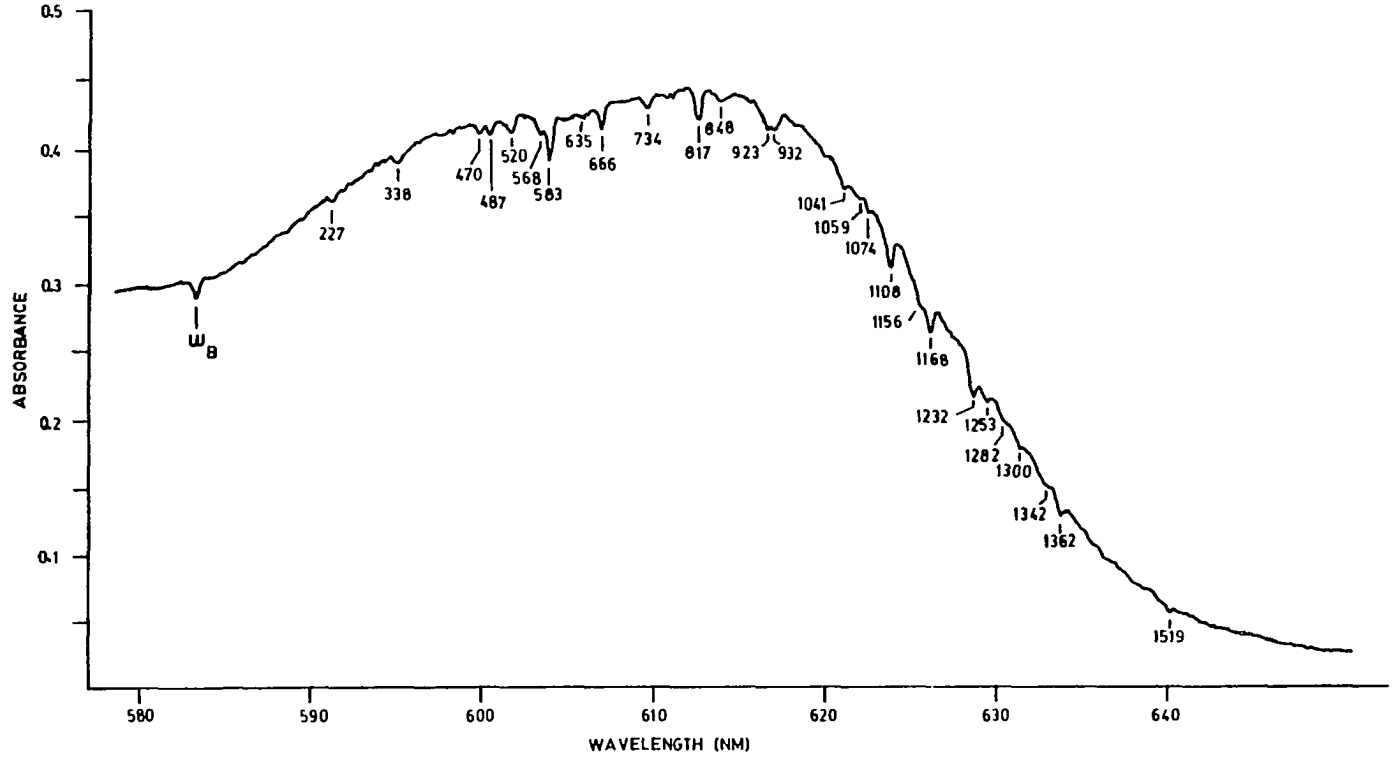
0.5
0.4
0.3
0.2
0.1
ABSORBANCE
ω_B
227
338
470
487
520
568
583
635
666
734
817
848
923
932
1041
1059
1074
1108
1156
1168
1232
1253
1282
1300
1342
1362
1519
580
590
600
610
620
630
640
WAVELENGTH (NM)

additional inhomogeneous broadening through either charge transfer interactions or a strong electron-phonon coupling, can be utilized to ensure that the electron-TLS coupling will lead to hole formation. For example, shown in Figure 2 is a portion of the absorption spectrum of cresyl violet perchlorate in polyvinyl alcohol (PVOH). The individual vibronic bands are all inhomogeneously broadened with widths greater than the vibronic splittings (i.e., $\Gamma_{inhom} \geq 500\ cm^{-1}$). Thus, prior to hole burning, the spectrum consists of a single unstructured absorption with a width on the order of 1000 cm^{-1}. As shown in the figure, the underlying vibronic structure can be revealed by the use of hole burning. In this particular case, a hole was burned at frequency ω_B, on the high energy side of the broad absorption. The satellite holes appearing at lower energy correspond to the fundamental vibrations of the molecule, as well as combinations and overtones of the fundamentals. In general, the sample may be burned anywhere in the broad absorption and vibronic holes will appear to both higher and lower energy. It should be pointed out that whether or not the resolution shown in Figure 2 is obtainable is dependent upon the linear electron-phonon coupling between the molecule and the matrix as well as other factors. When the coupling is strong, the hole (and the satellite holes) will be accompanied by a phonon sideband hole. The relative intensities of phonon-less and phonon sideband holes is determined by the Debye-Waller factor for the transition. When the Debye-Waller factor is small, the phonon sideband holes will be intense and may limit the resolution of vibronic bands.

A somewhat unusual example of phonon sideband holes is shown in

Figure 3. Hole burning of oxazine 725 perchlorate in a) PVOH and b) PAA. Both holes were burned at 632.8 nm with a flux of ~ 25 mW/cm^2 , with T = 5 K. Spectrum a) was burned for 2 min.; b) for 12 min

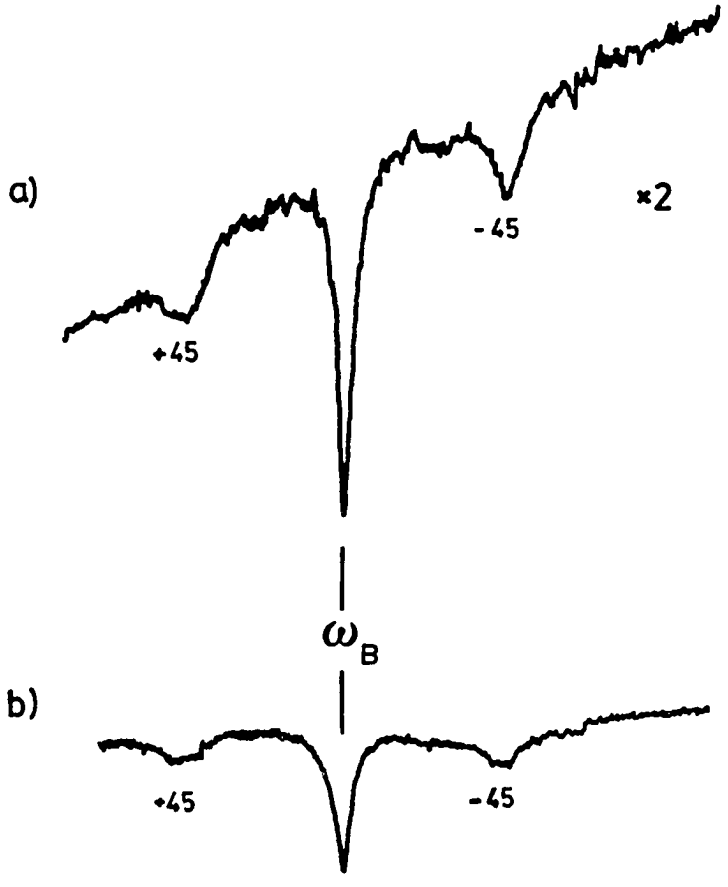
a)
×2
-45
+45
ω_B
b)
+45
-45

Figure 3. For these systems: oxazine 725 perchlorate in PVOH and in polyacrylic acid (PAA), well resolved phonon sideband holes symmetrically displaced at $\pm$ 45 cm^{-1} relative to the burn frequency are observed. The observation of both lower and higher energy sideband holes is explained by considering that the broad absorption consists of a distribution of homogeneously broadened absorptions consisting of a phononless line and a higher energy phonon hole. For other sites which absorb at the burn frequency through their phonon side bands, a hole due to zero-phonon absorption will occur at lower energy. In many cases, only the lower energy phonon hole is observed due to a large Debye-Waller factor.

One final comment on Figures 2 and 3 is that both of these systems, ionic dyes in hydrogen bonding polymers, are representative of a class of systems in which NPHB is very efficient. Measurable holes can be produced in these systems with exposure times of a few seconds and laser fluxes of ~ 1 - 25 mW/cm^2 [10].

NPHB of Biomolecules

As described above, the availability of a diverse selection of solvents which form amorphous solids provides matrices for the study of a variety of classes of molecules. As a prelude to the study of excitonic effects in self-aggregates (dimers) of chlorophylls, NPHB of chlorophyll monomers has recently been studied [11]. This work is somewhat akin to photochemical hole burning studies on free-base porphyrin derivatives (see **e.g.** Thijssen et al. [12]). In those studies, a hole is produced via photo-tautomerization of the porphyrin

ring protons. In chlorophyll however, the ring protons are replaced by a Mg II ion, blocking the photochemical mechanism. Hole burning of chlorophyll in ether has previously been observed and attributed to a nonphotochemical process [13]. In the present work NPHB was observed for both chlorophyll **a** and chlorophyll **b** in a polystyrene film.

Figure 4 shows holes burned in the spectra of chlorophyll **b**, and also illustrates laser induced hole filling of the initial hole by subsequent burns at frequencies away from the initial burn frequency. Burn 1 at 15441.6 cm^{-1} represents a change in optical density (Δ OD) of 10% produced by a 1 minute burn with a laser power density of ~ 5 mW/cm^2. The width of the hole is 0.16 cm^{-1}. Shifting the burn frequency to lower energy and with a similar exposure a second hole is produced with a depth and width similar to the initial hole. The burning of this hole results in a decrease in the intensity of the initial hole by ~ 13%. A third burn at higher energy again produces a hole with Δ OD ~ 10%, and with width ~ 0.16 cm^{-1} and fills both lower energy holes. Hole 1 is now reduced by 33% of its initial depth and hole 2 by 31%. This hole filling, as well as thermal annealing data [11], are indicative of the nonphotochemical nature of the holes [3,4].

Hole burning in the chlorophylls was extremely facile, **i.e.** relatively deep holes are produced with short exposure times and low power density. The holes produced, although somewhat broader than those observed in photochemical hole burning, are still narrow enough so that splittings which might occur (**e.g.**, vibronic holes) would still be resolved. Thus, NPHB is a promising method of studying photophysics of

Figure 4. Hole burning of chlorophyll b in polystyrene. Holes were burned for 1 min. at 647.6 nm with a flux of ~ 5 mW/cm^2, T=1.9 K

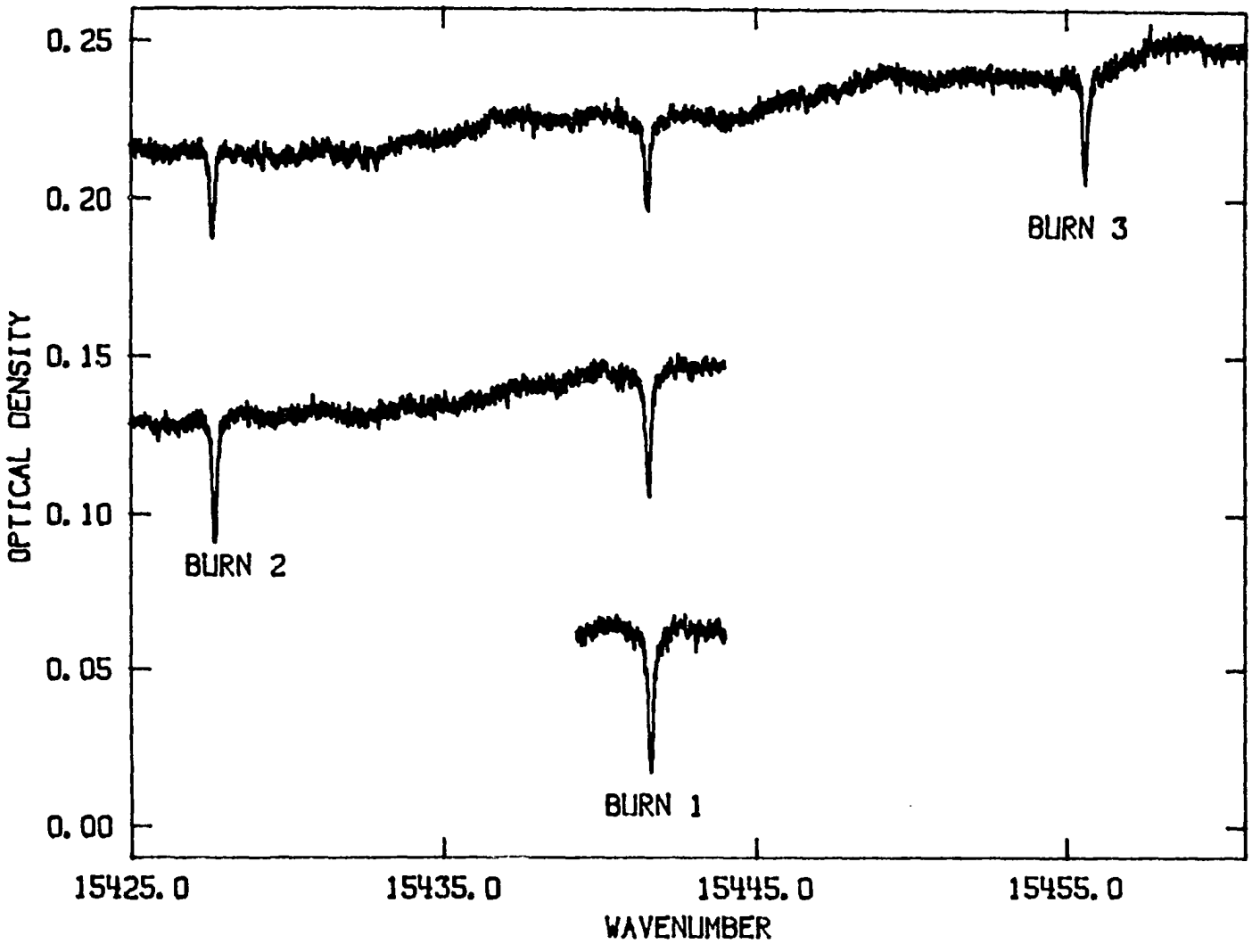
0.25
0.20
0.15
0.10
0.05
0.00
OPTICAL DENSITY
BURN 3
BURN 2
BURN 1
15425.0
15435.0
15445.0
15455.0
WAVENUMBER

biologically significant molecules.

Optical Dephasing in Amorphous Solids

A general feature of homogeneous optical linewidths in both organic and inorganic glasses and in polymers at low temperatures is that they are 1-2 orders of magnitude greater than those observed in crystalline solids. This difference as well as differences in the thermal variation of linewidths between crystalline and amorphous solids has been probed not only by NPHB but also by photochemical hole burning, fluorescence line narrowing and photon echoes. The variety of systems and techniques which are involved has prompted a number of theories which attempt to explain these large differences in dephasing times. In Table II, we have listed the various theories which have been proposed.

The starting point for all of the theories is that the dephasing anomaly is primarily due to the glass TLS, which are coupled to the impurity. Additionally, one must consider the vibrational modes of the solid (phonons). The coupling of the phonons to the TLS and/or to the impurity can be included in the system Hamiltonian. In Table II, we have described which of the possible coupling modes are included in the various theoretical models. Having developed a model, it is then possible to obtain a solution for the optical lineshape assuming fixed values for the system coordinates. However, the TLS have a broad distribution of energy asymmetries, barrier heights and tunneling frequencies. This in turn causes differences in the strengths of the impurity-TLS coupling and the TLS-phonon coupling. Thus, it is necessary to average the lineshape function over the various distributions.

It is in the details of taking this average that the major differences between the theories arise. It is beyond the scope of this paper to delve into the intricacies of the various averaging procedures. Rather, we will restrict ourselves to a few general comments. In most of the theories, following the model of Anderson **et al.** [5] and of Phillips [6] the averaging assumes that the TLS density of states is constant. In some of the more recent theories, this condition is relaxed so that the density of states is considered to vary slowly with the energy, **i.e.** $n(E) \propto E^{\mu}$; $\mu < 1$. The exception to this general trend is the paper by Hayes **et al.** [14]. They argue that the dephasing is dominated on average by one type of TLS with a dephasing frequency in a maximum range or interval. The distribution function for these particular TLS may then be sharply peaked although the entire TLS distribution will still obey the near constant density of states relationship.

Finally, let us remark that a fully satisfactory theory remains to be developed. Those theories which purport to explain all of the observed experimental data tend to do so at the expense of being predictive, **i.e.**, the parameters required to reconcile theory and experiment are themselves not available but must be inferred from experiment.

Table II. Theories of optical dephasing in glasses

REFERENCE	MODEL USED	TEMPERATURE DEPENDENCE
Reinecke [15]	spectral diffusion due to strain mediated coupling of impurity to TLS	$\propto T$ (n(E) = constant)
Reineker and Morawitz [16]	coupling of TLS to impurity and to phonons	T (except at very low T)
Hayes **et al.** [17,14]	coupling of impurity to a subset of TLS with maximum PAT rates	$T \rightarrow T^2$ as $T \rightarrow 0$ K
Morawitz and Reineker [18]	coupling of impurity to TLS and to low lying optical and librational modes	T (except at very low T)
Reineker **et al.** [19]	coupling of TLS to impurity and to phonons	T (except at very low T)
Lyo [20,21]	diagonal coupling of TLS and impurity with phonon modulation of TLS	$T^{4+\mu-9/s}$ ($V \propto r^{-s}$; $n \propto E^{\mu}$)
Jackson and Silbey [22]	addition of dephasing due to local libration to the model of Hayes **et al.**	$T^{1.3}$
Lyo and Orbach [23]	considered role of fractons in place of phonons in previous theory of Lyo	$T^{1+d/4}$ ($N_{fr} \propto E^{d-1}$)
Huber **et al.** [24]	spectral diffusion due to diagonal interaction between impurity and TLS	$T^{1+\mu}$ ($n \propto E^{\mu}$)
Mollenkamp and Wiersma [25]	dipolar coupling of impurity and TLS	$T^{1+\mu}$ ($n \propto E^{a}$)
Lyo and Orbach [26]	off-diagonal electrostatic coupling of TLS and impurity with diagonal phonon modulation	$T \rightarrow T^2$ as $T \rightarrow 0$ K (n(E) = constant)

REFERENCES

1. B. M. Kharlamov, R. I. Personov and L. A. Bykovskaya, Opt. Commun. 12, 191 (1974).

2. B. M. Kharlamov, R. I. Personov and L. A. Bykovskaya, Opt. Spectrosc. 39, 137 (1975).

3. J. M. Hayes and G. J. Small, Chem. Phys. 27, 151 (1978).

4. J. M. Hayes and G. J. Small, Chem. Phys. Lett. 54, 435 (1978)

5. P. W. Anderson, B. I. Halperin and C.M. Varma, Philos. Mag. 25, 1 (1972).

6. W. A. Phillips, J. Low Temp. Phys. 7, 351 (1972).

7. G. J. Small in: "Modern Problems in Solid State Physics. Molecular Spectroscopy", V. M. Agranovich and R. M. Hochstrasser, eds., North-Holland: Amsterdam, 1983.

8. T. P. Carter, B. L. Fearey, J. M. Hayes and G. J. Small, Chem. Phys. Lett. 102, 272 (1983) and references therein.

9. B. L. Fearey, R. P. Stout, J. M. Hayes and G. J. Small, J. Chem. Phys. 78, 7013 (1983).

10. B. L. Fearey, T. P. Carter and G. J. Small, J. Phys. Chem. 87, 3590 (1983).

11. T. P. Carter and G. J. Small, Chem. Phys. Lett. 120, 178 (1985).

12. H. P. H. Thijssen, R. E. van den Berg and S. Volker, Chem. Phys. Lett. 103, 23 (1983).

13. R. Avarmaa, K. Mauring and A. Suisalu, Chem. Phys. Lett. 77, 88 (1981).

14. J. M. Hayes, R. P. Stout and G. J. Small, J. Chem. Phys. 74, 4266 (1981).

15. T. L. Reineke, Solid State Commun. 32, 1103 (1979).

16. P. Reineker and H. Morawitz, Chem. Phys. Lett. 86, 359 (1984).

17. J. M. Hayes, R. P. Stout and G. J. Small, J. Chem. Phys. 73, 4129 (1980).

18. H. Morawitz and P. Reineker, Solid State Commun. 42, 609

(1982).

19. P. Reineker, H. Morawitz and K. Kassner, Phys. Rev. B 29, 4546 (1984).

20. S. K. Lyo, Phys. Rev. Lett. 48, 688 (1982).

21. S. K. Lyo in: "Electronic Excitations and Interactions in Organic Molecular Aggregates", P. Reineker, H. Haken and H. C. Wolf eds., Springer Series in Solid State Physics, Vol. 49 Springer: Berlin, 1983.

22. B. Jackson and R. Silbey, Chem. Phys. Lett. 99, 381 (1983).

23. S. K. Lyo and R. Orbach, Phys. Rev. B 29, 2300 (1984).

24. D. L. Huber, M. M. Broer and B. Golding, Phys. Rev. Lett. 52, 2281 (1984).

25. L. W. Mollenkamp and D. A. Wiersma, J. Chem. Phys. 83, 1 (1985).

26. S. K. Lyo and R. Orbach, Phys. Rev. B 22, 4223 (1980).

PAPER II.

EFFICIENT NONPHOTOCHEMICAL HOLE BURNING OF DYE MOLECULES IN POLYMERS

EFFICIENT NONPHOTOCHEMICAL HOLE BURNING OF DYE MOLECULES IN POLYMERS

THOMAS P. CARTER, B. L. FEAREY and GERALD J. SMALL

Ames Laboratory-USDOE and Department of Chemistry
Iowa State University, Ames, Iowa 50011

Journal of Physical Chemistry 87, 3590 (1983)

INTRODUCTION

The connection between nonphotochemical hole burning (NPHB) of the optical absorption bands of impurities imbedded in amorphous hosts and the disorder of the latter was drawn by Hayes and Small [1,2] and Hayes **et al.** [3]. These and other works related to solid state hole burning spectroscopy have recently been reviewed [4]. A distribution of two-level systems (TLS) associated with asymmetric double-well potentials [5,6] was used to model the disorder. Relaxation between TLS tunnel states, triggered by the impurity transition electron-TLS interaction was proposed as the hole formation mechanism [1,2]. Because the hole burning process was too slow to account for the large homogeneous hole widths observed, it was further proposed that the impurity interacts with two "types" of TLS, distinguished by whether or not their tunnel states are in equilibrium when the impurity is in its ground state [3]. Those which are <u>not</u> in equilibrium can, at a given burn temperature T_B, give rise to persistent [7] holes. Those which <u>are</u> in equilibrium are responsible for rapid optical dephasing by phonon-assisted tunneling (PAT) between tunnel states. The PAT accounted for the linear dependence of hole width on T_B observed for tetracene in organic glasses [3,8]. This dependence arises in the high T limit when kT > width of $f(\varepsilon)$, where ε is the zero-point splitting between local oscillators of a TLS and f is a distribution function. The problem of PAT dephasing in amorphous solids has now been considered by a number of groups [9-11]. With the exception of reference [11], the high-T and low-T limits of these theories yield a linear and approximately quadratic dependence of

dephasing on T, respectively. In contrast with organic glasses and polymers, several experiments on rare earth ions in "hard" inorganic glasses have demonstrated, with one exception [12], the latter dependence in the low T regime [13]. In [11], the dephasing of the impurity is argued to be due to diagonal (**versus** off-diagonal) modulation of the impurity optical levels. If the density of TLS states is constant, the theory finds the temperature dependence of the dephasing to be $T^{1.0}$, $T^{1.75}$, and $T^{2.12}$ for dipole-dipole, dipole-quadrupole and quadrupole-quadrupole impurity-TLS coupling, respectively.

Importantly, NPHB has been observed in a wide variety of amorphous molecular solids [4, 14-17] and very recently, in Eu^{3+} and Pr^{3+} doped silicate glasses [12]. Thus, it is likely that NPHB will be added to the list of techniques [18] important for the study of disorder. Of course, photochemical hole burning of photoreactive species can also be used to probe dephasing in amorphous solids [19-21]. However, NPHB affords greater flexibility. For example, one can study the irreversible thermal annealing of holes burned at different T_B [3], the dependence of the integrated hole intensity on T_B and the filling of a primary hole produced by subsequent burns at different frequencies located within the same inhomogeneously broadened profile [2].

Unfortunately, data from these latter types of experiments are limited because the experiments are very time consuming for low NPHB quantum yields. With one exception [15], the molecular systems studied have exhibited low yields ($\lesssim 10^{-5}$) [4]. For this reason, we have been exploring the generality of NPHB and its efficiency in widely differing

(molecular) systems. Earlier results indicated that amorphous hosts with hydrogen bonding are promising although it was noted that efficient NPHB has been reported for some non-hydrogen bonding matrices [16]. This led to a study of a series of ionic dyes embedded in poly(vinyl alcohol) and poly(acrylic acid) polymers. We report here some of our results because they indicate that such dyes in polymers may form a class of efficient NPHB systems particularly convenient for future detailed studies. In addition, the NPHB spectra provide detailed vibronic structural information on the lowest excited singlet state of the ionic dye molecules.

EXPERIMENTAL

Holes were probed with a double-beam spectrometer whose construction is described below. Light from a continuous 700 W xenon arc lamp is first dispersed by either a 1 m Jarrel-Ash 75-150 Czerny-Turner fast spectrometer or a 1.5 m Jobin-Yvon HR-1500 monochromator and then split into two beams, each of which is mechanically chopped (Laser Precision CTX-534) at a different frequency, and then passed through identical optics. Only air was present in the reference beam. After passage through the sample, the beams are recombined and monitored by the same photomultiplier tube (RCA C31034 cooled to ~ -15° C in a PTR TE-104-RF housing) whose output was provided to two identical lock-in amplifiers (Ithaco 391A) each referenced to one of the chopping frequencies. A logarithmic ratiometer (Evans Associates) provided a signal proportional to sample absorbance. Extreme care was taken to ensure that the probe beam cross-sectional area at the sample was smaller than the cross-sectional area of the burn laser beam. A Janis variable temperature helium cryostat was utilized.

For all of the cresyl violet and hole filling experiments, the holes were burned with a Nd:YAG laser pumped dye laser (Quantel) with a linewidth < 0.2 cm^{-1}. In all other experiments, a cw He-Ne laser with a linewidth < 0.02 cm^{-1} was employed. Photon fluxes and burn times are given in the figure captions. The objectives of these experiments did not necessitate utilizing a narrow monochromator band pass. The band pass utilized was typically 0.5 cm^{-1}.

Poly(vinyl alcohol) (PVOH) and poly(acrylic acid) (PAA) polymer films were prepared as follows: polymer powder (Aldrich) was dissolved in hot water to produce a syrupy consistency. Crystals of the dye (Exciton) were added to the polymer solution and the mixture was stirred. Undissolved material was removed with a filter syringe. Aliquots of the solution were then poured onto 2 in. square glass plates and allowed to dry into thin (~ 100 μ) films which were subsequently removed from the plate. Film sections were then selected for optical density and high optical quality.

RESULTS AND DISCUSSION

The two lower traces of Figure 1 are hole burned spectra obtained with a pulsed Nd:YAG laser pumped dye laser for cresyl violet in a PVOH polymer. Burning and recording were performed at T = 7 K. Spectrum a) is the absorption prior to the burn; its breadth and lack of structure should be noted. Spectrum b) results from an initial burn at ω_{B1} = 650.0 nm which is ~ 1000 cm^{-1} to higher energy of the absorption onset. The zero-phonon hole at ω_{B1} is accompanied by a 32 cm^{-1} low energy phonon side band hole [1, 22] as well as about a dozen reproducible zero-phonon intramolecular satellite holes to lower energy from ω_{B1}. The displacements of the satellite holes from ω_{B1} yield the optically active fundamental vibrational frequencies of the S_1 state of cresyl violet. For example, the 527 cm^{-1} hole is due to cresyl violet sites whose zero-point level lies at ω_{B1} - 527 cm^{-1} and which absorb ω_{B1} via their 527 cm^{-1} vibronic band. Thus, cresyl violet exhibits extensive vibronic activity of lower frequency fundamentals which, along with inhomogeneous line broadening, is responsible for the structureless absorption spectrum, a). Satellite activity to higher energy from ω_{B1} is very weak because ω_{B1} lies in a region where absorption by sites with zero-phonon origin absorption constitutes only a small fraction of the total optical density. It is interesting that the linear electron-phonon coupling, as judged by the phonon side band hole intensity, is weak for an ionic dye.

The nonphotochemical nature of the holes is confirmed by spectrum c) obtained following spectrum b) with a second burn at ω_{B2} (600.0 nm).

Figure 1. Hole burning and filling for cresyl violet perchlorate in PVOH at 7 K. Spectrum a) is the inhomogeneous profile before hole burning; trace b) shows the same sample after burning with the dye laser for 10 min. with ~ 5 mW/cm^2 at 605 nm. Frequency displacements of the satellite holes from the burn frequency are given in cm^{-1}; trace c) is the spectrum of the same sample subsequently burned for 10 min. at 600 nm with the same flux

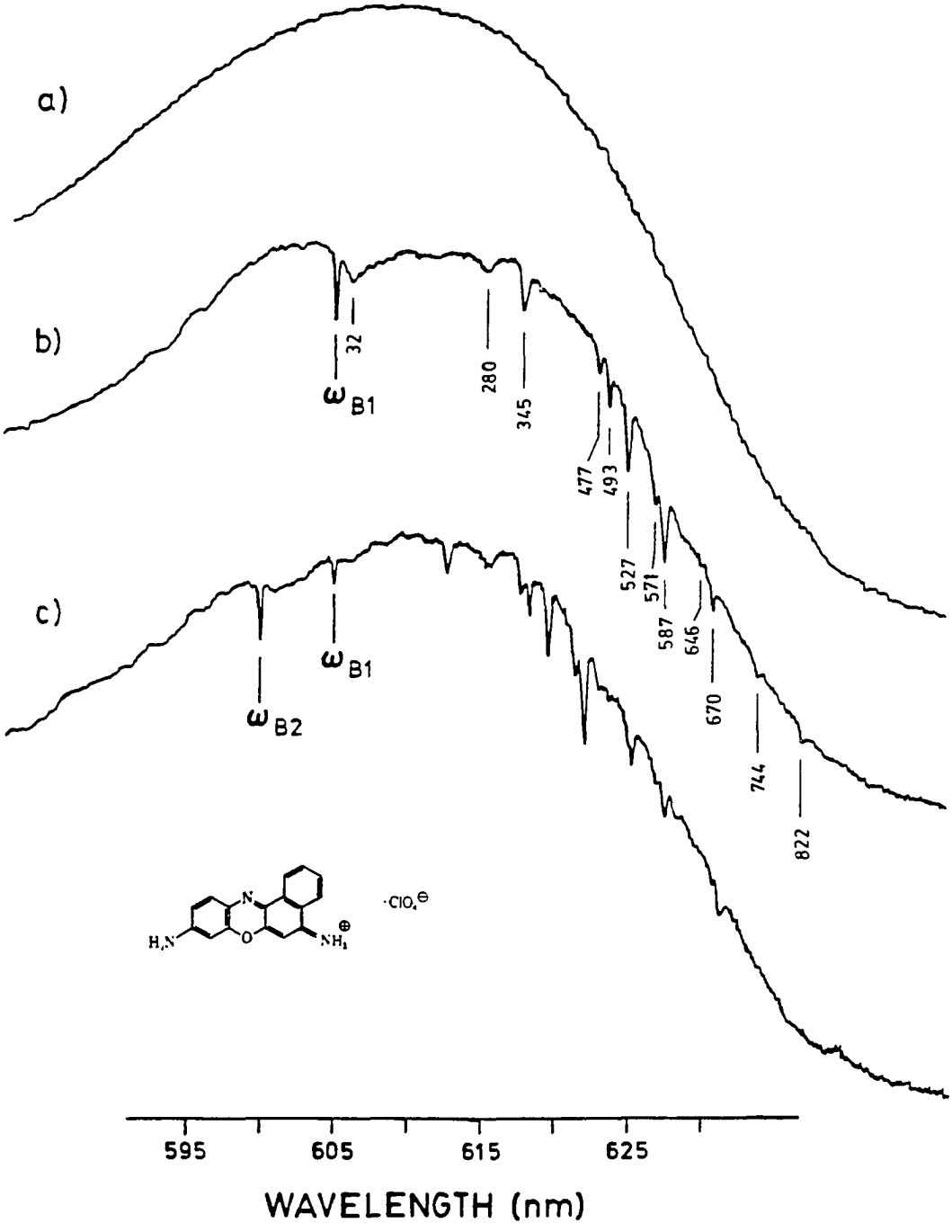
a)
b)
c)
ω B1
ω B2
32
280
345
477
493
527
571
587
646
670
744
822
595
605
615
625
WAVELENGTH (nm)

This hole filling experiment [2] clearly shows how the holes in spectrum b) are substantially filled by the ω_{B2} burn lying ~ 150 cm^{-1} to higher energy of ω_{B1}. Thus it is demonstrated that, with NPHB, hole filling can occur when $\omega_{B2} > \omega_{B1}$ in addition to $\omega_{B2} < \omega_{B1}$ [2]. Given that inhomogeneous broadening in polymers is severe, say a few hundred cm^{-1}, it is particularly interesting that a second burn so far removed from the first shows such a high degree of selectivity for producing impurity-TLS configurations which absorb at frequencies corresponding to those photobleached by the primary burn ω_{B1}. If we note that the burn times for spectra b) and c) are identical and that their holes coincident with the burn frequency have nearly the same intensity, it seems unlikely that the selective filling is a result of bulk heating due to the laser. This possibility, along with the interesting question of selective hole filling due to disorder induced cooperative effects, are to be investigated further.

In comparing the satellite hole structure produced by ω_{B2} with that in spectrum b), one can see that the two are essentially identical in vibronic frequencies and intensities. Given that ω_{B2} and ω_{B1} are so different, this may mean that the relative satellite hole intensities are a qualitative measure of the relative vibronic absorption cross sections. Further studies with a wide variety of burn frequencies are required to establish this with certainty. From spectra b) and c) it can be seen that the linewidth of a number of vibronic satellite holes are considerably broader than the hole coincident with ω_B (see also Figures 2 and 3). The reason for this has not been established but one possibility is that the impurity site distribution function depends on

Figure 2. Hole burning for nile blue perchlorate at 5 K with a cw helium-neon laser. Spectrum a) is in PVOH burned for 7 min. with ~ 25 mW/cm^2. Displacements of the sat-satellite holes from the burn frequency are given in cm^{-1}; spectrum b) is in PAA burned for 12 min. with the same flux

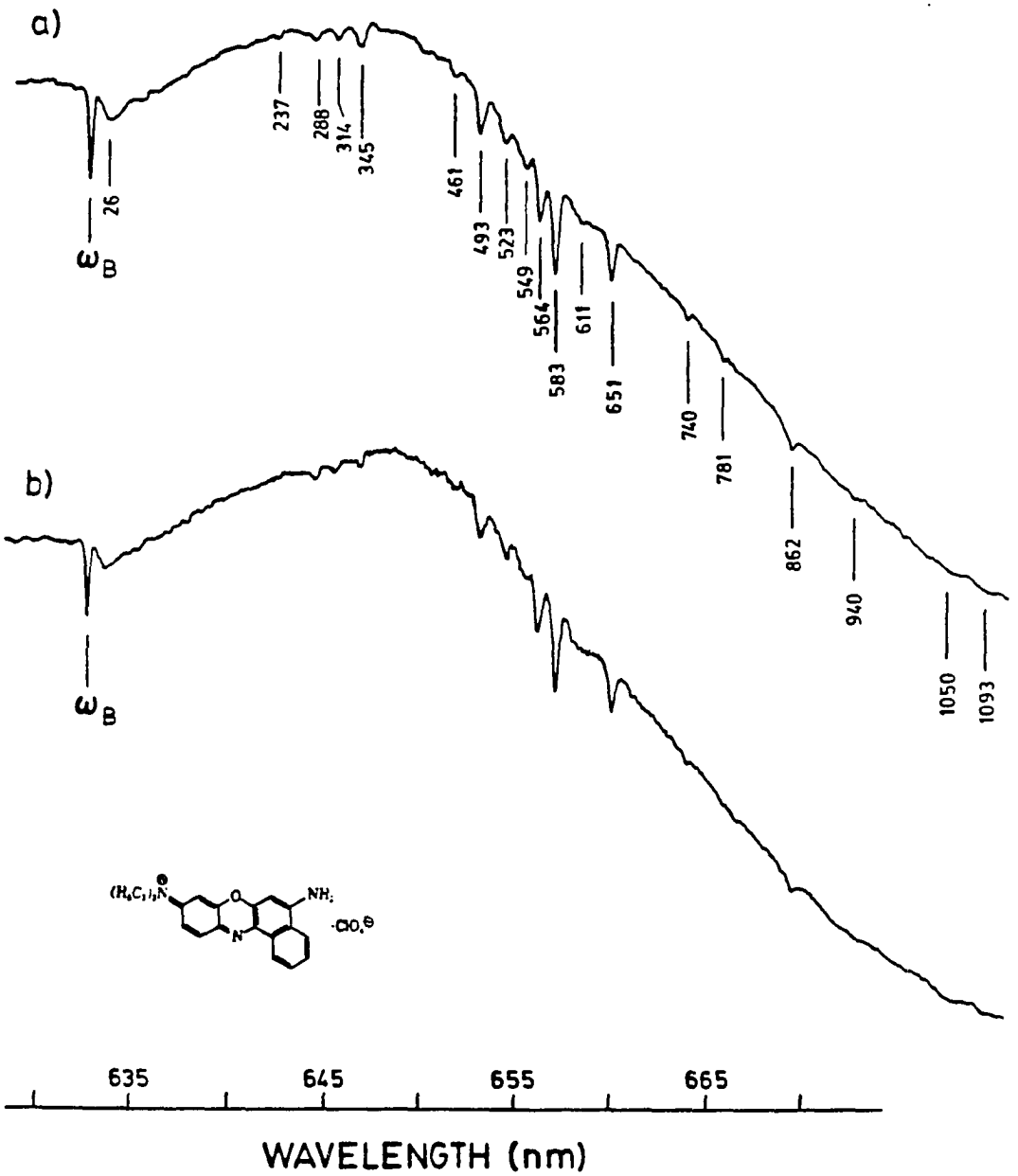
a)
237
288
314
345
461
493
523
549
564
583
611
651
740
781
862
940
1050
1093
26
ω_B
b)
ω_B
635
645
655
665
WAVELENGTH (nm)

Figure 3. Hole burning for oxazine 720 perchlorate at 7 K with a cw helium-neon laser. Spectrum a) is the unburned inhomogeneous profile in PVOH; spectrum b) is the same sample burned for 7 min. with ~ 25 mW/cm^2. Frequency displacements from ω_B are given in cm^{-1}. The host in spectrum c) is PAA which was burned for 12 min. with the same flux

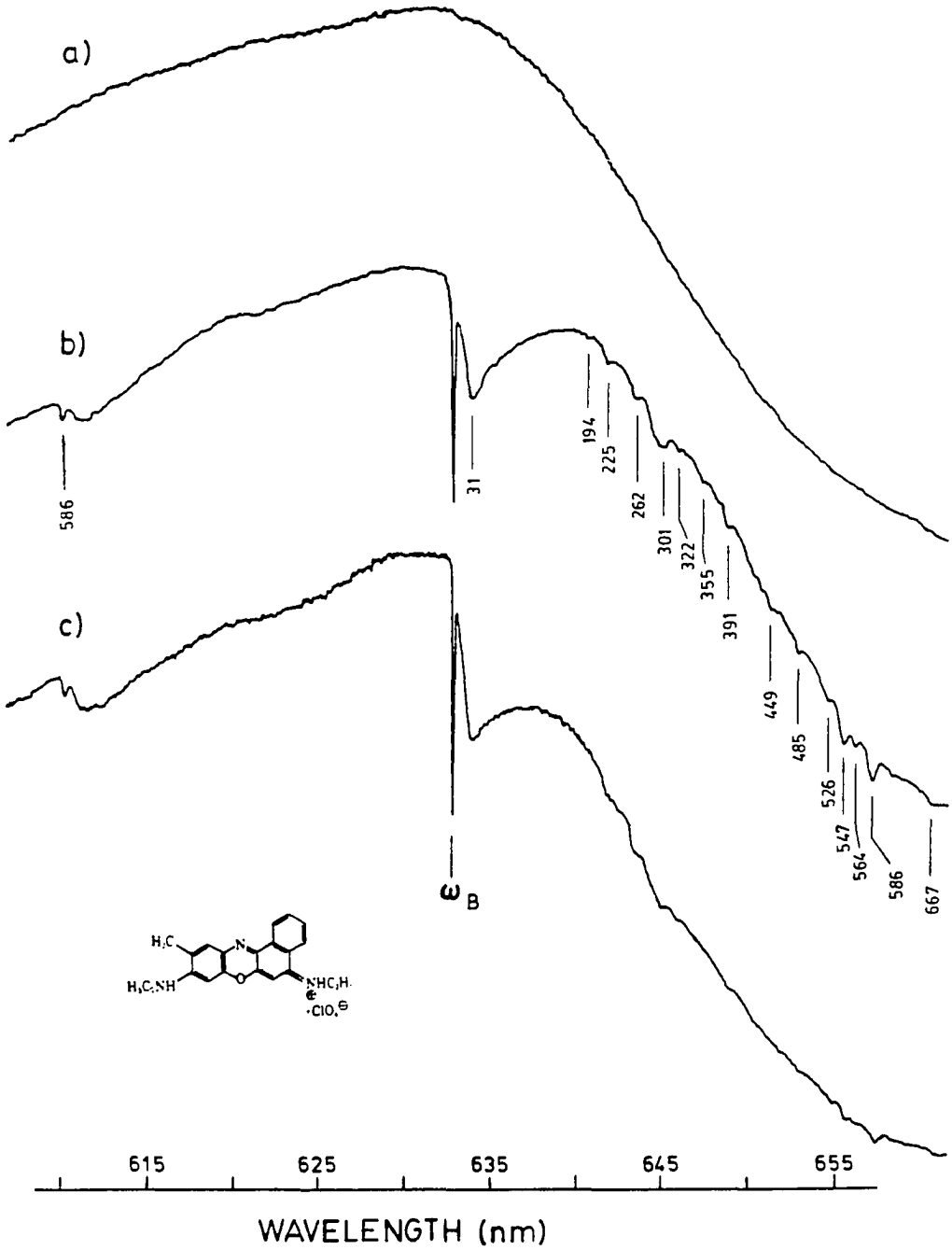
a)
b)
c)
586
31
194
225
262
301
322
355
391
449
485
526
547
564
586
667
ε B
615
625
635
645
655
WAVELENGTH (nm)

the vibrational sublevel of S_1.

The optical dephasing of cresyl violet in PVOH has been studied with the He-Ne laser at 632.8 nm (15803 cm^{-1}) [23]. In the course of this work, we determined that at 632.8 nm the saturated [24] hole intensity represents about a 50% optical density change. Using an approach identical to that found in [15] we estimated the NPHB quantum yield (average) to be ~ 10^{-2}.

The hole burned spectra in Figure 2 are for nile blue perchlorate in a)PVOH and b)PAA at a burn and recording temperature T = 5 K. Again, a rich vibronic satellite structure is observed which is essentially identical in the two polymers and is a signature for nile blue. The satellite holes labeled with vibronic frequencies are reproducible.

Finally, in Figure 3 we show the NPHB spectra for oxazine 720 perchlorate in PVOH for a) and b) and in PAA for c) all burned with a He-Ne laser. At saturation, the optical density change associated with the ω_B zero-phonon hole ~ 40%. The vibronic satellite structure is broader and less pronounced than in Figures 1 and 2. Note, however, the pronounced zero-phonon hole at 586 cm^{-1} to higher energy from ω_B, indicating there exists an appreciable number of sites with their origin transition at ω_B, which is approximately 800 cm^{-1} from the onset of the inhomogeneous distribution.

CONCLUSION

Ionic dye molecules in hydroxylated polymers exhibit efficient NPHB and rich vibronic satellite hole structure. Further, the systems studied thus far are characterized by linear electron-phonon coupling which is sufficiently weak to permit temperature dependent optical dephasing studies based on the zero-phonon hole profile. The observed efficiencies are sufficiently high to make this class of mixed polymer systems ideal for a wide range of studies targeted toward a better understanding of phonon assisted tunneling processes and disorder in polymers. Because of the high optical quality of the polymers it is hoped that photon echo experiments will prove feasible [25].

Although certain aspects of NPHB are fairly well understood, the criteria for efficient NPHB are not. This is a difficult problem because at the very least one must consider the microscopic disorder, electron-TLS coupling strength, the spatial extent and distribution of TLS and specific intermolecular interactions. For the systems considered here it may be that the ionic dye plays an important role, for NPHB of cresyl violet in a glycerol:water glass is also efficient [26]. On the other hand, NPHB of non-polar impurities in non-polar polymers has proven to be very inefficient [16,26]. Thus, it still appears to be that systems with extended hydrogen bonding networks form a class which is promising for efficient NPHB.

REFERENCES

1. J. M. Hayes and G. J. Small, Chem. Phys. 27, 151 (1978).

2. J. M. Hayes and G. J. Small, Chem. Phys. Lett. 54, 435 (1978).

3. J. M. Hayes, R. P. Stout and G. J. Small, J. Chem. Phys. 74, 4266 (1981).

4. G. J. Small in: "Modern Problems in Solid State Physics. Molecular Spectroscopy", V. M. Agranovich and R. M. Hochstrasser, eds., North-Holland: Amsterdam, 1983.

5. P. W. Anderson, B. I. Halperin and C.M. Varma, Philos. Mag. 25, 1 (1972).

6. W. A. Phillips, J. Low Temp. Phys. 7, 351 (1972).

7. In a number of systems holes have been observed to persist unchanged for many hours provided the sample is maintained at or below the burn temperature; see [4].

8. J. M. Hayes, R. P. Stout and G. J. Small, J. Chem. Phys. 73, 4129 (1980).

9. S. K. Lyo and R. Orbach, Phys. Rev. B 22, 4223 (1980).

10. P. Reineker and H. Morawitz, Chem. Phys. Lett. 86, 359 (1984).

11. S. K. Lyo, Phys. Rev. Lett. 48, 688 (1982).

12. R. M. Macfarlane and R. M. Shelby, Opt. Commun., 45, 46 (1982).

13. A number of systems exhibit close to a T^2 dependence from very low T to $\geq$ 300 K; see [12] for references to studies from M. A. El-Sayed's and W. M. Yen's laboratory.

14. E. Cuellar and G. Castro, Chem. Phys. 54, 217 (1980).

15. R. Jankowiak and H. Bassler, Chem. Phys. Lett., 95, 124 (1983).

16. B. L. Fearey, R. P. Stout, J. M. Hayes and G. J. Small, J. Chem. Phys. 78, 7013 (1983).

17. And in a hydrogen bonded single crystal; see R. W. Olson, H. W. H. Lee, F. G. Patterson, M. D. Fayer, R. M. Shelby, D. P. Burum and R. M. Macfarlane, J. Chem. Phys. 77, 2283 (1982).

18. See "Topics in Current Physics", Vol. 24, W. A. Phillips, ed. Springer-Verlag: Berlin, 1981.

19. H. Thijssen, S. Volker, M. Schmidt and H. Port, Chem. Phys. Lett. 94, 53 (1983).

20. A. Gorokhovski, J. Kikas, V. Pal'm and L. A. Rebane, Solid State Phys. 23, 1040 (1981).

21. F. Burkhalter, G. Suter, U. Wild, V. D. Samoilenko, N. Rasumova and R. I. Personov, Chem. Phys. Lett. 94, 483 (1983).

22. J. Friedrich, J. D. Swalen and D. Haarer, J. Chem. Phys. 73, 705 (1980).

23. T. P. Carter, B. L. Fearey, J. M. Hayes and G. J. Small, Chem. Phys. Lett. 102, 272 (1983).

24. With NPHB, only a subset of the total number of impurity-TLS systems absorbing at ω_B undergo hole burning at any given T_B; see [4].

25. Such experiments are planned in collaboration with A. Zewail and co-workers.

26. T. P. Carter, B. L. Fearey and G. J. Small, Ames Laboratory and Iowa State University, unpublished results.

PAPER III.

NEW STUDIES OF NONPHOTOCHEMICAL HOLES OF DYES AND RARE EARTH IONS IN POLYMERS. II. LASER INDUCED HOLE FILLING

NEW STUDIES OF NONPHOTOCHEMICAL HOLES OF DYES AND RARE EARTH IONS IN POLYMERS. II. LASER INDUCED HOLE FILLING

T. P. CARTER, B. L. FEAREY and GERALD J. SMALL

Ames Laboratory-USDOE and Department of Chemistry
Iowa State University, Ames, Iowa 50011

Chemical Physics 101, 279 (1986)

INTRODUCTION

In a previous paper, spontaneous hole filling of rhodamine 640 (R640), Nd^{3+} and Pr^{3+} in poly(vinyl alcohol) (PVOH) were presented and discussed [1]. Here, we are concerned with the phenomenon of laser induced hole filling as it occurs in the same and other systems. By LIHF we mean the partial or complete filling of a hole burned at ω_{B1} which results from subsequent laser irradiation at a frequency removed from ω_{B1}. Interestingly, LIHF is the least studied aspect of hole burning in amorphous hosts even though it may be the most intriguing. The first LIHF experiment was performed on tetracene in an ethanol/methanol glass in order to argue that the hole burning mechanism is nonphotochemical (photophysical) rather than photochemical in nature [2]. It is conceivable that LIHF can also occur for photochemical holes burned in glassy hosts. Undoubtedly, LIHF and hole erasure due to white light irradiation are related phenomena. Gutierrez **et al.** [3] have studied the latter for quinizarin in the ethanol/methanol glass. White light erasure has also been observed by us [4] for cresyl violet perchlorate (CV) in PVOH. It is important to note that we do not ascribe LIHF or white light erasure to a bulk heating effect. It is easy to identify and, consequently prevent interference due to thermal erasure since it is generally accompanied by spectral diffusion and hysteresis whose T-dependences can be characterized by separate thermal erasure (thermal cycle) experiments [5,6].

Returning to the tetracene in ethanol/methanol glass system, it was reported that significant LIHF occurs only when the second irradiation

frequency lies within ~ 2 cm^{-1} of the primary hole at ω_{B1} [2]. Although a mechanism for LIHF was not given, it might be inferred that the LIHF is due to reversion of originally burned impurity-TLS sites back to their configurations prior to the burn (presumably due to excitation of anti-hole sites). LIHF due to reversion following excitation of anti-holes has been firmly established for pentacene in benzoic acid crystals [7,8].

Following the observation [9,10] that LIHF for CV in PVOH is facile for secondary irradiation frequencies (ω_{B2}) far removed from ω_{B1} ($|\omega_{B2} - \omega_{B1}| \simeq 100$ cm^{-1}), it was decided to study the phenomenon in far greater detail. Given the large inhomogeneous absorption linewidths of dyes in polymers (500-1000 cm^{-1}) and apparent large widths of the anti-holes (~ 100 cm^{-1} [1]), the above observation for CV/PVOH suggested that reversion resulting from anti-hole excitation may not be the dominant mechanism for LIHF in dye/polymer systems. Other possibilities include a mechanism based on spectral diffusion which depends on connectivity between the different TLS of the polymer which couple to the impurity. That is, secondary irradiation (or the resulting hole formation) may trigger configurational changes at impurity-TLS sites which are spatially removed from those involved in the primary burn or the secondary light absorption process. Another possibility is that LIHF can result from intermolecular energy transfer. To begin to understand the LIHF process it was judged important to first determine relative LIHF efficiencies as a function of the sign and magnitude of $\omega_{B1} - \omega_{B2}$ while, at the same time, to ascertain whether LIHF is accompanied by broadening of the primary hole. The results of such studies on R640,

Nd^{3+} and Pr^{3+} in PVOH are reported. These data prompted us to perform LIHF experiments on the mixed dye system of rhodamine 560 (R560) and CV in PVOH. These experiments speak to the question of intermolecular energy transfer and the results of such are also reported and discussed.

EXPERIMENTAL

Experimental details are given in [1]. Here we present the protocol for the LIHF experiments. The basic procedure for studying LIHF is analogous to the SPHF experiments. First, the initially burned hole ωB_1 was repeatedly scanned as in [1] with zero time being measured from the end of the initial burn. This then was followed by the fill burn ω_{B2} (noting the time at the end of this burn) and again the initial hole was repeatedly scanned. Typical results following the above procedure are shown in Figures 1 and 2. Once the quantity of spontaneous hole filling is established and shown to be a constant from sample to sample [1]), then by ensuring that further LIHF experiments follow a set sequencing and time scale, the SPHF can easily be removed from any additional studies of LIHF for each system. It should be pointed out that, in most cases, each set of data represents an "identical" unique sample (samples reproducibly prepared and cooled were found to yield identical results from sample to sample [1,9]), which allows for many similar experiments to be performed in a single run, such as where one burns a new initial burn at ω_{B1} for each sample followed by a different ω_{B2} for each.

Figure 1. LIHF of R640 in PVOH at 1.7 K. Burns were performed with a ring dye laser using a flux of 1 mW/cm^2; the sample was burned for 75 sec. at ω_{B1} = 582.5 nm. The data points show the measured hole areas as a function of time. The dashed lines are fits for the spontaneous hole filling contribution as in [1]. The sharp discontinuity at 800 sec. is the result of the secondary burn at ω_{B2} = 576.2 nm for 250 sec., corresponding to a laser induced filling of 12%

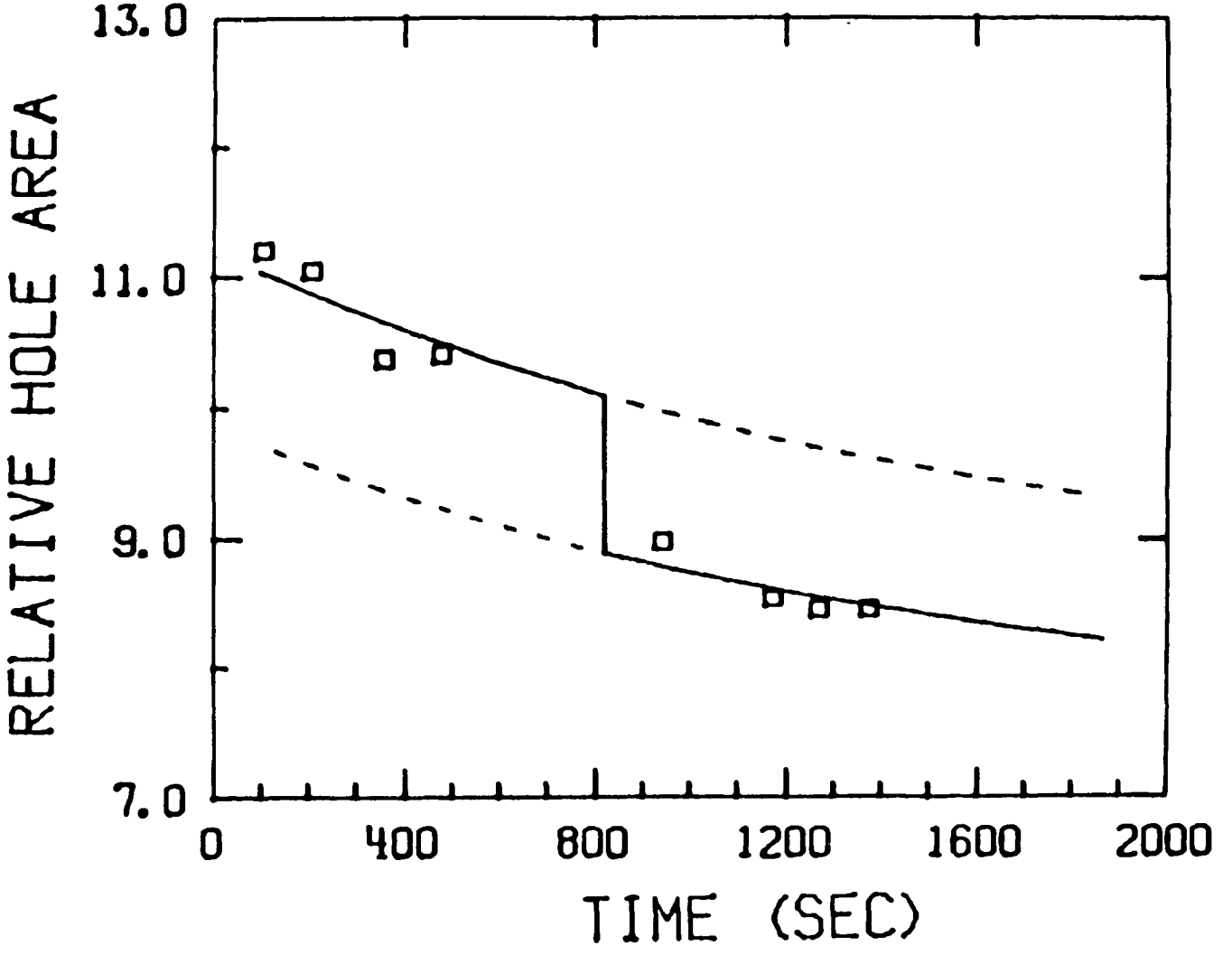
13.0
11.0
9.0
7.0
RELATIVE HOLE AREA
0
400
800
1200
1600
2000
TIME (SEC)

Figure 2. LIHF of R640 in PVOH at T = 1.7 K with ω_{B1} = 582.5 nm and ω_{B2} = 588.9 nm. The data points indicate the measured holes. Burn fluxes and times are as in Figure 1. Under these conditions, the hole has filled 6%

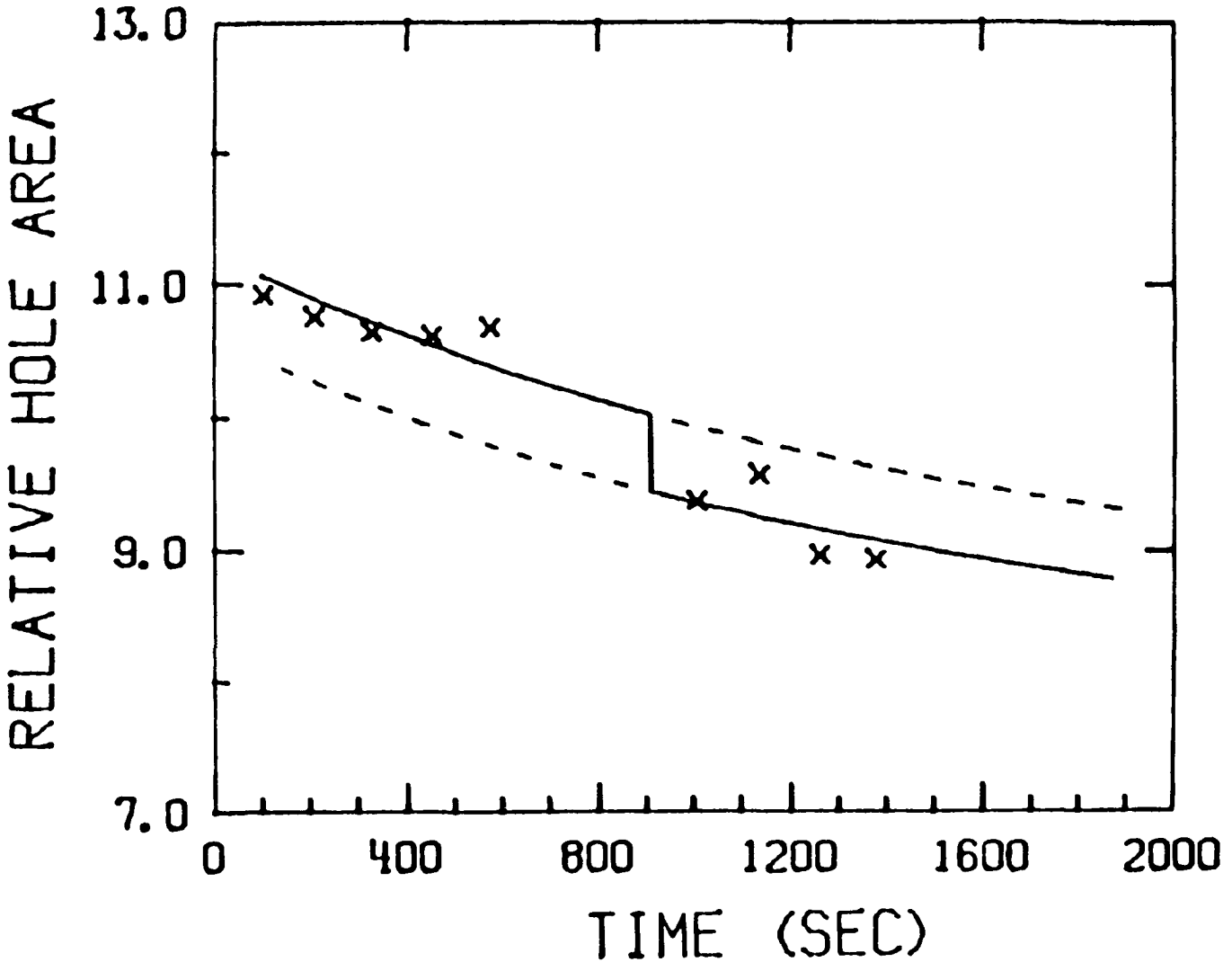
13.0
11.0
9.0
7.0
RELATIVE HOLE AREA
0
400
800
1200
1600
2000
TIME (SEC)

RESULTS AND DISCUSSION

Rhodamine 640 in Poly(Vinyl Alcohol)

A nonphotochemically hole burned spectrum of R640 in PVOH is shown in [1] where SPHF data are presented and discussed. Because SPHF occurs during the time scale of the LIHF experiments, it was essential to subtract out the contribution of SPHF to the filling. The results of [1] allow this to be done in a reliable manner. Two examples of how this was accomplished are shown in Figures 1 and 2. Both figures are derived from a primary burn at ω_{B1} = 582.5 nm with secondary irradiation frequencies at ω_{B2} = 576.2 and 588.9 nm for Figures 1 and 2 respectively. Burn times and intensities are indicated in the figure captions. It should be noted that the vertical segment of the solid line in each figure indicates the time at which the ω_{B2} irradiation terminates. Prior to and following the ω_{B2} irradiation, the SPHF is monitored and the primary hole decay fit to the equation

$$I(t) - I(\infty) \propto \exp(-Kt) \; . \quad (1)$$

Here, I(t) and I(∞) are the integrated hole areas at time t and at infinite time and the parameters are determined by a least squares fit. Good agreement for the SPHF parameters with those reported in [1] was found. Thus the dashed line extensions are calculated. The difference between the upper and lower curves in each figure yield the percent hole filling due only to LIHF. These percentages for Figures 1 and 2 are 12% and 6%, respectively. Therefore, LIHF for R640/PVOH is significantly

more facile when $\omega_{B2} > \omega_{B1}$ than when $\omega_{B2} < \omega_{B2}$. Still, the observation that LIHF does occur for the latter case is important.

Figure 3 summarizes the results of our 1.7 K LIHF studies on R640/PVOH. The arrow at ω_{B1} locates the primary burn frequency (582.5 nm) and the smaller arrows locate the secondary irradiation frequencies, ω_{B2}. For each and every ω_{B2}, a fresh primary hole at ω_{B1} was burned for 75 sec. with a burn flux of 1 mW/cm^2. The same flux was also used for all ω_{B2} irradiations. Focusing on the small arrow near 594.5 nm, the X, o and + percent hole area change (filling) data points correspond to ω_{B2} irradiation times of 75, 150 and 225 sec, respectively. We note that for the burn flux and times utilized, the zero-phonon holes were not saturated (**i.e.**, were not burned to maximum depth) and that phonon side bands and vibronic satellite holes were not observed. Separate thermal annealing and thermal cycle experiments confirmed that hole filling from bulk heating does not contaminate the data. Specifically, when a sample which had been burned at 1.7 K was raised rapidly to some higher temperature (T_h) and then promptly recooled to 1.7 K, significant hole broadening was observed when the resultant hole filling was comparable to that in LIHF experiments. For example, for filling of ~ 10% (T_h = 10 K), a broadening of ~ 20% occurred. This is in marked contrast to LIHF, where no broadening is observed.

The absence of bulk heating is also consistent with one of the two most striking aspects of the data in Figure 3, the "discontinuity" or step in LIHF efficiency which occurs at ω_{B1}. The second is the apparent insensitivity of the LIHF facility to ω_{B2} on both the low and high energy sides of ω_{B1}. Clearly, LIHF facility is not obviously related to

Figure 3. LIHF of R640 in PVOH as a function of filling frequency. The initial burn at ω_{B2} = 582.5 nm was burned with 1 mW/cm^2 for 75 sec in each experiment. A new sample and initial hole was burned for every different ω_{B2} which are marked by the arrows. The observed percent hole area changes versus secondary burn frequency are marked by the points; different symbols denote different secondary burn times. Crosses indicate 75 sec., circles 150 sec. and plusses 225 sec

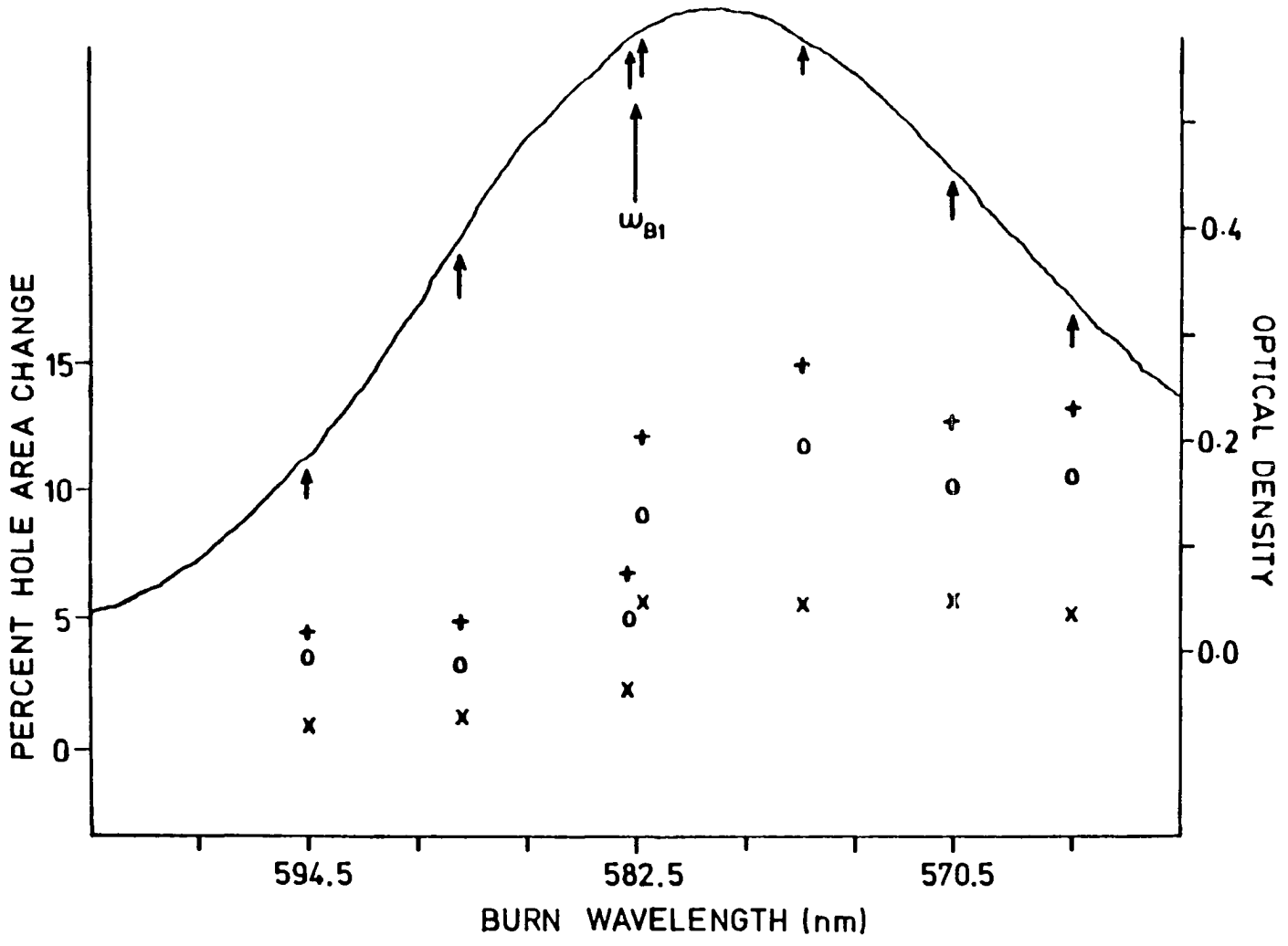
PERCENT HOLE AREA CHANGE
15
10
5
0
ω_{B1}
0·4
0·2
0·0
OPTICAL DENSITY
594.5
582.5
570.5
BURN WAVELENGTH (nm)

optical density at ω_{B2}. A third important observation is that LIHF of the primary hole occurs without hole broadening. Our linewidth measurements are accurate to within ~ 6% and the FWHM of the initial holes burned at 582.5 nm was constant at 0.45 cm^{-1} for T = 1.7 K.

An obvious question is whether the LIHF of the primary hole is the result of the secondary hole formation at ω_{B2} itself rather than just absorption of ω_{B2} irrespective of hole burning. The data in Figure 4 speak to this question and were obtained with a burn flux ~ 1 mW/cm^2 and a burn time of 75 sec. The dependence of the zero-phonon hole burning efficiency on ω_{B1} is shown to decrease in a linear fashion with increasing ω_{B1}. In comparing Figures 3 and 4, ω_{B1} = 582.5 nm corresponds to 17167 cm^{-1}. In the LIHF experiments, the secondary holes at ω_{B2} were also monitored and these results along with those of Figure 4 show that LIHF efficiency is not simply related to the intensity (depth) of the secondary hole. This point will be returned to later. One final point is that the hole profiles corresponding to the different data points in Figure 4 exhibit the same FWHM (0.45 cm^{-1}).

Because of their possible connection with the data of Figure 3, the data of Figure 5 are presented. Figure 5 shows the percent hole depth (ω_{B1} = 594.5 nm) for R640/PVOH as a function of burn flux at a constant fluence. The manner in which the hole depth initially decreases with increasing flux and then plateaus is similar to that observed by Romagnoli **et al.** [11] for phthalocyanine. In their work, the flux dependence was nicely explained in terms of a population bottleneck due to the lowest triplet state. Intersystem crossing from S1 of phthalocyanine has a very high quantum yield. This, however, is not the

Figure 4. Hole burning efficiencies as a function of burn frequency for R640 in PVOH. Holes were burned with 1 mW/cm^2 for 72 sec. at 1.7 K. Hole depth is expressed as a percentage of the initial (unburned) optical density

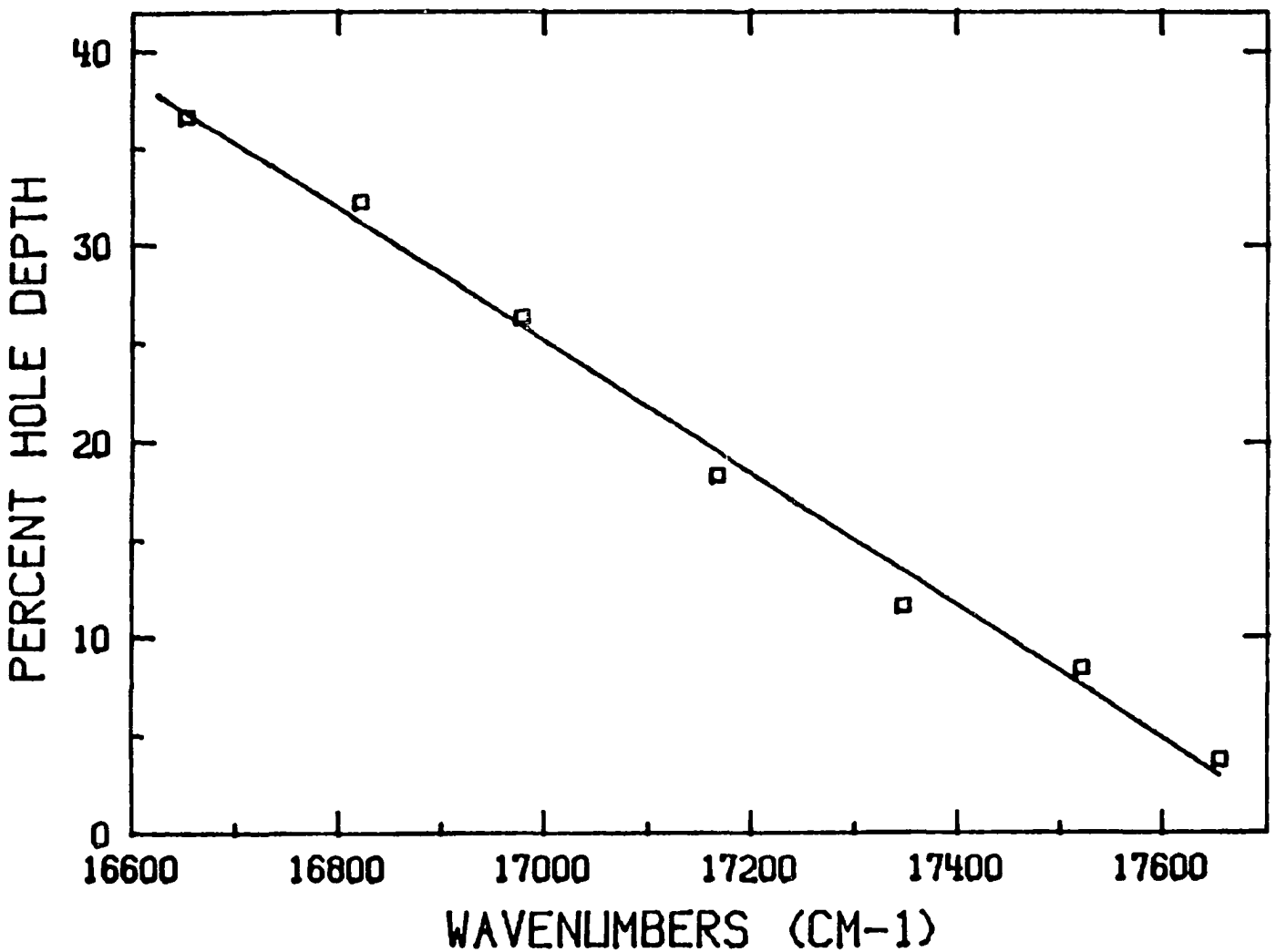
PERCENT HOLE DEPTH
40
30
20
10
0
16600
16800
17000
17200
17400
17600
WAVENUMBERS (CM-1)

case for R640. A likely candidate for the bottleneck of R640/PVOH is the subset of R640-TLS sites which undergo the initial step of hole burning in the excited electronic state but which undergo ground state tunneling back to their original configurations during the course of the burn. That this might occur is not surprising in view of the SPHF results of [1]. It would be worthwhile to determine whether the saturation behavior of Figure 5 can be explained by a simple dispersive kinetic model.

Binary Dye Mixture in Poly(Vinyl Alcohol)

The data in Figure 3 for R640/PVOH and similar data for Nd^{3+} and Pr^{3+} in PVOH (**vide infra**) show that LIHF occurs for $\omega_{B2} < \omega_{B1}$. The mechanism for LIHF when $\omega_{B2} < \omega_{B1}$ cannot be due to intermolecular energy transfer (spatial diffusion) between R640 sites. The step function behavior at ω_{B1} in Figure 3 might suggest that a second mechanism for LIHF is operative for $\omega_{B1} > \omega_{B2}$. One possibility is intermolecular energy transfer from sites at ω_{B2} to lower energy anti-hole sites produced by the burn at ω_{B1}. Within the TLS model [6,12,13], this means that reversion (by phonon assisted tunneling) from the excited state of the anti-hole tunnel state occurs. LIHF would then be viewed as an excited electronic state process.

We have explored this possibility by performing LIHF on a binary mixture of CV and rhodamine 560 (R560) in PVOH. Their absorption spectra exhibit minimal overlap [λ_{max}(CV) = 610 nm; λ_{max}(R560) = 510 nm] but the fluorescence spectrum of R560 provides an excellent match for the absorption spectrum of CV. Thus, for the concentrations involved,

Figure 5. Hole depth of R640 as a function of burn flux at a constant fluence (i.e. burn power and irradiation time both varied, keeping the total number of photons a constant) of 75 mJ

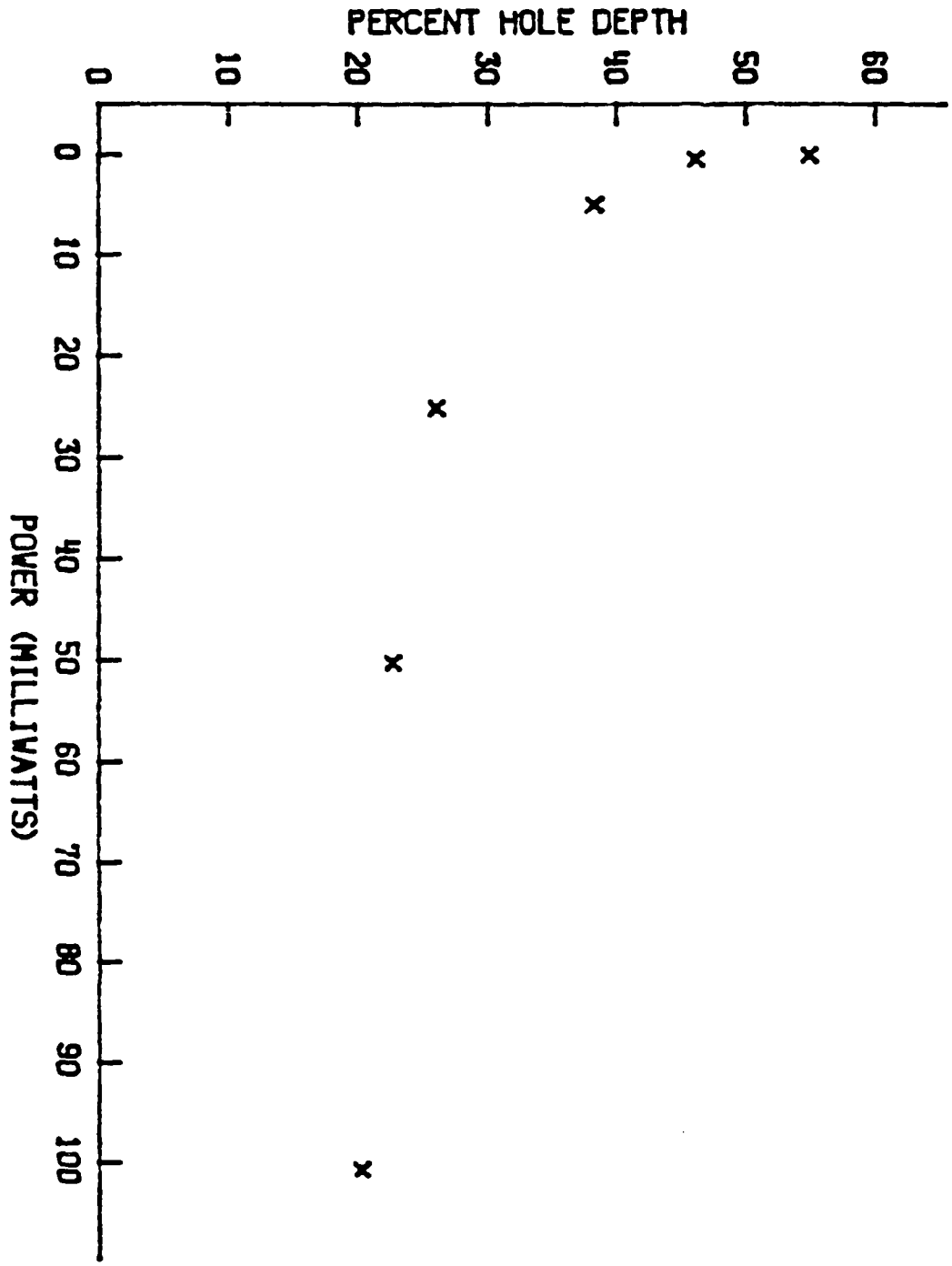
PERCENT HOLE DEPTH
0
10
20
30
40
50
60
POWER (MILLIWATTS)
0
10
20
30
40
50
60
70
80
90
100

the probability for Forster energy transfer is maximized [14].

The results of the experiments are given in Table I. The conditions used to obtain the data are similar to those used for the R640 experiments. Samples were immersed in pumped helium (T = 1.7 K) and all burns were performed with a flux of ~ 1 mW/cm^2. The burn times are indicated in Table I. The ω_{B1} burn times for R560 are longer than for CV because the NPHB facility of the former is lower. In order to obtain good results, a reasonably deep primary hole is required. For clarity, the order in which the primary and secondary burns were performed is depicted in the crude spectra included in Table I. The four sections of the table will be referred to as rows 1-4 (starting with **mixed dye** at the top). Further, numbers in parentheses refer to the percent hole depth following a burn while the numbers in brackets refer to the percent of the initial hole depth which is lost after the secondary burn at ω_{B2}.

Inspection of the data in rows 1 and 2 show that energy transfer is not involved in LIHF for the mixed dye system. Note that the protocols for rows 1 and 2 are identical except that for row 2 the R560 dye is absent. That is, the 15% LIHF is the same whether or not this dye is present. We hasten to add that for both samples the optical density of CV at ω_{B2} = 514.5 nm was 0.08. Consider next rows 3 and 4 which correspond to a sequence opposite to the above. For both rows, the primary burn (ω_{B1}) is in the R560 profile. The only difference between rows 3 and 4 is that the sample used for the latter contained no CV. Thus, the presence of CV appears to reduce the LIHF for the primary hole in R560. One additional point from Table I is that the presence of the

Table I. Mixed dye data. See text for explanation

System Studied \ Lambda Burn	(R560) 514.5 nm	(CV) 617.0 nm	Schematic Spectrum
Mixed Dye ω_{B_1} = 617.0, t_1+		(27)*	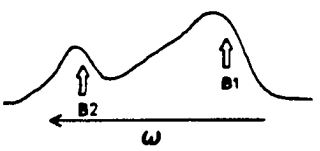
ω_{B_2} = 514.5, t_1	(10)	[15]**	
CV Dye ω_{B_1} = 617.0, t_1		(27)	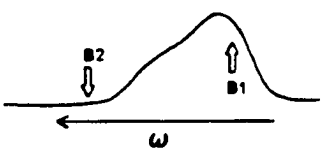
ω_{B_2} = 514.5, t_1		[15]	
Mixed Dye ω_{B_1} = 514.5, t_2++	(16)		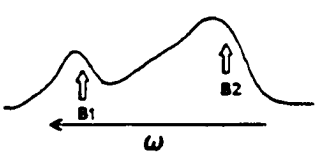
ω_{B_2} = 617.0, t_1	[7]	(28)	
R560 Dye ω_{B_1} = 514.5, t_2	(13)		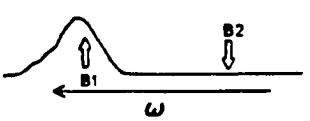
ω_{B_2} = 617.0, t_1	[13]		

* () = percent burn hole depth.
** [] = percent fill of initial hole.
\+ t_1 = 75 second burn time.
++ t_2 = 225 second burn time.

second dye does not seem to affect the hole burning efficiency of the other.

Nd3+ and Pr3+ in Poly(Vinyl Alcohol)

The optical transitions of Nd^{3+} and Pr^{3+} which were studied were the $(^2G_{7/2}, ^4G_{5/2}) \leftarrow {}^4I_{9/2}$ transitions of Nd^{3+} and the $^1D_2 \leftarrow {}^3H_4$ transition of Pr^{3+}. Hole burning was performed on the lowest energy J component of each transition. In fact, attempts to hole burn the higher energy components were not successful, presumably due to their rapid radiationless decay [15].

The experimental procedure used for LIHF was essentially identical to that used for R640/PVOH. Figure 6 shows the result of one LIHF run for Nd^{3+} which is of the type shown in Figures 1 and 2 for R640. We note that high rare earth ion (RE^{3+}) concentrations corresponding to a number density of ~ 10^{21} cm^{-3} or to an average interionic separation of ~ 1 nm were employed. The LIHF results for Pr^{3+} and Nd^{3+} are shown in Figures 7 and 8. The indicated LIHF (filling) percentages are corrected for SPHF. The numbers in square brackets correspond to the percent optical density change due to hole burning at the indicated burn frequencies. The numbers without brackets correspond to the percent filling of a hole due to subsequent irradiation at some ω_{B2}. With reference to trace b) of Figure 7, irradiation at ω_{B2} produces a 17% hole at ω_{B2} while filling the ω_{B1} hole by 4%. Similarly, trace c) shows that irradiation at ω_{B3} fills the hole at ω_{B2} by 15%. Trace d) was obtained with secondary irradiation at 594.0 nm which is in the second J component of the transition.

Figure 6. LIHF of Nd^{3+} in PVOH with ω_{B1} at 579.0 nm and ω_{B2} at 578.75 nm; both burns were for 10 min. with 100 mw/cm^2. The triangles give the measured hole depth; the hole was "read" four times before the secondary burn and four times after, to determine the SPHF contribution shown as the solid lines. The vertical discontinuity is the result of the secondary burn at t = 1350 sec. and corresponds to a 15% change in hole depth

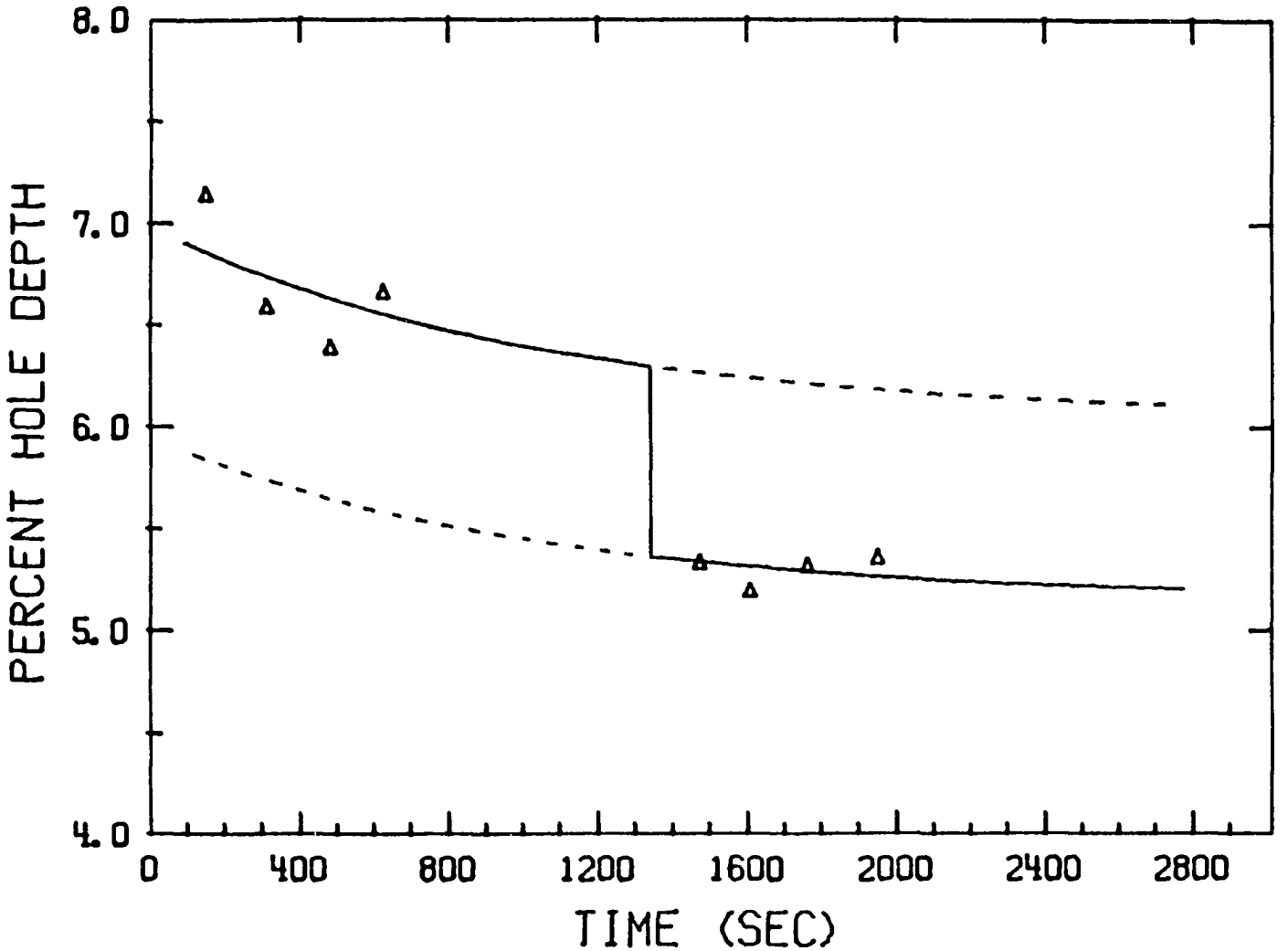
8.0
7.0
6.0
5.0
4.0
PERCENT HOLE DEPTH
0
400
800
1200
1600
2000
2400
2800
TIME (SEC)

From Figure 7, we conclude that for Pr^{3+} in PVOH, LIHF is significantly more efficient when the secondary irradiation frequency is displaced to higher energy from the hole being filled, as is the case for R640 in PVOH. Another similarity is that the LIHF does not broaden the hole being filled.

The absence of broadening accompanying LIHF is also observed for Nd^{3+} in PVOH. However, this system behaves in a qualitatively different manner than Pr^{3+} or R640 in that the LIHF is more efficient for a secondary irradiation lying to the red of the hole being filled. We return to this point later.

Finally, we have performed preliminary experiments on a binary mixture of Nd^{3+} and Pr^{3+} in PVOH. More extensive measurements are planned, but the results obtained indicate that $Nd^{3+}(^2G_{7/2}, ^4G_{5/2}) \rightarrow Pr^{3+}(^1D_2)$ energy transfer is not an efficient mechanism for filling of Pr^{3+} holes. This may occur, however, because the $^2G_{7/2}$ and $^4G_{5/2}$ states of Nd^{3+} possess a very short lifetime [16].

The Puzzle

We begin by summarizing the key results from the preceding section. They are:

1) LIHF of a primary hole at ω_{B1} occurs for both $\omega_{B2} > \omega_{B1}$ and $\omega_{B1} < \omega_{B1}$.

2) Except for Nd^{3+} the LIHF efficiency for $\omega_{B2} > \omega_{B1}$ is significantly greater than that for $\omega_{B2} < \omega_{B1}$.

3) For R640 the LIHF efficiency exhibits a step behavior at ω_{B1}. The dependence of the LIHF efficiency on $|\omega_{B2} - \omega_{B1}|$ is weak.

Figure 7. Hole burning and LIHF data for Pr^{3+} in PVOH. All burns were performed using 100 mW/cm^2 for 10 min. The figure shows a portion of the Pr^{3+} $^1D_2 \leftarrow {}^3H_4$ transition. Trace a) shows the primary hole; trace b) shows the result after burning again but to lower energy; trace c) is the result after still another burn but to higher energy from both a) and b); trace d) is the result after burning again but into another transition at 594.0 nm. The bracketed numbers are the initial percent hole depths and the unbracketed numbers are the percentage hole filling values due to the previous burn. The experiment was performed at 1.7 K

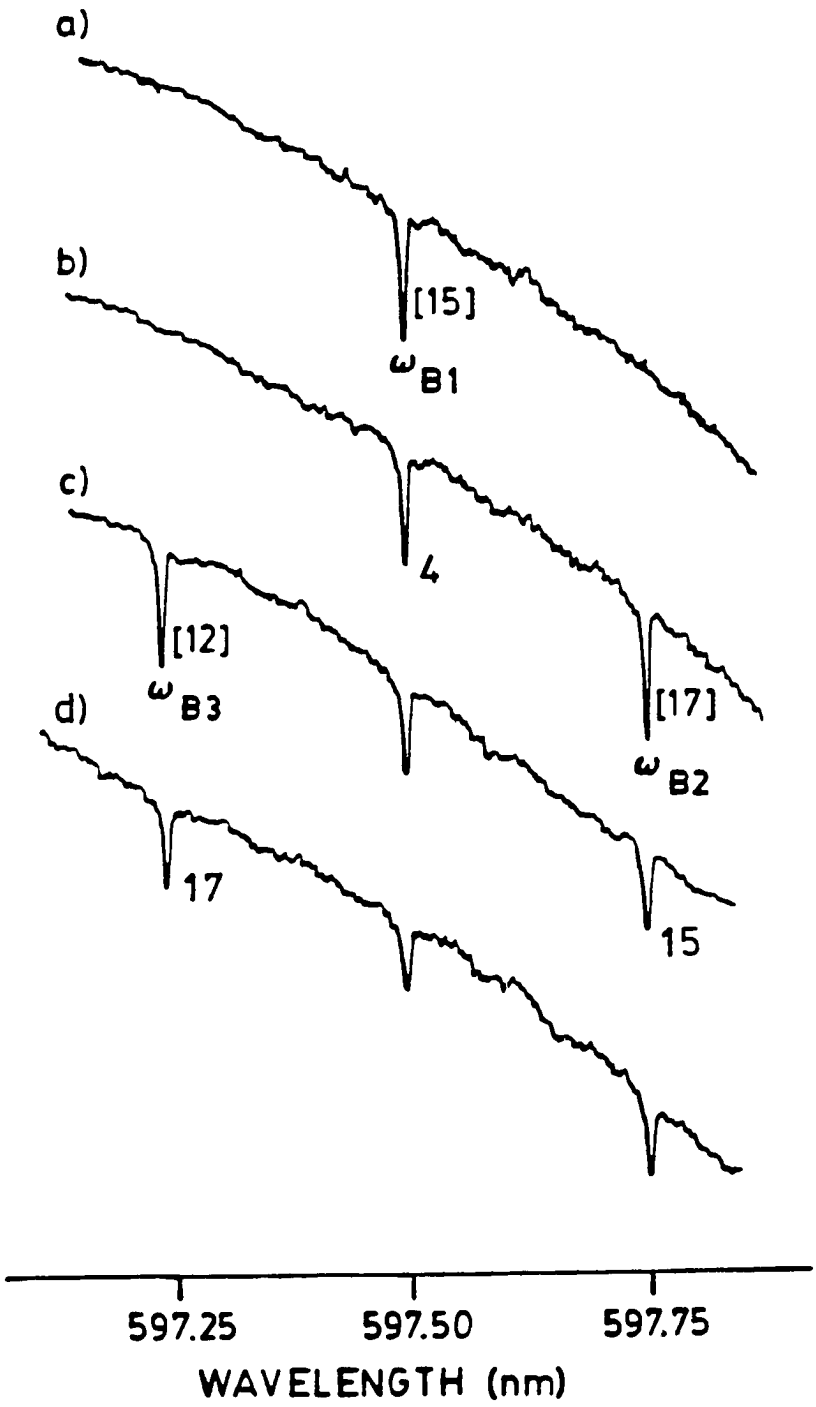
a)
b)
[15]
ω_{B1}
c)
4
[12]
ω_{B3}
[17]
ω_{B2}
d)
17
15
597.25
597.50
597.75
WAVELENGTH (nm)

Figure 8. Hole burning and LIHF of Nd^{3+} in PVOH at 1.7 K. Trace a) shows a ω_{B1} hole burned into the $(^2G_{7/2}, ^4G_{5/2}) \leftarrow {}^4I_{9/2}$ transition; trace b) shows the result after burning again to lower energy; trace c) shows the further result after burning again but to higher energy from ω_{B1}. The numbers in brackets are the initial (unfilled) percentage hole depths and the unbracketed numbers are the percentage hole filling values due to the previous burn. All holes were burned with 100 mW/cm^2 for 10 min

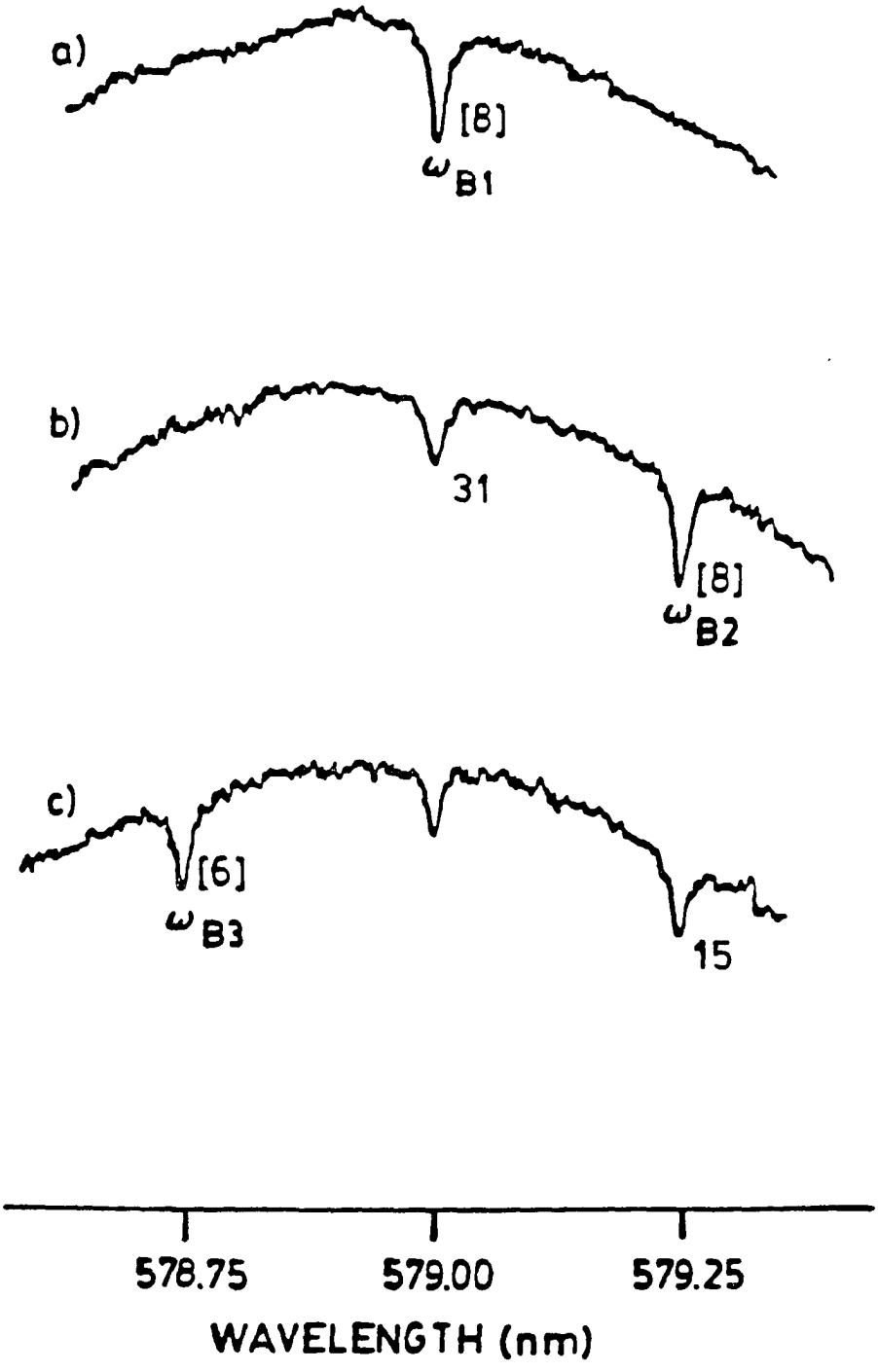
a)
[8]
ω_{B1}
b)
31
[8]
ω_{B2}
c)
[6]
ω_{B3}
15
578.75
579.00
579.25
WAVELENGTH (nm)

4) LIHF does not produce any perceptible broadening of the primary hole (within our holewidth measurement accuracy, ~6%).

In reference to result 2, the behavior of R640 and Pr^{3+} has also been observed for chlorophyll **a** [17], chlorophyll **b** [17,18] and the self-aggregated dimer of chlorophyll **a** [19] in polystyrene films. With regard to result 1, the observation that LIHF is operative for $\omega_{B2} < \omega_{B1}$ establishes that a mechanism for filling other than intermolecular energy transfer (ET) exists.

Taken as a whole, the above results present an intriguing puzzle. An attempt will be made to explain them but first we argue against a number of possibilities as plausible significant mechanisms for LIHF.

In doing so, we recall that the anti-holes associated with the primary burn can, in principle, lie to higher and lower energy of ω_{B1} and must be very broad relative to the zero-phonon hole width [1,20,21]. Furthermore, the conditions of the LIHF experiments (**e.g.**, narrow line excitation) show that the LIHF is surprisingly efficient when the large inhomogeneous profiles in absorption and the large anti-hole width (relative to the laser line width) are considered. This, together with the insensitivity of LIHF to $|\omega_{B2} - \omega_{B1}|$ (result 3 above) precludes direct anti-hole site excitations followed by reversion to original (pre-burn) configurations as a likely mechanism [2]. This line of argument also eliminates local heating as a plausible mechanism. A third possibility is ET. In view of the CV/R560 in PVOH results and the insensitivity of LIHF efficiency to ω_{B2} when $\omega_{B2} > \omega_{B1}$ (see Figure 3), we are inclined to reject ET as a significant contributor. The CV/R560 results also rule out a trivial emission-reabsorption (the "white light" erasure) mechanism.

It follows that LIHF cannot be understood by a local (simple) impurity-TLS model. By local, we mean that model which is typically used to explain the phenomenon of nonphotochemical hole production itself [2,6]. In this model, each impurity undergoing hole burning is associated with a single two level system and connectivity (communication) between different impurity-TLS is not considered. It leads naturally to the notion that LIHF is due to a reversion process occurring in isolated impurity-TLS. Nor can the simple impurity-TLS model account for hysteresis effects in NPHB thermal cycle experiments.

A Tentative Model for LIHF

The glassy state which we associate with glasses and polymers depends on how that state was prepared. Prior to a burn there are points in configuration space which are thermally accessible to the initially prepared state. The simple TLS model was designed to describe this state of affairs [2,6]. With this in mind, NPHB leading to stable holes can be viewed as a process which produces a glassy state which is thermally inaccessible to the pre-burn state. In our view, LIHF or thermal erasure of a hole in excitation frequency space should not be viewed as a return of the system to its original state. Rather, both are likely irreversible in nature, given the essential continuum of glassy configurations which exist.

An obvious difficulty with the TLS model as it is applied to most systems is that something as fundamental as the spatial extents of the TLS are not known. Without this information for the host (intrinsic TLS) and those which may be introduced by the impurity (extrinsic TLS),

the concept of TLS connectivity is impossible to quantify. Nevertheless, we proceed to explore a model for LIHF which is based on the premise that filling involves communication between impurity sites excited by the secondary irradiation and those which are not and are, therefore, spatially removed from the sites in resonance with the primary burn. In doing so, we pursue the idea that we can divide the TLS distribution into two sets, one whose members are weakly coupled to the impurity and the others whose members are strongly coupled [22]. For convenience we refer to the former as intrinsic and the latter as extrinsic. The extrinsic TLS would include those which lead to hole formation by phonon-assisted tunneling. Their spatial extent may be considered as localized relative to the intrinsic TLS. For polymers in particular, a large spatial extent for intrinsic TLS is not unreasonable since polymer chain "snaking" along the channel or "tube" formed by its neighbors can presumably occur to some degree even at liquid helium temperatures. Leger and de Gennes [23] and de Gennes [24] have referred to such motion as reptation. Now for each and every extrinsic TLS we associate a potential energy curve $V_{ex}^{j}(q,\xi)$ where q is the usual intermolecular double-well coordinate associated with the extrinsic (subscript ex) TLS [6]. The superscript j labels the ground or excited electronic state of the impurity. The variable ξ denotes the coordinates of the atoms associated with the intrinsic TLS. Within the Born-Oppenheimer approximation one can view V_{ex}^{j} as depending parametrically on ξ. Thus, $\langle V_{ex}^{j}(q,\xi)\rangle_{gls}$ represents the extrinsic TLS potential for a particular glassy state (subscript gls). The subscript gls defines the value of ξ and is governed by the intrinsic TLS which surround the extrinsic TLS.

LIHF is then viewed as resulting from irreversible gls → gls' glassy state transitions triggered by secondary light absorption by extrinsic impurity-TLS different from those involved in the primary burn. The initial excitation (**via** the secondary irradiation) and coupling between the extrinsic excited impurity-TLS and intrinsic TLS leads to the irreversible evolution of the gls'. The time scale may be long with much of the configurational change associated with gls → gls' occurring with the impurity in its ground electronic state. The energies V_{ex}^{j} respond adiabatically to the glassy state transition (we have used the term "glassy state" interchangeably with the state of the intrinsic TLS which surround and influence the extrinsic TLS). Thus, provided that the spatial extent of the intrinsic TLS is large, the excitation frequencies of extrinsic impurity-TLS spatially removed from those directly excited can be altered. The picture which emerges is that excitation of a spectrally narrow isochromat causes excitation frequency diffusion over a broad segment of excitation frequency space.

We proceed now to discuss the results 1 through 4 (**vide supra**) in terms of this model (referred to hereafter as model A). Consider first the part of result 3 and Figure 3. Our initial interpretation of the step behavior at ω_{B1} was that there are two LIHF mechanisms, only one of which is operative for $\omega_{B2} < \omega_{B1}$. At the present time this possibility has not been excluded, although we are not able to suggest another plausible model. Thus, we consider here only model A. We suggest that the behavior shown in Figure 3, the results from Figures 7 and 8 and other LIHF results for LIHF in polystyrene [17,19] are explicable using model A. An important clue is provided in Figure 8 which shows that

Nd^{3+} is intriguingly different in that LIHF is more efficient for $\omega_{B2} < \omega_{B1}$. This leads us to consider correlation effects between impurity site excitation energies and glassy state (intrinsic TLS) absolute energies. By positive (negative) correlation, we mean that increasing excitation energy is associated with increasing (decreasing) absolute energy of the intrinsic TLS. Although the zero-point splittings, barrier heights, etc., of extrinsic impurity-TLS may be dominated by interatomic interactions from within their domains, the intrinsic TLS which envelop them may be a major contributor to the determination of the excitation frequencies within the inhomogeneously broadened absorption profile. It is reasonable to suggest that the absolute energies of intrinsic TLS are quite insensitive to the state of the impurity due to their assumed large spatial extent. In addition to correlation, we introduce the notion that an arbitrary perturbation (like secondary irradiation in LIHF) is, on average, far more disposed to promote gls → gls' configurational transformations in which E(gls') < E(gls). This is not unreasonable for transformations at liquid helium temperatures. Thus, for positive correlation and within the framework of model A, secondary irradiation would cause red shifts with a wide distribution of excitation energies while for negative correlation, blue shifts would occur. Given the gradient in excitation frequency space due to the primary hole, these shifts lead to hole filling.

With this in mind, one can qualitatively understand the step behavior for R640, Figure 3, and the results for Pr^{3+} in Figure 7. For both there is a significant amount of positive correlation, albeit not perfect since some filling is observed for $\omega_{B2} < \omega_{B1}$. On the other hand

for Nd^{3+}, as shown in Figure 8, a significant amount of negative correlation is indicated.

Consider next result 4, in which we state that the hole broadening accompanying LIHF is imperceptible. The analogous spectral diffusion problem pertaining to thermally induced spectral diffusion (hole broadening) and hysteresis has been treated theoretically by Friedrich **et al.** [25]. The associated problem for SPHF is considered in [1]. Friedrich **et al.**'s theory [25] is, with slight modification, a reasonable starting point for LIHF and model A. If the probability function for an excitation frequency shift $\omega' \rightarrow \omega' + \Delta\omega$ has an effective width σ and is independent of ω', the theory shows that hole broadening would be difficult to observe (with our 6% accuracy and the extent to which we fill the holes) for $\sigma \geq 10\gamma$, where γ is the width of the hole prior to filling. Thus, failure to observe hole broadening is not necessarily in contradiction with model A.

Thus far, model A has qualitatively accounted for all the results listed at the beginning of this section except the second part of result 3 (illustrated in Figure 3). Although one can understand why LIHF can occur for large $|\omega_{B2} - \omega_{B1}|$ (with ω_{B2} within the absorption profile), it is difficult to explain why LIHF is insensitive to changes in $|\omega_{B2} - \omega_{B1}|$. For the same ω_{B2} flux and irradiation time, one would reasonably assume that the percent hole filling would follow the variation in optical density across the absorption profile. In addition, the first two rows in Table 1 indicate that irradiation of R560 near the peak of its absorption yields a percent LIHF for holes in CV identical to that obtained with the same ω_{B2}, burn flux and burn time but with R560 absent

from the sample (in the latter case, the OD at ω_{B2} was 0.08, compared to OD 0.35 in the former case). Further experiments are required to understand the above behavior, including studies with substantially reduced (<< 1 mW/cm^2) ω_{B2} fluxes. Given the saturation (bottleneck) behavior for NPHB shown in Figure 5, it is possible that LIHF itself is being affected by a saturation effect.

CONCLUSION

The model presented for LIHF is based on the idea of connectivity or communication between spatially separated extrinsic impurity-TLS. For the concentrations used in the R640 and CV/R560 experiments, the average distance between impurities is about 22.5 nm. The idea that the relatively localized impurity-TLS is enveloped by spatially extended intrinsic TLS and that the impurity excitation frequencies depend in an adiabatic manner on the configuration of the intrinsic TLS is introduced. The latter can be viewed as being a type of embedding glassy state (gls) for each and every impurity-TLS. A possible mechanism for the above long-range communication for polymer hosts could involve subtle reptation-type motions of the polymer chains. Accepting that a perturbation of the system, such as ω_{B2} irradiation, produces a preponderance of downward (energy lowering) gls transitions, much of the LIHF data presented can be qualitatively explained when one additional ingredient is introduced: that some degree of correlation exists between impurity site excitation energies and the absolute gls energies.

The general features of LIHF shown here for R640, Pr^{3+}, Nd^{3+} and R560/CV in PVOH have also been observed for chlorophyll **a** and **b** [17,18] and chlorophyll **a** dimers [19], all in polystyrene. More recently, they have been observed for oxazine 720 in PVOH [26]. Given the range of the impurities studied, it may be that LIHF is general for hole burning in polymers.

However, the above model should be viewed as tentative. There are a number of experiments which may be used to test it; for example, LIHF as

a function of impurity concentration and the determination of the $|\omega_{B2} - \omega_{B1}|$ dependence of LIHF in non-polymeric hosts such as aprotic and alcoholic glasses. Such experiments are planned. In addition, the R640 results shown in Figure 3 suggest that it will be important to determine how the $|\omega_{B2} - \omega_{B1}|$ dependence is affected by reductions in secondary irradiation flux.

REFERENCES

1. B. L. Fearey and G. J. Small, Chem. Phys. 101, xxx (1985).

2. J. M. Hayes and G. J. Small, Chem. Phys. 27, 151 (1978).

3. A. R. Gutierrez, J. Friedrich, D. Haarer and H. Wolfrum, IBM J. Res. Develop. 26, 198 (1982).

4. T. P. Carter and B. L. Fearey, Ames Laboratory and Iowa State University, unpublished results.

5. J. M. Hayes and G. J. Small, J. Luminescence 18/19, 219 (1979).

6. J. M. Hayes, R. P. Stout and G. J. Small, J. Chem. Phys. 74, 4266 (1981).

7. R. W. Olson, H. W. H. Lee, M. D. Fayer, R. M. Shelby, D. P. Burum and R. M. Macfarlane, J. Chem. Phys. 77, 2283 (1982).

8. H. W. H. Lee, C. A. Walsh and M. D. Fayer, J. Chem. Phys. 82, 3948 (1985).

9. T. P. Carter, B. L. Fearey, J. M. Hayes and G. J. Small, Chem. Phys. Lett. 102, 272 (1983).

10. B. L. Fearey, T. P. Carter and G. J. Small, J. Phys. Chem. 87, 3590 (1983).

11. M. Romagnoli, W. E. Moerner, F. M. Schellenberg, M. D. Levenson and G. C. Bjorklund, J. Opt. Soc. Am. 1, 341 (1984).

12. S. K. Lyo and R. Orbach, Phys. Rev. B 22, 4223 (1980).

13. P. Reineker and H. Morawitz, Chem. Phys. Lett. 86, 359 (1984).

14. T. Foster, Ann. Physik 2, 55 (1948).

15. R. M. Macfarlane and R. M. Shelby, in: "NATO Workshop on Coherence and Energy Transfer in Glasses", P. A. Fleury and B. Goldin, eds., Plenum Press: New York, 1982.

16. J. K. Tyminski, R. C. Powell and W. K. Zwicker, Phys. Rev. B2,6074 (1984).

17. T. P. Carter and G. J. Small, Chem. Phys. Lett. 120, 178 (1985).

18. T. P. Carter, B. L. Fearey, J. M. Hayes and G. J. Small, Int.

Rev. Phys. Chem., accepted.

19. T. P. Carter and G. J. Small, submitted to J. Chem. Phys.

20. B. L. Fearey, R. P. Stout, J. M. Hayes and G. J. Small, J. Chem. Phys. 78, 7013 (1983).

21. H. F. Childs and A. F. Frances, J. Phys. Chem. 89, 466 (1985).

22. B. Golding, M. von Schickfus, S. Hunklinger and K. Dransfeld, Phys. Rev. Lett. 43, 1817 (1979).

23. L. Leger and P.-G. de Gennes, Ann. Rev. Phys. Chem. 33, 49 (1982).

24. P.-G. de Gennes, Phys. Today 33 (June, 1983).

25. J. Friedrich, D. Haarer and R. Silbey, Chem. Phys. Lett. 95, 119 (1983).

26. M. Kenney, Ames Laboratory and Iowa State University, unpublished results.

ADDITIONAL RESULTS AND DISCUSSION

Persistent hole burning techniques have now been proven by many researchers to be an important and extremely useful technique in investigations of the basic properties of disordered systems. Many different types of systems have been studied for a wide variety of reasons, ranging from obtaining pure dephasing information for a particular substance, to trying to identify photoreactive mechanisms in biological systems, to studying the properties of materials in an effort to determine those which might be useful in the manufacture of optical storage devices based on persistent hole burning, to studying the details of the energetics of amorphous solids. Several good recent reviews of the topic are available to guide those who wish to read more [6-8].

The studies reported above (and others not included here [17,18]), were undertaken as first steps toward a deeper understanding the details of the amorphous state. Much of what has been accomplished is viewed as preliminary, that is, our work has provided the foundation for more detailed studues yet to come.

Even so, much detail about NPHB processes has been determined as a result of these efforts. Three new and interesting classes of hole burning systems have been discovered: organic ionic dyes in hydrogen bonding polymers, rare earth ions in the same polymers and chlorophylls in polystyrene, all of which are appreciably more efficient hole burning systems than many others which are known.

From the work on the ionic dye molecules, many new and interesting results have been obtained. A new mechanism for hole production has been identified (the non-resonant vibronic holes at frequencies lower than ω_B) which may have use as a means of obtaining excited state vibronic frequencies even when other methods may fail (as they do for some of the dye molecules used in this work). Also, these systems were the first for which LIHF was observed to be virtually insensitive to the absorption of radiation by the impurity, and the first systems in which the significant change in LIHF efficiency was observed for different relative positions of ω_{B2} and ω_{B1}. It may be that this last observation has profound implications as to the microscopic details of amorphous systems, since it seems to imply that the energies of the extrinsic (impurity) TLS are directly correlated with the absolute energy of the intrinsic (host) TLS, and that the intrinsic TLS have a large spatial extent. Moreover, these same details for LIHF behavior have also been observed in the rare earth ion and chlorophyll systems and therefore seem to be general, at least in polymeric hosts.

The hole burning of the rare earth ions was the first example of NPHB for other than a molecular species in organic hosts, and seems to be dependent upon the state of solvation for the ion, since only incompletely dried samples showed NPHB. The significance of the NPHB in the chlorophyll systems is presented in detail in Section II.

Paper II, above, presents results of NPHB experiments on three dye molecules: cresyl violet, nile blue, and oxazine 720, each doped into two polymers, PVOH and PAA. Not mentioned are the additional observations of efficient NPHB in the same two polymers when doped with

oxazine 725, oxazine 750, rhodamine 560, rhodamine 640, methylene blue, indigo carmine, malachite green, and 1,1'-methylene-2,2'-cyanine iodide, none of which have been studied in any detail. Each of these systems is characterized by efficient NPHB with a small electron-phonon coupling, varying degrees of vibronic hole intensities relative to the resonant hole intensity, and large pure dephasing contributions to the hole width at 1.8 K (as presumed from the observed hole width, in relation to that expected if the width were determined solely by the molecular radiative lifetime). These results have provided additional conformation of the existence of rapid pure dephasing processes occurring in amorphous organic matrices which are one or two orders of magnitude faster than those observed in crystalline substances or "hard" inorganic glasses at 1.8 K.

Future Work

Whether or not the homogeneous line width as determined by NPHB will approach the lifetime limit as T_B goes to 0 K is still a matter of conjecture at this time; determination of this point is the objective of planned future experiments using a liquid ^3He cryostat now under construction. It is believed that this indeed will be the case, as is observed for several other NPHB systems [19, and references therein]. Also, since it has been observed that hole burning in hydrogen bonding matrices seems to be especially efficient, studies are planned to determine the effects of deuteration of the hydrogen bonding protons on the NPHB of such systems.

The rare earth ions Nd^{3+} and Pr^{3+} each have several excited states which are fluorescent as does the organic molecule azulene [21]; it is thought that since these states are radiative, and hence rapid internal conversion or intersystem crossing are not occurring, then these states may each be available for hole burning (as has been demonstrated for Eu^{3+} in silicate [20]). Experiments are planned to study the effects on the NPHB behavior when the different states of these systems are irradiated.

Of course there has always been the intention to investigate some or all of the above mentioned dye/polymer systems in much greater depth, including dephasing as a function of temperature, LIHF, spontaneous hole filling, deuteration effects, etc., as well as extending the study to other dyes or polymers, hydrogen bonding or not.

The informed reader may be aware that the method used for probing NPHB holes in this work is not the method of choice if very high resolution reading is important (as would be the case if dephasing data at very low temperatures is needed). The ideal method would be to use the cw ring dye laser for hole probing (via fluorescence excitation) as well as burning, since its line width when actively stabilized is ~ 5 MHz. However, the scanning option for this dye laser was not available to us when these studies were performed, and the absorption spectrometer was. Moreover, the scanning option for the laser, as provided by the manufacturer, is capable of scanning only over a 30 GHz (1 cm^{-1}) region, and the hole widths for many of these systems are a significant fraction of this width, even at 1.8 K; thus, scanning over the complete hole including the "wings" of the Laurentzian lines would be impossible by

this method. In addition, if fluorescence excitation were used, it would have been very difficult to obtain the wide range scans which are easy to obtain by absorbance, and perhaps many interesting phenomena (non-resonant hole formaton, **e.g.**) would not have been observed. Still, measures are being taken to allow for dye laser scans of up to 90 GHz by interfacing the dye laser scan controller with a computer, which will perform etalon mode hops together with cavity length tuning in a controlled fashion.

It is hoped that many new and interesting details of the NPHB process will be learned as a result of future studies based on the work reported herein. The implications as to the profound complexity of the amorphous state which have been gleaned from past NPHB experiments holds promise of much more interesting science to come.

REFERENCES

1. A. Carrington and A. D. McLachlan: "Introduction to Magnetic Resonance", Harper and Row: New York, 1969.

2. R. L. Shoemaker in: "Laser and Coherence Spectroscopy", J. I. Steinfeld, ed., Plenum Press: New York, 1978.

3. R. G. Brewer and R. L. Shoemaker, Phys. Rev. Lett. 27, 631 (1971).

4. R. G. DeVoe, A. Szabo, S. C. Rand and R. G. Brewer, Phys. Rev. Lett. 42, 1560 (1979).

5. R. I. Personov, in: "Spectroscopy and Excitation Dynamics of Condensed Molecular Systems", V. M. Agranovich and R. M. Hochstrasser, eds., North-Holland: New York, 1983.

6. G. J. Small, in: "Spectroscopy and Excitation Dynamics of Condensed Molecular Systems", V. M. Agranovich and R. M. Hochstrasser, eds., North-Holland: New York, 1983.

7. J. Friedrich and D. Haarer, Angew. Chem. Int. Ed. Engl. 23, 113 (1984).

8. J. M. Hayes, R. Jankowiak and G. J. Small in: "Persistent Spectral Hole Burning: Science and Applications", W. E. Moerner, ed., Springer-Verlag, in preparation.

9. B. M. Karlamov, R. I. Personov and L. A. Bykovskaya, Opt. Commun. 12, 191 (1974).

10. B. M. Karlamov, R. I. Personov and L. A. Bykovskaya, Opt. Spectrosc. 39, 137 (1975).

11. A. A. Gorokhovskii, R. K. Kaarli and L. A. Rebane, JETP Lett. 20, 216 (1974).

12. J. Friedrich and D. Haarer, Chem. Phys. Lett. 74, 503 (1980).

13. J. M. Hayes and G. J. Small, J. Lumin. 18/19, 219 (1979).

14. See Paper II, Section I.

15. J. M. Hayes and G. J. Small, Chem. Phys. 27, 151 (1978).

16. S. G. Rautian, Soviet Phys. Uspekhi 66, 245 (1958).

17. T. P. Carter, B. L. Fearey, J. M. Hayes and G. J. Small, Chem. Phys. Lett. 102, 272 (1983).

18. B. L. Fearey, T. P. Carter and G. J. Small, J. Lumines. 31 & 32, 792 (1984).

19. H. P. H. Thijssen, R. E. van den Berg and S. Volker, Chem. Phys. Lett. 103, 23 (1983).

20. R. M. Macfarlane and R. M. Shelby, Opt. Commun. 45, 46 (1983).

21. G. D. Gillispie and E. C. Lim, J. Chem. Phys. 68, 4578 (1978).

SECTION II.

NONPHOTOCHEMICAL HOLE BURNING OF PHOTOSYNTHETIC PIGMENTS

INTRODUCTION

The various chlorophyll (chl) molecules, which are the primary photoacceptors in photosynthesis and therefore are of direct or indirect importance to nearly every living organism, have been the subject of intense study over the years, and determining the state of **in vivo** chl has been a primary concern in photosynthesis research. To define what I mean by "the state of **in vivo** chl" I will paraphrase a definition used by Katz **et al.** [1]: "the three-dimensional arrangement of chlorophyll molecules in the antenna (light-harvesting) and reaction center (photoreactive) units that together compose the photosynthetic system of living organisms". It wasn't until very recently (late 1984) that any detailed information about the structure of antenna or reaction centers of photosynthetic organisms was determined.

It has long been accepted by researchers that the chl in a photosynthetic unit has very little (if any) of the magnetic, redox, and most importantly, the optical properties of a chl solution in ordinary polar solvents where chl exists as a monomer. While the chemical structure of the chl molecules in ordinary solvents is identical to that in the antenna and reaction centers of photosynthetic organisms, it is the different organizations of the chl molecules **in vivo** which give them the ability to perform their specialized tasks. The ultimate objective of photosynthesis research is the understanding of the photoprocesses of the **in vivo** systems and a necessary preliminary to this is the understanding of the photophysical and photochemical properties of monomeric chl.

A review of the literature of photosynthesis research, even that from recent years, shows that much of what is known about chl is based on low resolution optical spectroscopy. This is in part due to the fact that chl is highly colored because of its strong ($\varepsilon \simeq 6 \times 10^4$) visible absorption, that the monomer and **in vivo** chl species have appreciable fluorescence quantum yields ($\phi_F \simeq 0.3$), and that the instrumentation for these types of studies is readily available. However, it has become more and more evident that more detailed, higher resolution information needs to be determined for chl before a true understanding of photosynthesis can be reached.

Although chl has been studied spectroscopically for more than 100 years [see **e.g.**, 2,3], it wasn't until the early 1970s that vibronically well resolved spectra of the fluorescence and absorption (actually the fluorescence excitation) spectra for chl monomers were obtained. There are some good reasons for this: chl is a large and asymmetric molecule which doesn't substitute in a well defined way in any known host crystal which rules out using mixed crystal techniques (including Shpol'skii matrices), and the vapor pressure of chl below its decomposition point is too low to be of use in supersonic jet spectroscopy. The only method of obtaining such spectra which has been successfully applied to chl is fluorescence line-narrowing spectroscopy [4], which requires the use of tunable lasers as an excitation source. A review of the high-resolution optical spectroscopy of chl which has been performed to date has recently been published [5].

In order to better understand that which follows, a brief introduction to chl optical spectroscopy is called for, and to do this

one must also discuss the aggregation behavior of chl as well. Figure 1 shows the structure of chl **a** which is composed of a substituted porphyrin ring whose four pyrrole nitrogens are ligated to a magnesium II ion, together with a long aliphatic side chain known as the phytyl group. The magnesium ion has a coordination number of four and therefore is coordinatively unsaturated, and this fact is important in almost every aspect of chl spectroscopy. The unsaturation may be alleviated through axial ligation to the magnesium by one or two molecules possessing a lone pair of electrons; in this sense chl is acting as an acceptor and the ligating molecule as a donor of electron density. It should be noted that chl is unusual in that it possesses both of the necessary functional groups for donor-acceptor interactions, **vide infra.**

In monomeric form, chl is acting in its acceptor aspect. There is no unequivocal evidence for chl having Mg with coordination number four and therefore the spectral (and other) properties of chl are more correctly attributed to *mono- or* biaxially ligated chl, chl·L_1 and chl·L_2, respectively. If solutions of chl in non-polar (non-Lewis base) solvents are prepared and no steps are taken to exclude adventitious nucleophiles (usually, water) then it should be assumed that the solution is at least equimolar in chl and water. Chl crystallizes only as a hydrate, and when dry it is very hydroscopic. When "wet" (or in the prescence of nucleophilic solvents or impurities), the room temperature solution spectrum of chl a appears as shown in Figure 2. There are actually two electronic transitions in the red absorption: the $S_1 \leftarrow S_0$ or Q_y transition near 15000 cm^{-1} (667 nm) which is polarized

Figure 1. Molecular structure of chlorophyll a

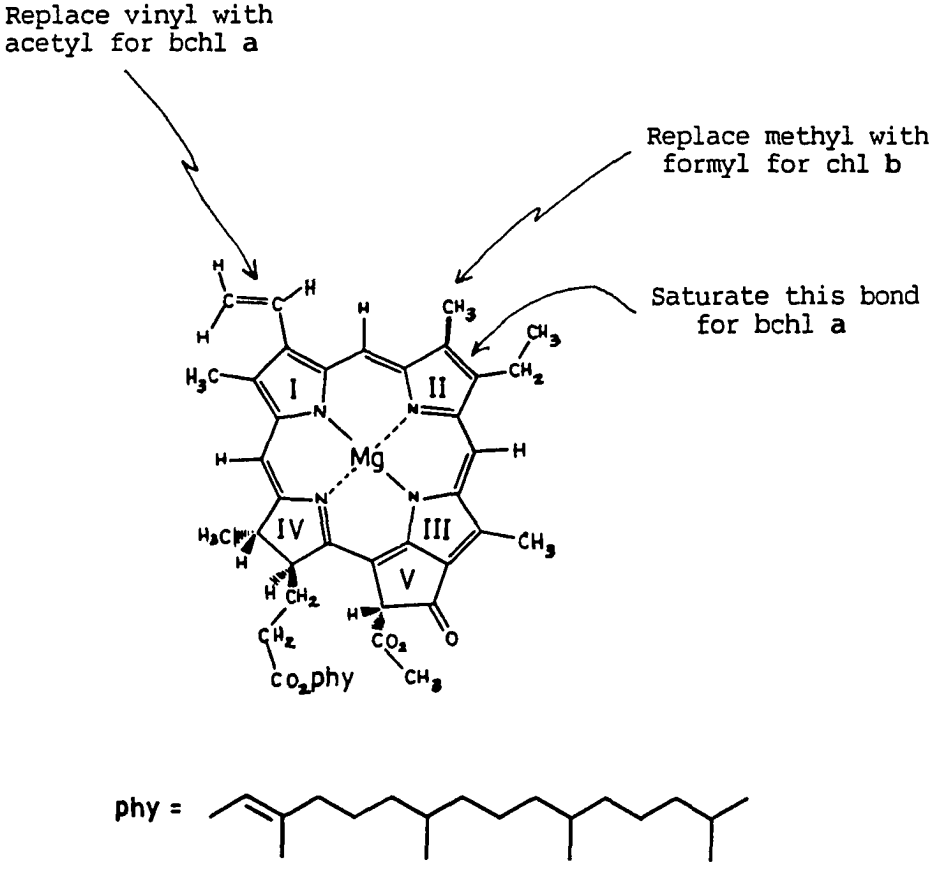
Replace vinyl with
acetyl for bchl a
Replace methyl with
formyl for chl b
Saturate this bond
for bchl a
I
II
III
IV
V
Mg
phy =

in the porphyrin plane with a transition dipole oriented nearly along the N1 - N3 axis, and the $S_2 \leftarrow S_0$ or Q_x transition near 17500 cm^{-1} (575 nm) which is also in-plane polarized with a transition dipole roughly perpendicular to Q_y and having a much lower oscillator strength. The energies of these transitions are to some degree solvent dependent but a more profound shift depends on the number of axial ligands. When mono-ligated, the two electronic transitions are fairly well separated as in the spectrum of Figure 2, but when two nucleophiles are ligated, there is a differential red shift; Q_y shifts to lower energies but to a lesser degree than does Q_x, which then lies only a few hundred cm^{-1} higher than Q_y. This biaxial ligation occurs only in the presence of strong nucleophiles such as pyridine.

The basic features of chl-chl interactions are most readily apparent in chl **a** dimers [(chl **a**)$_2$]. Direct molecular weight measurements show that in polarizable media such as benzene or carbon tetrachloride, chl **a** exists almost entirely as the dimer (chl **a**)$_2$ over a wide range of concentrations (10^{-6} - 10^{-2} M) [6]. Various methods such as infrared, NMR and electronic transition spectra have provided information on the structure of (chl **a**)$_2$. The dimerization is a result of the fact that chl **a** can act as both donor and acceptor in lone-pair electron sharing, and it has been determined that (chl **a**)$_2$ is formed through the ring V keto oxygen of one chl **a** donating lone pair density to another chl **a**'s

Figure 2. Room temperature solution absorption spectrum of chlorophyll a in toluene

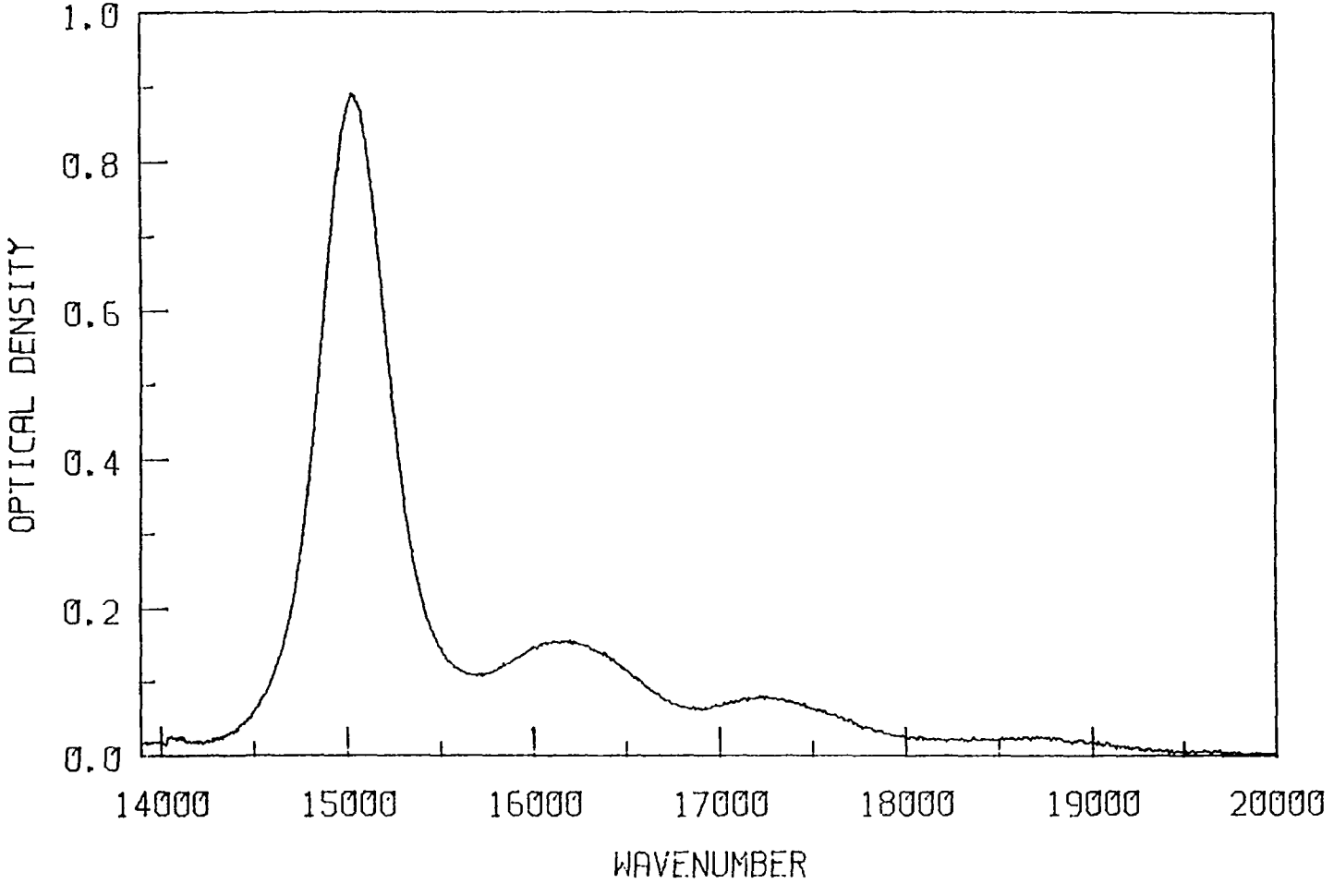
1.0
0.8
0.6
0.4
0.2
0.0
OPTICAL DENSITY
14000
15000
16000
17000
18000
19000
20000
WAVENUMBER

Mg II ion. On the time scale of NMR experiments, these two components of the dimer are interconverting in room temperature solutions, that is, exchanging roles of donor and acceptor, and the NMR spectra show signals for only one average structure. However, the interconversion is slow on the time scale of electronic transitions because the absorption spectrum of (chl **a**)$_2$ shows two unresolved features of comparable intensity, one of which is nearly where Q_y is observed in monomeric solutions and the other shifted a few hundred cm^{-1} to lower energy. It should be understood that there will be a distribution of structures for the dimer, which is roughly T-shaped. There will be a distribution of angles between porphyrin planes as well as a distribution describing various conformers related through rotation about the keto-Mg bond. However, in rigid solutions at low temperatures the interconversion between donor and acceptor should be frozen out, as will most, if not all, of the other conformational interconversions.

The exact mechanism which produces the double transition observed in the Q_y region for (chl **a**)$_2$ has been the subject of some discussion. Some researchers argue that two large molecules with high oscillator strengths interacting in such a close manner must necessarily be coupling in a excitonic fashion. However, it seems that the particular orientation of the two chl **a** dimer components is highly unfavorable for such an interaction in that their transition dipoles are nearly perpendicular. Also, if excitonic coupling is assumed as the mechanism for producing the observed spectrum, then the problem of how to account for the near equal intensities for the two dimer transitions arises. It is perhaps not surprising then that there is no direct experimental evidence to support the supposition of excitonic coupling in (chl **a**)$_2$.

There is another proposed mechanism for producing the observed doubling in (chl a)$_2$. Briefly, the two chl a molecules in the dimer are inequivalent in that one is acting as an electron donor and the other as an acceptor, and it is this difference which is responsible for the observed doubling. Studies using reagents which act as acceptors and preferentially bind to the ring V keto group of chl a (thus mimicking the acceptor chl a in the dimer) produce a chl a spectrum with a single Q_y transition but shifted to lower energy to a position nearly the same as that observed for the low energy component in the (chl a)$_2$ spectrum. It should be recalled that the ring V keto group participates in the electronic resonance structure for the porphyrin ring, and thus donor-acceptor interactions involving this moiety can affect the Q_y transition energy, while axial ligation through the Mg has little effect. This and other evidence indicate that the inequivalent donor and acceptor chl a molecules in (chl a)$_2$ do have differential "environmental" shifts and are not excitonically coupled to any great degree. In this view then, the interpretation of the (chl a)$_2$ Q_y spectrum is that the lower energy transition D_l is due to the donor chl a half of the dimer and the higher energy transition D_u is due to the acceptor half.

One possible complication that arises in interpreting our data is due to the fact that D_u occurs at almost the same energy as Q_y for the monomer, and therefore it is difficult to assess the amount of residual monomer present in (chl a)$_2$ samples. Further discussion of this is left for Paper II.

Following the detailed experimental description of the methods used in this work, given below, are the two publications that describe our

work on the nonphotochemical hole burning experiments which have been performed on monomeric chl **a** and chl **b** as well as (chl **a**)$_2$, each of which was doped into polystyrene and then cast as a film. The monomer experiments were primarily performed to provide a benchmark to use in interpreting the results for (chl **a**)$_2$, and the motivations for that work were to see if hole burning would be able to detect any excitonic behavior between dimer components, and whether any differences in the hole burning behavior of these components would be observable. Also, hole burning provides a means of high resolution information: homogeneous linewidths (and hence, dephasing times) as well as, in some instances, detailed vibronic information for the excited state (see Section I). Two component aggregates of chl are of special interest in photosynthesis research since it has long been postulated that such a pair of chl molecules is the primary photoelectron donor of **in vivo** reaction centers. The details of the structure of (with one exception, **vide infra**) and interactions which occur between these so-called special pairs is as yet unknown, and any information about the interactions of **in vitro** dimers is useful in this regard.

EXPERIMENTAL METHODS

Sample Preparation

Samples of monomeric chl **a** and chl **b** in polystyrene films were prepared using techniques analogous to those used for the hydrogen bonding polymers discussed in Section I. The chl **b** from spinach (Sigma Chemicals) was used without further purification as was the chl **a** from clover (generously provided by Dr. James R. Norris, Argonne National Laboratory). The polystyrene pellets (Aldrich) were dissolved in reagent grade toluene; unlike the hydrogen bonding polymers however, the dissolution of the polystyrene did not require heating. After the desired consistency was obtained by either adding more toluene or more polymer pellets, aliquots of a concentrated solution of chl were stirred in until the desired optical density was reached. Round microscope cover slips were used as substrates for film growth as with the previous samples. Allowing the films to dry in the open was unsatisfactory because the rather high vapor pressure of toluene caused them to dry too rapidly producing a very poor film surface. The solvent evaporation was slowed down by placing the film preparations in a vacuum desiccator (without desiccant) which had been modified by the addition of a small hole drilled in the lid. A slow stream of dry N_2 gas was then flowed through the desiccator to carry away the evaporating toluene. The samples were carefully demounted from their cover slips and either cut into pieces and individually taped over holes in the sample holder or the entire film was taped directly to the sample holder and each hole in the holder treated as a different "sample" (the former method was used

when quantitative information was desired). All other methods were as reported in Section I.

For the dimeric chl **a** samples a much more stringent regimen was used for sample preparation since it was necessary to both eliminate any nucleophilic impurities which were already present and exclude those which might be introduced during preparation and handling. By far the most common nucleophilic impurity which interferes in the self aggregation of chl **a** is water. A "dry" dilute solution of (chl **a**)$_2$ will substantially or totally revert to hydrated monomers if exposed to atmospheric moisture for a few minutes (one ml of a 10^{-5}M solution of (chl **a**)$_2$ needs only 2 x 10^{-8} moles or 360 ng of water to be equi-molar in water). Therefore the procedure which follows (which was shown to me by Dr. James R. Norris to whom I am grateful) was carried out entirely within a dry box.

All glassware used in subsequent steps was baked overnight in a vacuum oven at 80° C and transferred while hot into the dry box. A rather dilute solution (roughly four times less concentrated than that used to produce films) of polystyrene in toluene was prepared previously and stored for several days in a tightly stoppered flask over freshly activated type 4A molecular sieve and swirled several times a day to ensure complete drying. Similarly dried toluene and CH_2Cl_2 were prepared in other flasks. Crystals of chl **a** were dried by placing them in a small sample vial and dissolving them in a small amount (1 ml) of CH_2Cl_2. Then, while swirling the solution in the vial, it is evaporated to dryness using a fairly rapid stream of dry N_2. The intention is to get the chl to form a very thin film on the wall of the vial so that no

trapped solvent remains with the solid and any nucleophilic impurity evaporates with the solvent as an azeotrope. This solution-evaporation was repeated twice more with CH_2Cl_2 and three times with toluene. The dilute "dry" polystyrene solution was then evaporated using a stream of N_2 until the desired viscosity was reached. The dried crystals were then redissolved in toluene and added to the polystyrene solution. Film preparation was then performed as above. When completely dried the films were then taped to the sample holder while still in the dry box and transferred to the cryostat inside a rubber glove; in this way their exposure to ordinary air was limited to a few seconds.

Other Methods

For cryogenic, hole burning and hole probing methods, see Section I.

PAPER I.

NONPHOTOCHEMICAL HOLE BURNING OF CHLOROPHYLL **a** AND **b** IN POLYSTYRENE

NONPHOTOCHEMICAL HOLE BURNING OF CHLOROPHYLL **a** AND **b** IN POLYSTYRENE

THOMAS P. CARTER and GERALD J. SMALL

Ames Laboratory-USDOE and Department of Chemistry
Iowa State University, Ames, Iowa 50011

Chemical Physics Letters 120, 178 (1985)

INTRODUCTION

It has been several years since the connection between nonphotochemical hole burning (NPHB) of the optical absorption spectra of dopants in amorphous solids and the two-level systems (TLS) of the glassy state was drawn [1,2]. The TLS form a distribution of asymmetric intermolecular double-well potentials and are used to model those glassy configurations which are accessible from a particular glassy state by phonon assisted tunneling (PAT). Because the holes formed by NPHB can be stable [3], it follows that the TLS which couple to the impurity and are responsible for stable hole formation form a subset of the total distribution [4]. Each TLS belonging to the subset is characterized by the fact that its two tunnel states do not interconvert on the time scale of the experiment when coupled to the impurity in its ground state. That is, the tunnel states are not in thermal equilibrium. The permanent impurity-TLS configurational change which leads to NPHB arises from PAT of the TLS interacting with the impurity in its excited state. In other words, in cycling the impurity from its ground to its excited state and back to its ground state, a glassy configuration is reached which is not thermally accessible from the configuration which existed prior to burning at $T = T_B$ (the burn temperature). As expected, nonphotochemical holes do undergo irreversible thermal annealing [5,6].

At the time the above mechanism for NPHB was developed it was apparent that the dephasing of molecular electronic transitions in glasses was anomalously fast and peculiar in its T-dependence [2,5,6]. Similar behavior had already been observed for trivalent rare earth ions

(RE^{3+}) in inorganic glasses by fluorescence line narrowing [7]. A variety of theories have now been developed [8] to explain this dephasing in a large number of systems [5,6,9-15]. They all invoke PAT of TLS coupled to the impurity as the underlying physics for the anomalous dephasing. The principal difficulty (uncertainty) is associated with the problem of performing the ensemble average over the TLS responsible for the dephasing. Since the quantum efficiencies for NPHB are generally low ($\sim 10^{-5}$), the TLS responsible for dephasing cannot be those responsible for hole formation [4]. The former are believed to have tunnel states which are in thermal equilibrium when the impurity is in its ground state. It is plausible to suggest that the dephasing and hole producing TLS are associated with distinctly different configurational coordinates. For each coordinate, there will be a distribution of TLS as a result of the inherent disorder.

Nonphotochemical hole burning spectroscopy was reviewed in 1982 [4]. In comparing the experimental data available then and now, it is clear that many exciting developments have occurred in three years. For example, NPHB has been observed for a wide variety of dye molecules in polymers [16-18], RE^{3+} ions in inorganic glasses [19] and organic polymers [18], aromatic molecules in amorphous aromatic hydrocarbon hosts [13,20] and in organic mixed crystals in which the host is characterized by H-bonding [21]. We have observed NPHB for over 10 dye molecules in polymers like polyvinyl alcohol and polyacrylic acid [22]. Thus, NPHB can now be considered to be a quite common phenomenon. Although NPHB appears to be favored in H-bonding hosts, this is not a hard and fast rule.

A case in point is the subject of this paper in which we report efficient NPHB for chlorophyll a (chl a) in polystyrene polymer films. The motivation of these studies stems from our desire to apply NPHB to the study of the excitonic effects in self-aggregated dimers of chl a which can be formed in aprotic solvents [23]. As a first step it was important to establish that NPHB can be observed for chl a monomers in an aprotic host. Somewhat related to this work are the photochemical hole burning studies on free-base porphyrin derivatives in various host media [12]. In all cases, hole formation is attributed to a tautomeric rearrangement of the two protons in the center of the porphyrin ring. In the chlorophylls however, these protons are replaced by a Mg(II) ion thereby precluding this PHB process. Hole burning has been reported for protochlorophyll a and chl a in ether and attributed to a NPHB mechanism [24,25].

In the present studies extreme care has been taken to ensure that the species involved in hole burning are chl a and b (rather than pheophytin). Thermal cycling and laser induced hole filling data are presented which support NPHB as the mechanism. In contrast with laser dyes and RE^{3+} ions in hydrogen bonding polymers [18], no partial spontaneous hole filling is observed. Finally, preliminary dephasing data have been obtained and yield a power law of $T^{1.3 \pm 0.2}$.

EXPERIMENTAL

Pure chl **a** from clover was obtained courtesy of Dr. James R. Norris, Argonne National Laboratory. Samples were prepared by mixing a solution of chl **a** in toluene with a viscous solution of polystyrene in toluene and then pouring the resulting mixture onto a circular microscope cover slip and allowing it to dry slowly to a film.

The hole burning and measuring techniques used in this work have been described elsewhere [17]. Briefly, the holes were burned with a single frequency cw ring dye laser attenuated to 0.1 - 50 mW/cm^2 and the holes were "read" using a home built double beam absorption spectrometer whose bandwidth is ~ 0.08 cm^{-1} in the spectral region examined in the experiments described here. Samples were cooled in a liquid helium immersion cryostat.

Close inspection of the visible and near UV absorption spectra of the samples used and comparison with known samples checked by IR and NMR confirmed that they were indeed chl **a** monomers and not either pheophytin **a** or chl **a** aggregates. While aggregation is usually only a problem when the sample is kept scrupulously free of any adventitious nucleophiles, it can be a problem at high concentrations [23]. Pheophytinization (abstraction of the Mg II ion) however, is very facile and must be guarded against [26], especially since the red absorptions of pheophytin **a** and chl **a** are very similar.

In all cases, the holes, were burned into the low energy side of the Q_y transition of chl **a** which in these samples at 1.8 K has a maximum at 665 nm (15038 cm^{-1}) with a FWHM of about 420 cm^{-1}.

RESULTS AND DISCUSSION

We consider first the laser induced hole filling (LIHF) data for chl **a** in polystyrene shown in Figure 1. The results for chl **b** are similar and are reported elsewhere [22]. The data of Figure 1 were obtained with a burn flux of 10 mW/cm^2. The top trace in Figure 1a shows the hole burned at 1.9 K and the trace below it shows the result after burning the same sample spot again with a burn frequency $\omega_{B2} \sim 15\ cm^{-1}$ to the red of the primary burn. The primary hole at ω_{B1} is slightly filled (~ 10%) but the filling is <u>not</u> accompanied by broadening. Figure 1b shows the results of the same experiment but with the secondary burn located to higher energy of the primary burn. Again, no broadening of the primary hole results from filling. The absence of spectral diffusion accompanying LIHF and the fact that LIHF is substantially more efficient when the secondary irradiation lies to higher energy of the primary burn frequency are entirely consistent with the results from far more detailed studies on Pr^{3+}, Nd^{3+}, and rhodamine 640 in polyvinyl alcohol [18]. In this work (as in the present studies, **vide infra**) the LIHF is not a result of bulk or local heating. Furthermore, the LIHF is argued in reference 18 to be the result of secondary irradiation only rather than the formation of the secondary hole. At least two mechanisms for LIHF are indicated (corresponding to $\omega_{B2} > \omega_{B1}$ and $\omega_{B2} < \omega_{B1}$) [18]. The proposed mechanisms need not concern us here. The key point is that observation of LIHF with no spectral diffusion is consistent with NPHB as the mechanism for hole production of chl **a** and **b** in polystyrene.

Figure 1. LIHF in chl a / toluene at 1.9 K. The top trace in a) shows the initial hole burned in a sample and the trace below it is the same sample burned again about 15 cm^{-1} to lower energy. The initial hole has filled ~ 12% without broadening. The top trace in b) shows the initial burn in a new sample and the trace below it shows the result after burning again ~ 15 cm^{-1} to higher energy. This time the initial hole has filled ~ 70%, again without broadening. All holes were burned with 10 mW/cm^2 for 10 minutes

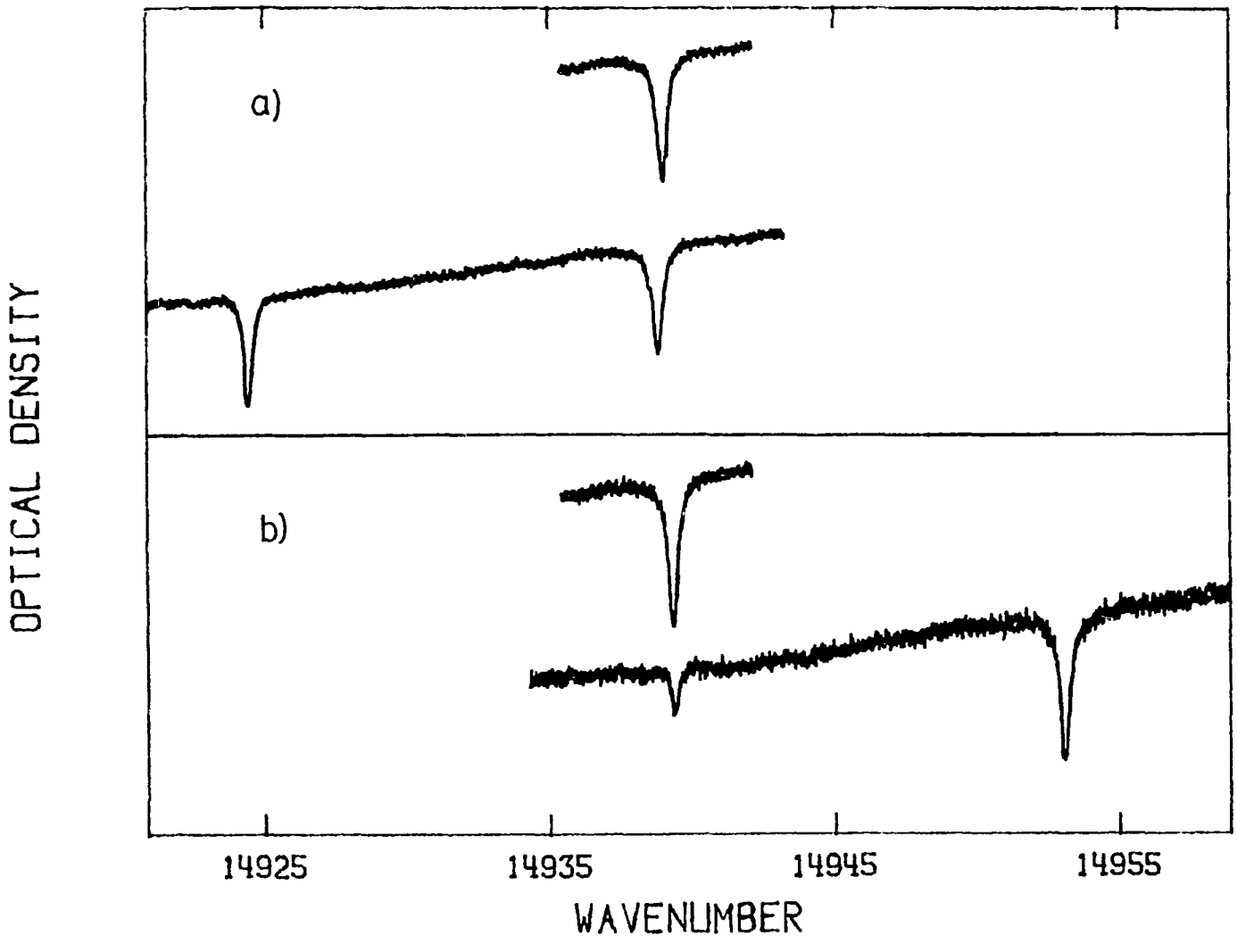
a)
b)
OPTICAL DENSITY
14925
14935
14945
14955
WAVENUMBER

Further support derives from our thermal cycling studies. The experiment involves a burn and read at a minimum temperature T_B (here 1.9 K) followed by reads at successively higher temperatures. Following a higher temperature read, the sample cam be cooled to T_B and reread so that hysteresis effects [27] can be studied. For chl **a** in polystyrene the thermal broadening follows a $\Gamma = 0.07\ T^{1.3 \pm 0.2}\ cm^{-1}$ behavior up to 8.8 K (the highest T studied). The initial hole burned at 1.9 K exhibited a FWHM of $0.18 \pm 0.01\ cm^{-1}$ (burn flux 2 mW/cm^2). Large hysteresis is observed; for example, following the cycle 1.9 K → 8.8 K → 1.9 K the holewidth at 1.9 K is diminished from the 8.8 K value of 1.2 cm^{-1} by ~ 20%. This hysteresis effect indicates that the above thermal broadening is to a large extent due to spectral diffusion arising from TLS relaxation associated with the ground electronic state of chl **a**. Friedrich **et al.** [28] have developed a theory which examines the combined effect of spectral diffusion and optical dephasing on hole widths in the above burn-read sequence. The diffusion process is driven by the gradient in frequency space due to the hole and all impurity-TLS sites are treated in a more or less egalitarian manner. Naturally, the theory predicts that hole filling should accompany thermal broadening. In the above T range, no hole filling (a decrease in the integrated hole area) is observed for chl **a** in polystyrene. However, the uncertainty in the area measurements at the highest temperatures is ± 15-20%. Taken together, the LIHF and thermal cycling data make a convincing case for NPHB as the mechanism for hole production.

In our NPHB studies of Nd^{3+}, Pr^{3+} and rhodamine 640 in polyvinyl alcohol, significant spontaneous hole filling (~ 25-75% depending on the

system) is observed following a burn at 1.7 K [18]. The hole filling at 1.7 K terminates after ~ 17-200 minutes depending on the system. Interestingly, in these systems the spontaneous hole filling is not accompanied by broadening and, thus, cannot be explained by a general spectral diffusion process [28]. We wish to note here that $T_B \approx 1.9$ K holes for chl **a** and **b** in polystyrene exhibit no spontaneous hole filling.

At the lowest burn temperature (1.9 K) and burn flux (130 $\mu W/cm^2$) used in this study, chl **a** exhibits a hole width of 0.17 ± 0.01 cm^{-1} (corrected for monochromator resolution; the observed width being 0.19 cm^{-1}). As illustrated in Figure 2, the hole is predominantly Lorentzian in shape. Further reductions in burn flux and fluence did not produce narrower holes. This hole width is about a factor of three larger than the broadest hole observed by photochemical hole burning for free-base porphins (in MTHF glasses) [12] and free-base phthalocyanine in sulfuric acid [29] at $T_B = 1.9$ K. It is about a factor of 17 broader than that observed at $T_B = 1.8$ K for chl **a** in ether [25] but a factor of two narrower than that reported for protochlorophyll **a** in ether-butanol. However, it is well established that the homogeneous hole widths of free-base porphins depend strongly on the amorphous host medium [12]. The same dependence should exist for the chlorophylls due to variations in the impurity-TLS and TLS-phonon bath coupling strengths. A preliminary T-dependence dephasing study for chl **a** in polystyrene has been performed between a T_B of 1.9 and 8.2 K. The sequence used involves a series of burn at T_B - read at T_B measurements with different sections of the polymer film being used for each T_B [16]. The thermal

Figure 2. Hole burned in the absorption spectrum of chl a at 1.9 K with 250 $\mu W/cm^2$ in 30 seconds. The depth of the hole corresponds to a 13% change in optical density. The circles and triangles are calculated fits to Lorentzian and Gaussian line shapes, respectively

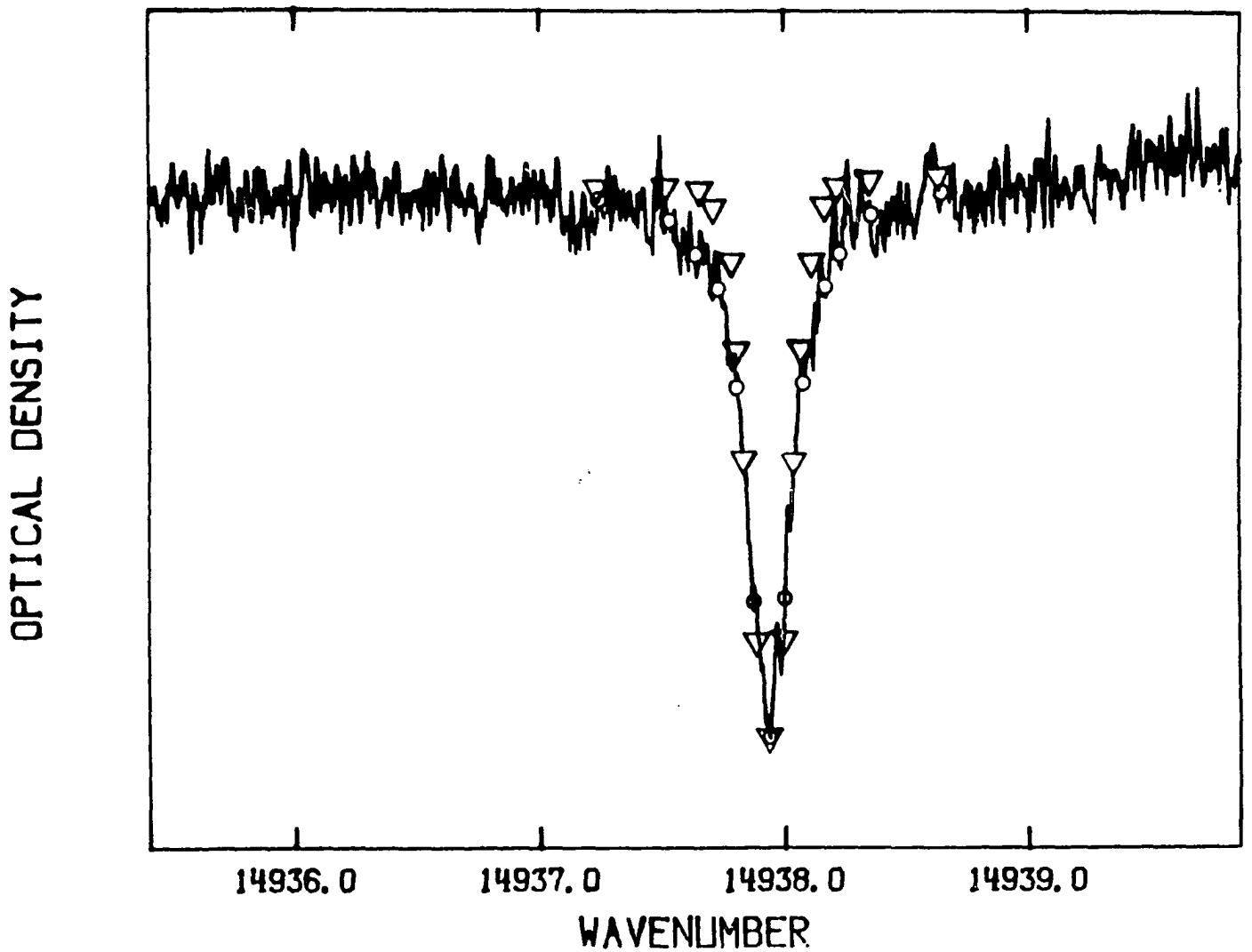
OPTICAL DENSITY
14936.0
14937.0
14938.0
14939.0
WAVENUMBER

dephasing (broadening) follows a $\Gamma = 0.066\ T^{1.3 \pm 0.2}\ cm^{-1}$ behavior over this temperature range. This power law is, within experimental uncertainty, the same as has been observed for a number of other molecules in glasses and polymers [12]. It is capable of being explained by several theories [4,8] which take into account PAT of TLS coupled to the impurity. Unfortunately, our level of understanding of the structures and distribution functions associated with the TLS is far too primitive to allow for an assessment of the accuracy or appropriateness of the theories to be made at this time. We hasten to add that the power laws with $n \simeq 2$ have also been observed for molecules imbedded in polymers and glasses [9,29]. Further measurements of the dephasing of chl **a** at lower temperatures with the purpose of determining the residual linewidth as $T \rightarrow 0$ K need to be performed.

CONCLUDING REMARKS

In previous studies [22], we have found that polystyrene does not afford facile NPHB. For example, NPHB was not observed for pentacene, tetracene, and two laser dyes, rhodamine 640 and DCM, when doped into polystyrene. In light of this, the results reported here for chl **a** and **b** are surprising. An explanation may stem from the fact that the chlorophylls used were wet (the Mg II was ligated by H_2O). Thus, the NPHB mechanism may be associated with quite local TLS associated with the water. Future studies in which H_2O is replaced by D_2O and other ligands, **e.g.**, pyridine, are planned to test this idea.

The observation of facile NPHB for chlorophyll momomers in an aprotic solvent, polystyrene, opens up the possibility of using NPHB to perform accurate measurements of Davydov splittings associated with chlorophyll dimers. Such studies with self-aggregated (as well as synthetically linked) dimers are planned. If successful, important information about excitonic interactions as a function of the dimer environment as well as the population decay times of the upper Davydov component could be obtained. It is conceivable that NPHB can be applied to reaction centers imbedded in polymer matrices.

REFERENCES

1. J. M. Hayes and G. J. Small, Chem. Phys. 27, 151 (1978).

2. J. M. Hayes and G. J. Small, Chem. Phys. Lett. 54, 435 (1978).

3. Although after burning some systems exhibit some degree of spontaneous hole filling at short times, the holes at longer times become stable indefinitely.

4. G. J. Small in: "Modern Problems in Solid State Physics. Molecular Spectroscopy", V. M. Agranovich and R. M. Hochstrasser, eds., North-Holland: Amsterdam, 1983.

5. J. M. Hayes, R. P. Stout and G. J. Small, J. Chem. Phys. 73, 4129 (1980).

6. J. M. Hayes, R. P. Stout and G. J. Small, J. Chem. Phys. 74, 4266 (1981).

7. P. M. Selzer, D. L. Huber, D. S. Hamilton, Y. M. Yen and M. J. Weber, Phys. Rev. Lett. 36, 813 (1976).

8. P. Reineker, H. Morawitz and K. Kassner, Phys. Rev. B 29, 4546 (1984) and references therein.

9. A. A. Gorokhovskii, J. V. Kikas, V. V. Pal'm and L. A. Rebane, Sov. Phys. Solid State 23, 602 (1981).

10. H. P. H. Thijssen, A. I. M. Dicker and S. Volker, Chem. Phys. Lett. 92, 7 (1982).

11. H. P. H. Thijssen, S. Volker, M. Schmidt and H. Port, Chem. Phys. Lett. 94, 53 (1983).

12. H. T. H. Thijssen, R. van den Berg and S. Volker, Chem. Phys. Lett. 97, 295 (1983).

13. R. Jankowiak and H. Bassler, Chem. Phys. Lett. 95, 310 (1983).

14. L. A. Rebane, A. A. Gorokhovskii and J. V. Kikas, Appl. Phys. B 29, 235 (1982).

15. F. A. Burkhalter, G. W. Suter, U. P. Wild, V. D. Samoilenko, N. V. Rasumova and R. I. Personov, Chem. Phys. Lett. 94, 483 (1983).

16. T. P. Carter, B. L. Fearey, J. M. Hayes and G. J. Small, Chem. Phys. Lett. 102, 272 (1983).

17. T. P. Carter, B. L. Fearey and G. J. Small, J. Phys. Chem. 87, 3590 (1983).

18. T. P. Carter, B. L. Fearey, and G. J. Small, Chem. Phys., in press.

19. R. M. MacFarlane and R. M. Shelby, Opt. Commun. 45, 46 (1983).

20. R. Jankowiak and H. Bassler, Chem. Phys. Lett. 95, 124 (1983).
R. Jankowiak and H. Bassler, Chem. Phys. Lett. 101, 274 (1983).

21. F. G. Patterson, H. W. Lee, R. W. Olson, and M. D. Fayer, Chem. Phys. Lett. 84, 59 (1981).

22. T. P. Carter, J. M. Hayes, B. L. Fearey and G. J. Small, Accepted, Intl. Rev. Phys. Chem.

23. J. J. Katz, L. L. Shipman, T. M. Cotton and T. R. Janson in: "The Porphyrins", Volume V, Physical Chemistry, Part C, D. Dolphin, ed., Academic Press: New York, 1978.

24. R. Avarmaa, K. Mauring and A. Suisalu, Chem. Phys. Lett. 77, 88, (1982).

25. K. K. Rebane and R. A. Rebane, Chem. Phys. 68, 191 (1982).

26. G. R. Seely in: "The Chlorophylls", L. P. Vernon and G. R. Seely, eds., Academic Press: New York, 1966.

27. J. Friedrich, H. Wolfram and D. Haarer, J. Chem. Phys. 77, 2309 (1982).

28. J. Friedrich, D. Haarer and R. Silbey, Chem. Phys. Lett. 95, 119 (1983).

29. H. W. H. Lee, A. L. Huston, M. Gehrtz and W. E. Moerner, Chem. Phys. Lett. 114, 491 (1985).

PAPER II.

NONPHOTOCHEMICAL HOLE BURNING OF SELF-AGGREGATED DIMERS OF CHLOROPHYLL a IN POLYSTYRENE

NONPHOTOCHEMICAL HOLE BURNING OF SELF-AGGREGATED DIMERS OF CHLOROPHYLL a IN POLYSTYRENE

THOMAS P. CARTER and G. J. SMALL

Ames Laboratory-USDOE and Department of Chemistry
Iowa State University, Ames, IA 50011

Submitted to the Journal of Physical Chemistry
February, 1986

RESULTS AND DISCUSSION

Application of a variety of spectroscopic techniques to isolated reaction centers (RC), intact photosynthetic organisms and artificial chlorophyll (chl) and bacteriochlorophyll (bchl) aggregates (especially dimers) has produced important insights [1,2]. Notable is the postulation of the chlorophyll special pair (chl_{sp}, $bchl_{sp}$) as the primary electron donor in RC [3,4]. It was, in part, a comparison of low resolution optical absorption spectra of artificial dimers of chlorophyll molecules with those of the RC which led to this postulation. Recently, a crystal structure determination of the RC isolated from the purple bacterium **Rhodopseudomonas viridis** has identified a substructure which appears to be the $bchl_{sp}$ unit [5].

High resolution optical spectra for artificial aggregates would be valuable for the interpretation of spectra from **in vivo** systems or isolated RC. We report here the first observation of nonphotochemical hole burning (NPHB) [6] for a self aggregated chlorophyll dimer: chl **a** dimer [$(chl\ a)_2$] [7] in polystyrene. Holes burned in the lowest energy Q_y component (D_1) of the dimer absorption are narrow in contrast to the transient holes observed for the lowest energy absorption component of the isolated RC of **Rps. sphaeroides** [8,9]. We also observed NPHB in the region corresponding to the absorption of the upper dimer component, D_u.

The NPHB apparatus has a burn and reading resolution of 0.001 and 0.08 cm^{-1}, respectively [10]. Details of the $(chl\ a)_2$/polystyrene film preparation are given elsewhere [11]. The absorption spectrum is shown in Figure 1. The D_1 and D_u components lie at 14655 cm^{-1} (681.9 nm) and 14990 cm^{-1} (667.1 nm), respectively. The chl **a** monomer transition lies

Figure 1. Absorption spectrum of (chl a)$_2$ in a polystyrene film at 1.8 K. The lowest energy peak corresponds to the overlapping Q_y transitions for D_L and D_U. The arrows mark the energies at which holes were burned

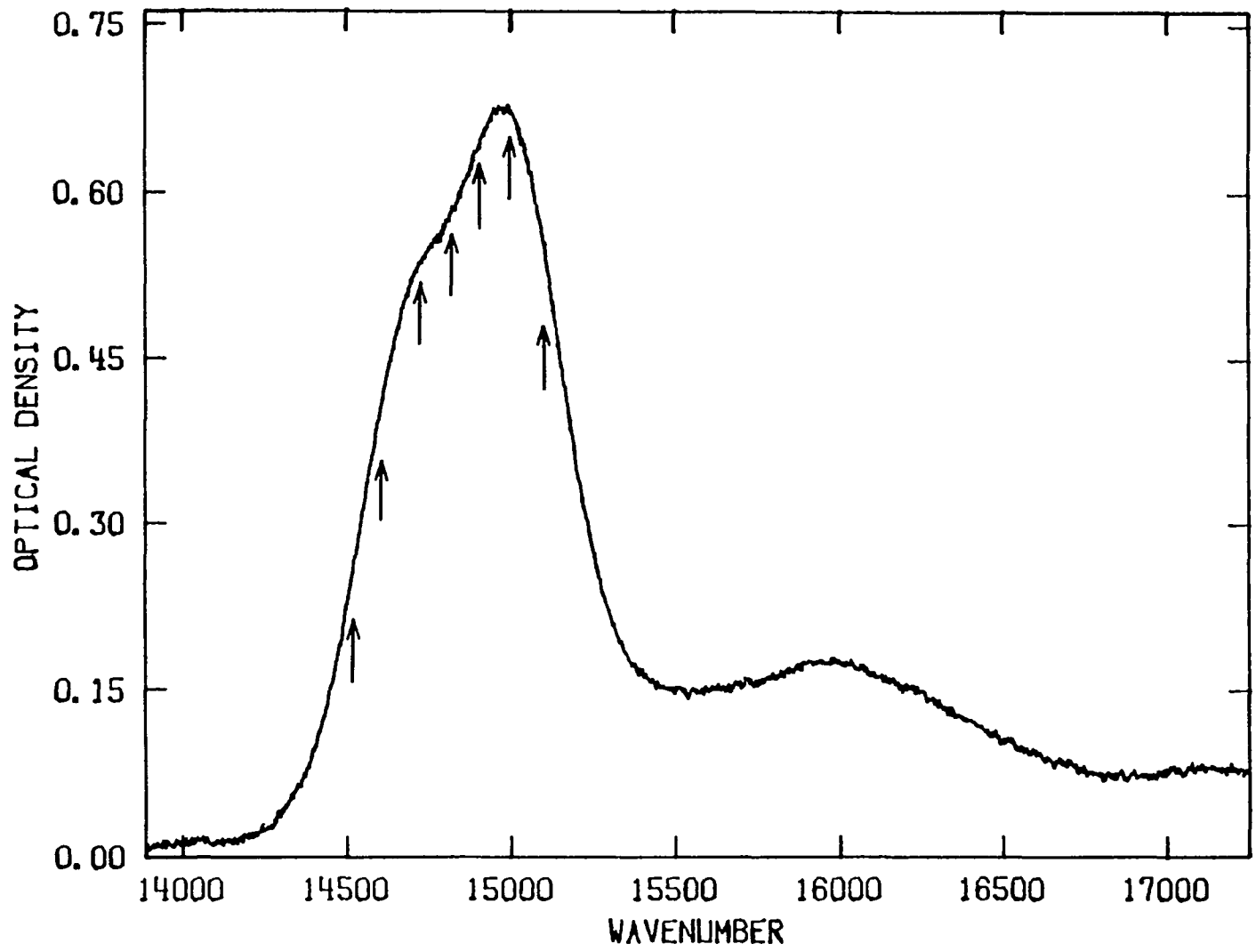
0.75
0.60
0.45
0.30
0.15
0.00
OPTICAL DENSITY
14000
14500
15000
15500
16000
16500
17000
WAVENUMBER

at 15040 cm^{-1} (664.9 nm) in polystyrene [12]. Hole burning was performed at the burn frequencies (ω_B) indicated by arrows. The spectrum in Figure 2 shows a hole (~ 5% O.D. change) burned with ω_B = 14515 cm^{-1} (688.9 nm). For the same burn intensity and burn time the hole depth decreases slowly with increasing ω_B, reaching a value of ~ 2% at ω_B = 15129 cm^{-1} (661.0 nm). These results, together with the fact that the contribution of the D_u absorption tail at ω_B = 14515 cm^{-1} is less than 10% indicate that D_u hole burning makes an insignificant contribution to the 5% hole at this frequency. In addition, if this were not the case, one would expect the hole depth to increase as ω_B increases from 14515 cm^{-1} into the D_u absorption. We conclude that the hole at 14515 cm^{-1} is due to NPHB of D_1. The possibility that this hole is due to residual monomer in the sample can be discounted on the basis of the following discussion on the question of residual monomer contributing to the absorption referred to as D_u.

Exposure of the (chl a)$_2$ films to ordinary air results in an absorption indistinguishable from that of hydrated chl a in polystyrene (which has a single origin band at 15040 cm^{-1} , FWHM = 425 cm^{-1}). Further, saturated hole depths for the hydrated chl a are ~ 20% [12] compared with a 4% value for holes in the (chl a)$_2$ spectrum at about the same frequency (near the peak of D_u). Thus, the contribution of monomer to the D_u absorption is $\leq$ 20% with the upper limit obtained when the D_u hole burning is due entirely to NPHB of the residual monomer. Very recently, we have obtained the line narrowed fluorescence excitation spectra associated with the D_1 and D_u emissions [13]. Emissions of the

Figure 2. A typical hole at the lowest burn frequency used; the hole was burned for 30 sec. with 1.5 mW/cm^2 and corresponds to a 5% change in optical density. The measured holewidth is $0.16 \pm 0.3\ cm^{-1}$

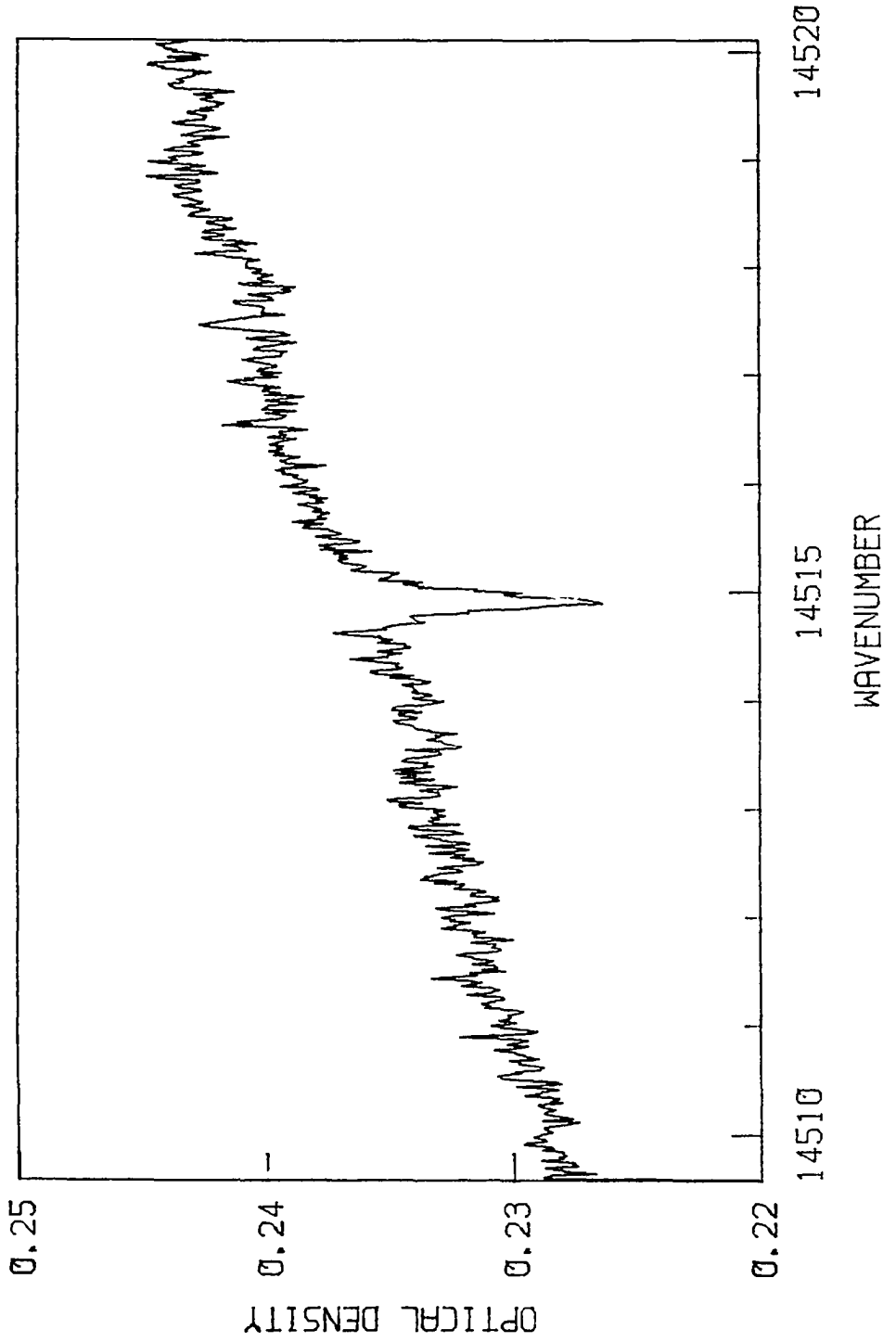
0.25
0.24
0.23
0.22
OPTICAL DENSITY
14510
14515
14520
WAVENUMBER

two components have comparable intensities and are markedly weaker than the fluorescence from chl **a** monomer in polystyrene. This would be expected [1] if the isolated monomer contribution to the absorption (and hence, the emission) is sufficiently low. Preliminary data suggest that the monomer contribution to the D_u absorption must be less than 20%.

This establishes that the D_1 hole at ω_B = 14515 cm^{-1} is due to the lower dimer component. For the conditions of Figure 2, the holewidth is 0.16 cm^{-1} (corrected for monochromator resolution, see Experimental, Section I) which, if taken as homogeneous, corresponds to a dephasing time of T_2 = 132 psec. However, there may be a spectral diffusion contribution to the holewidth. Aside from the observation of NPHB, it is the fact that the hole is narrow relative to the exceedingly broad (~ 400 cm^{-1}) transient holes observed for the isolated RC of **Rps. sphaeroides** which is noteworthy. This width is viewed as homogeneous and ascribed to an ultra-fast charge separation in the $bchl^{sp}$ prior to electron transfer [8,9]. However, the possibility that the broad hole caused by the "artificial" cyclic electron transfer in the isolated RC is inhomogeneous has not been ruled out. Our result is consistent with earlier persistent hole burning studies on intact cells of a mutant strain of **Chlamydomonas reinhardii**. Narrow holes (~ 0.2 cm^{-1}) were burned into the P700 (lowest energy) band which is believed to be due to the chl a_{sp} [14]. In that system and in ours, the absence of intense phonon sideband holes indicate that the charge transfer contribution to the dimer excited state is small.

The holewidths for the higher energy burns indicated in Figure 1 are independent of ω_B and are equal to that of the hole at the lowest

frequency ($\Gamma = 0.16 \pm 0.3$ cm^{-1}). With the assumption that the proposed [15] distribution of T-shaped dimer structures for (chl a)$_2$ is correct and that the D_u holes are due to the upper dimer component, it is appropriate to place a lower limit of $T_1 = 66$ psec for $D_u \Rightarrow D_l$ energy transfer (ET). Based on room temperature solution studies [16], the ET would be expected to be close to this value. However, it has been established that Forster ET in inhomogeneous media at liquid helium temperatures should be orders of magnitude slower than at room temperature [17]. Thus, it is most likely that the holewidths are determined by some combination of pure dephasing and spectral diffusion.

REFERENCES

1. J. J. Katz, L. L. Shipman, T. M. Cotton and T. R. Janson in: "The Porphyrins", Volume V, Part C, D. Dolphin, ed., Academic Press: New York, 1978.

2. J. J. Katz and J. C. Hindman in: "Biological Events Probed By Ultrafast Laser Spectroscopy", R. R. Alfano, ed., Academic Press: New York, 1982.

3. J. D. McElroy, D. C. Mauzerall and G. Feher, Biochim. Biophys. Acta 267,363 (1972).

4. J. R. Norris, R. A. Uphaus, H. L. Crespi and J. J. Katz, Proc. Natl. Acad. Sci. USA 68, 625 (1971).

5. J. Deisenhofer, O. Epp, K. Miki, R. Huber and H. Michel, J. Mol. Biol. 180, 385 (1984).

6. G. J. Small in: "Modern Problems in Solid State Physics. Molecular Spectroscopy", V. M. Agranovich and R. M. Hochstrasser, eds., North-Holland: Amsterdam, 1983.

7. By self-aggregated we mean chl a molecules interacting via the ring V keto - Mg interaction which has been shown to preferentially produce dimers in dry non-polar solvents at room temperature and at concentrations up to 10^{-2} M. See Reference [1].

8. S. R. Meech, A. J. Hoff and D. A. Wiersma, Chem. Phys. Lett. 121, 287 (1985).

9. S. G. Boxer, D. J. Lockhart and T. R. Middendorf, Chem. Phys. Lett., in press; cited by permission of the authors.

10. T. P. Carter, B. L.. Fearey and G. J. Small, J. Phys. Chem. 87, 3590 (1983).

11. See Experimental, Section II.

12. T. P. Carter and G. J. Small, Chem. Phys. Lett. 120, 178 (1985).

13. R. Jankowiak, T. P. Carter, J. K. Gillie and G. J. Small, Ames Laboratory and Iowa State University, unpublished results.

14. V. G. Maslov, A. S. Chunaev and V. V. Tugarinov, Mol. Biol. 15, 788 (1981).

15. C. Houssier and K. Sauer, J. Am. Chem. Soc. 2, 779 (1970); T. M. Cotton, A. D. Trifunac, K. Ballschmiter and J. J. Katz,

Biochim. Biophys. Acta 368, 181 (1974).

16. W. W. A. Keller, B. A. Albers, E. Strauss and K. Maier-Schwartz, J. Lumin. 31-32, 892 (1984).

17. K. D. Rockwitz and H. Bassler, Chem. Phys. 70, 307 (1982).

ADDITIONAL RESULTS AND DISCUSSION

As briefly mentioned in Paper I, nonphotochemical hole burning of chl **a** and **b** in diethyl ether or diethyl ether-butanol (EB) have been reported previously [7,8]. In those systems, the hole width in the short burn-time limit was found to be 0.01 cm^{-1} at 1.8 K, or a factor of 17 less than that measured in this work at the same T; this may be indicative of significantly faster pure dephasing processes occurring in the polymer samples.

It is also interesting to note that, in the EB system, the saturation hole depth and electron-phonon coupling are both significantly greater than what is observed for holes in polystyrene. It may well be that both of these observations are attributable to NPHB processes which are intimately involved with the ligation of the Mg to the available nucleophilic donor, which is likely to be the solvent itself in the case of the EB samples, but is the adventitious water in polystyrene samples.

The NPHB of chl **a** in polystyrene was characterized by a pronounced dependence of the apparent quantum yield upon laser intensity. In a cursory study of observed hole depth as a function of burn power at constant fluence, higher powers resulted in much shallower holes than lower powers. This is easily understood as being caused by a bottleneck occurring in the excitation process. If the molecules can populate some metastable state which does not lead to NPHB, then those molecules are not available for NPHB until they return to the ground state. Higher powers will increase the population of molecules in the metastable state

and lead to lower ostensible quantum yields. This bottleneck is reasonably identified as the triplet state which, for chl **a**, has a radiative lifetime of 0.8 ms with an intersystem crossing (ISC) quantum yield ($S_1 \rightarrow T_1$) of about 0.25 in ethanol at room temperature [9]. This hole burning saturation behavior is common and is, of course, much more readily observed in those systems which have large (ISC) yields and long metastable lifetimes (it was not nearly as pronounced in the laser dye NPHB experiments where the ISC yield is much lower). It is therefore important, in general, to use as low a burn power as possible in NPHB, especially when attempting to get quantitative information about the NPHB quantum yield.

One of the things which was investigated in the NPHB experiments on (chl a)$_2$ that was not mentioned in Paper II (for reasons of space in the original journal publication), was whether or not some information could be obtained as to nature of the dimer pair interaction. Our view was that, if the dimer pair were interacting excitonically, and the two absorption features labelled D_u and D_l were excitonic in nature, then burning a hole in D_l would produce a hole in D_u and **vice versa**. When this experiment was carried out, however, no such phenomena were observed. This should not be viewed as conclusive proof to the contrary, though, since there are possible reasons why these results could be obtained, even for an excitonic system. Since the saturation depth for NPHB in this system is very low (about 8%, at best) it is possible that the hole in the other component is very broad due to a poor correlation in transition energy distribution functions (and as a result, assuming equal oscillator strengths for the two components, very

shallow), so that the secondary hole is below the instrumental limit of detection. Another possibility is that the holes observed in D_u are due primarily to residual monomer (although we doubt this),and the hole in the D_u absorption due to the excitonic component is very broad (and therefore shallow) because of rapid energy transfer to D_1, and hence are also beneath the limit of detection.

Recently, isolated intact reaction centers of the photosynthetic purple bacterium **Rhodopseudomonas viridis** have been successfully crystallized and the structure determined at atomic resolution (0.3 nm) by x-ray crystallography [10]. This was the first (and remains to this time, the only) example of detailed structural information on an **in vivo** reaction center. The reaction center was found to contain four large protein subunits together with an arrangement of four bacteriochlorophyll **b** (Bchl **b**) molecules, two bacteriopheophytin **b** (BPh **b**) molecules (which are Bchl **b** with the Mg replaced by two protons), one non-heme iron, two quinones and four (possibly five) heme groups. In the structure, there is a pair of closely associated Bchl **b** molecules which is identified as the elusive "special pair"; their porphyrin planes are separated by an average distance of about 0.3 nm and they are at a 15° angle to one another. The two molecules interact most closely with their pyrrole rings I, which are stacked on top of each other; this allows the acetyl groups of rings I to be in direct contact with the Mg ion of the other Bchl **b** in the pair. It is interesting to speculate that, since the chl in plants and cyanobacteria contain no acetyl group in ring I, the special pairs in other types of photosynthetic systems may be different.

As was briefly mentioned in Paper II, reaction centers of a similar but different purple bacterium, **Rhodopseudomonas sphaeroides**, have recently been studied using transient hole burning [11,12] and accumulated photon echo [11] techniques at liquid helium temperatures. In both these works, holes were successfully burned into the lowest energy optical absorption band of the reaction center spectrum, but the holes recovered on a millisecond time scale; there was no observable persistent hole. Even more intriguing is the fact that the measured holewidth was on the order of several hundred cm^{-1}. Several reasons were considered for this observation including power broadening, extremely rapid vibrational relaxation or pure dephasing, large electron-phonon coupling, and rapid charge transfer in the excited state. The accumulated photon echo experiments [11] corroborated the likelihood that these holes are due to some rapid T_1 process on a sub-picosecond time scale, possibly a cyclic electron transfer analogous to that which occurs **in vivo** but altered by the fact that the RC are isolated from the rest of the **in vivo** photosynthetic system. It interesting to contrast these results with those obtained in a hole burning experiment performed at 4.2 K on intact cells of a mutant strain of **Chlamydomonas reinhardii**, where persistent holes with a width of ~ 0.4 cm^{-1} were observed.

Future Work

It may have been noticed by the careful reader that the holes observed in monomer chl **a**, chl **b** and (chl **a**)$_2$ were only moderately broader than the spectrometer's read resolution, and hence were

distorted to some degree in measurement, especially at the lowest temperatures. The obvious solution to this problem is to detect (read) the holes using fluorescence excitation with broadband emission detection using the single frequency dye laser as excitation source, as explained in Additional Results And Discussion, Section I. This is especially important in planned future experiments on the dephasing of these systems at temperatures below those used in this work, since the linewidth is expected to decrease further upon further cooling (the lifetime limit is about 10^{-3} cm^{-1}). Since the fluorescence quantum yield of monomeric chl is quite high (about 0.3 for chl **a**) this is a viable proposition for the monomeric systems. For the self-aggregated dimer this may not be the case however, since its fluorescence quantum yield is at least two orders of magnitude lower than the monomer's; still, it remains to be seen whether this technique will work for dimers.

Further studies are planned on different types of chl dimer systems: those which are linked by interactions with bidentate solvent molecules and those which are linked covalently by intermediary chains of various lengths. These dimer systems have different symmetries and some of them resemble the "special pair" configuration observed in the crystallized reaction centers. It would be interesting to see if any of these show behavior similar to that observed in references [11,12] (an unlikely probability), and if the addition of some type of electron trap to the sample to break any cycle which was occurring would then produce a <u>persistent</u> hole which could be more easily studied. Also planned are hole burning studies on the isolated reaction centers whose structure

has been determined, and perhaps the same type of trap addition could be applied to that system (assuming it behaves similarly to **Rps. sphaeroides**), as well as to isolated RC of other organisms. It has also come to our attention that these RC can be procured in various stages in the isolation process, and these may perhaps have interesting differences in their hole burning behavior which may provide new information on the early steps in the photosynthetic process. Additionally, hole burning studies on intact cells of various photosynthetic organisms (especially **Rps. viridis**) will be performed in the near future.

REFERENCES

1. J. J. Katz, L. L. Shipman, T. M. Cotton and T. R. Janson in: "The Porphyrins", Volume V, Part C, D. Dolphin, ed., Academic Press: New York, 1978.

2. G. G. Stokes, Ann. Physik 4, 220 (1854).

3. G. G. Stokes, Proc. Roy. Soc. 13, 144 (1864); J. Chem. Soc. 17, 304 (1864).

4. R. I. Personov in: "Spectroscopy and Excitation of Condensed Molecular Systems", V. M. Agranovich and R. M. Hochstrasser, eds., North-Holland: New York, 1983.

5. R. A. Avarmaa and K. K. Rebane, Spectrochimica Acta 41A, 1365 (1985).
6. K. Ballschmiter, K. Truesdell and J. J. Katz, Biochim. Biophys. Acta 184, 604 (1969).

7. K. K. Rebane and R. A. Avarmaa, J. Photochem. 17, 311 (1981).

8. R. Avarmaa, K. Mauring and A. Suisalu, Chem. Phys. Lett. 77, 88 (1981).

9. C. A. Parker, "Photoluminescence of Solutions", Elsevier: New York, 1968.

10. J. Deisenhofer, O. Epp, K. Miki, R. Huber and H. Michel, J. Mol. Biol. 180, 385 (1984).

11. S. G. Boxer, D. J. Lockhart and T. R. Middendorf, Chem. Phys. Lett. in press; cited by permission of the authors.

12. S. R. Meech, A. J. Hoff and D. A. Wiersma, Chem. Phys. Lett. 121, 287 (1985).

ACKNOWLEDGEMENT

First and foremost, I would like to express my deepest thanks and appreciation to my wife Linda, without whose love and support (financial and moral) I would have not succeeded. I may never be able to make it up to her.

I also would like to thank Dr. Gerald J. Small for everything he has done for me over the last four plus years; they are too numerous to mention here but suffice it to say that he has gone far above and beyond what most major professors do for their students, and for this I am truly grateful.

I am also indebted beyond repayment to Dr. Gregory D. Gillispie who, with the exception of my parents, was the first to recognize my abilities and give me my first opportunity at research; I would like to thank him for his infinite patience with me over the first few years.

My thanks are also due to Dr. John M. Hayes for his help with some of the experimental details and theoretical understanding.

It would have been far less interesting at Iowa State if I hadn't met Mike Kenney and become friends with him; he has shared the bad times with me and I really appreciate his understanding and support. I have also enjoyed the many hours spent running with him; they allowed me to vent off some steam in good company (but not much competition).

Lastly and most importantly, I would like to thank my parents who have always supported me and encouraged me in everything I've done. All I can do is say thank you, which doesn't nearly express the depth of my gratitude for having helped me along the way.

APPENDIX.

FORTRAN COMPUTER PROGRAM

TO CONTROL THE ABSORPTION SPECTROMETER

```
      PROGRAM IBSPEC
C
C
C
C     THIS PROGRAM MUST BE LINKED TO IBDAT,JYSCAN,YORN
C     NEWFIL,CHART,ONREC,IBGAIN,IBINIT AND PEN.
C
C     MODIFIED 7-18-85 TO AUTOMATICALLY INCREMENT THE DATA FILE'S
C     LAST THREE DIGITS (HENCE THE "FILETYPE", I.E THE CHARACTERS
C     TO THE RIGHT OF THE DECIMAL MUST BE NUMBERS WITH NO LEADING
C     ZEROES: LIKE NNNNNN.7, NOT NNNNNN.007)
C
C
      COMMON NREC,ICOUNT,ISENSE/BLK3/aGAIN,OFFSET
      common/sub1/jans,irpeat,inum,nam
      common/sub2/icntrl,irange,jstep,istep,ispace
      REAL*8 SLAMB,FLAMB,STEP,SCALE,STEP1,aGAIN,offset
      LOGICAL*1 NAM(14),file(14)
      LOGICAL*1 MESSAG(50)
5000  IRPEAT=1                    !THIS IS HOW MANY REPEAT SCANS ARE ASKED FOR
      INUM=0                      !THIS IS # OF TIMES OPENER IS CALLED
      IGO=0                       !KEEP TRACK IF REPEAT SCANS ARE WANTED
      N=0
      IPRM=0                      !TELLS IF SCAN PARAMETERS HAVE BEEN INPUT
      ispace=1
      TYPE *,'*********************************************'
      TYPE *,'*       J-Y SCAN AND ITHACO INTEGRATOR       *'
      TYPE *,'*             CONTROL PROGRAM                *'
      TYPE *,'*                                            *'
      TYPE *,'* REFERENCE LOCK-IN TO INTEGRATOR CHANNEL A  *'
      TYPE *,'*   SAMPLE LOCK-IN TO INTEGRATOR CHANNEL B   *'
      TYPE *,'*  RECORDER INTERFACE TO TERMINAL AUX. MODEM *'
      TYPE *,'*           DAC(1) TO PEN INPUT              *'
      TYPE *,'*                                            *'
      TYPE *,'*             ***IMPORTANT***                *'
      TYPE *,'*      DO NOT USE LEADING ZEROES IN THE      *'
      TYPE *,'*   "FILETYPE" PART OF YOUR FILE NAME IF     *'
      TYPE *,'*        YOU ARE DOING REPEAT SCANS.         *'
      TYPE *,'*                                            *'
      TYPE *,'*     EXAMPLE: USE NAME.7  NOT  NAME.007     *'
      TYPE *,'*********************************************'
      WRITE(7,10)
      CALL YORN                   !ASK IF REPEAT SCAN IS WANTED
      IF(JANS.EQ.0)GO TO 1        !IF YES ASK FOR FILE NAMES(ALSO IF NO)
      IGO=1
      WRITE(7,11)
      READ(5,12)IRPEAT                              !     ASK
      write(7,17)
17    format(x,'Do you want spaces between spectra? (Y,N) : ',$)
      call yorn
      if(jans.eq.0)ispace=0
1     WRITE(7,101)                                  !     FOR
      READ(5,107)NAM                                !     THE NAMES
```

```
      do 41 k=1,14
              file(k)=nam(k)
41    continue
27    OPEN(UNIT=1,NAME=NAM,TYPE='OLD',FORM='UNFORMATTED',ERR=2)
      CLOSE(UNIT=1)
      WRITE(7,102)              !IF NAMES ARE USED, ASK AGAIN
      GO TO 1
2     IF(IRPEAT.EQ.0.AND.INUM.GT.1)GO TO 9999      !ARE WE DONE?
      CALL NEWFIL
      IF(IGO.EQ.1.AND.IPRM.EQ.1)GO TO 888
      GO TO 89                  !GO ASK FOR SCAN PARAMETERS
87    WRITE(7,115)              !CHECK IF SCAN SENSE IS RIGHT
      CALL YORN
      IF(JANS.EQ.0)GO TO 89     !IF NOT, GET NEW PARAMETERS
      ISENSE=-1                 !KEEP TRACK OF DIRECTION
      GO TO 200                 !GET MORE PARAMETERS
88    WRITE(7,116)              !CHECK IF SCAN SENSE IS RIGHT
      CALL YORN
      IF(JANS.EQ.0)GO TO 89     !IF NOT, GET NEW PARAMETERS
      ISENSE=1                  !KEEP TRACK OF DIRECTION
      GO TO 200                 !GET MORE PARAMETERS
90    WRITE(7,112)              !STEP TOO LARGE!
      GO TO 89
91    WRITE(7,118)              !SAME LAMBDA FOR START & FINISH!
89    WRITE(7,103)                        !    ASK
      READ(5,108)SLAMB                    !    FOR
      WRITE(7,104)                        !   SCAN
      READ(5,108)FLAMB                    !  LAMBDAS
      IF(FLAMB.LE.SLAMB) GO TO 87         !CHECK FOR SENSE
      IF(FLAMB.EQ.SLAMB) GO TO 91         !CHECK FOR ZERO SCAN RANGE
      GO TO 88                            !CHECK FOR SENSE
200   WRITE(7,105)                        !ASK FOR STEPSIZE(NM/DATA POINT)
      READ(5,109)STEP
      IF(STEP.GT.ABS(FLAMB-SLAMB)) GO TO 90   !CHECK AGAINST SCAN INTERVAL
      ISTEP=(STEP*5.000D3) + 5.0D-1    !CALC. # OF PULSES/DATA STEP(5000/NM)
554   WRITE(7,113)
      READ(5,109)SCALE                    !SCALE = #NM/CM OF CHART
      STEP1=((SCALE/STEP)*5.D-3)          !#DATA/(CHART STEP)
      DO 555 N=1,1000
              MM=N                                !FIND
              R=N/STEP1                           !# OF CHART STEPS
              RD=R-(AINT(R))                      !PER MONOCHROMATOR
              IF(RD.EQ.(0.0)) GO TO 556           !STEP
555   CONTINUE
      TYPE *, 'CHART SCALE NOT CORRECT,TRY AGAIN'
      GO TO 554
556   JSTEP=R                             !# CHART STEPS/MONO. STEP
      IPRM=1                              !WE HAVE GOTTEN PARAMETERS
      ICNTRL=1
      CALL IBINIT
      WRITE(7,120)
      READ(5,121)GAIN
      aGAIN=4.096D3/GAIN
```

```
      WRITE(7,122)
      READ(5,121)OFFSET
      CALL CHART
      PAUSE 'SET J-Y TO START LAMBDA, PRESS <CR> WHEN READY'
888   IRANGE=(ABS(FLAMB - SLAMB)/STEP) + 0.5  !IRANGE KEEPS TRACK OF STEPS
6     IF(IRANGE.EQ.0) GO TO 9999              !DONE?
      CALL IBDAT                              !GO GET DATA
      IF(N.GT.0) N=N-1
      IF(N.EQ.0) CALL PEN
      IF(N.EQ.0) N=MM
      IRANGE=IRANGE - 1                       !ONE LESS STEP TO GO
      CALL JYSCAN                             !TAKE ANOTHER STEP
      GO TO 6                                 !GET MORE DATA
9999  CALL IBDAT                              !IBDAT WRITES TO FILE
      ICNTRL=2
      CALL CHART
      IF(IRPEAT.NE.0)GO TO 2
      CALL IPOKIO("167772,"024406)            !SET J-Y TO MANUAL
C
C     DONE!!!!
C
      WRITE(7,300)inum,FILE
902   WRITE(7,301)SLAMB
      WRITE(7,302)FLAMB
      WRITE(7,303)STEP
      WRITE(7,304)SCALE
      WRITE(7,307)GAIN
      WRITE(7,308)OFFSET
      WRITE(7,334)
      MESSAG(1)=63
      MESSAG(2)=13
      CALL IBSEOI(MESSAG,2,1)
      K=IBRECV(MESSAG,50,1)
      WRITE(7,335)(MESSAG(L),L=1,K)
      ICNTRL=3
      CALL CHART
      WRITE(7,333)
      CALL YORN
      IF(JANS.EQ.1)GO TO 5000
      STOP
C
10    FORMAT(//,X,'MORE THAN ONE SCAN OF THIS SPECTRUM? (Y,N): ',$)
11    FORMAT(X,'ENTER NUMBER OF SCANS: ',$)
12    FORMAT(I3)
99    FORMAT(X,'ENTER THE FIRST FILE NUMBER (AN INTEGER) :',$)
100   FORMAT(/////,10X,'J-Y COMPUTER CONTROL PROGRAM',/)
101   FORMAT(X,'ENTER DATA FILE NAME : ',$)
102   FORMAT(//,X,'FILE NAME ALREADY IN USE, PICK ANOTHER',/)
103   FORMAT(X,'ENTER STARTING WAVELENGTH IN NM (AS NNN.NN): ',$)
104   FORMAT(X,'ENTER END WAVELENGTH IN NM (AS NNN.NN): ',$)
105   FORMAT(X,'ENTER J-Y STEPSIZE IN NM (AS N.NNN): ',$)
107   FORMAT(30A,30A,30A,30A,30A)
108   FORMAT(F10.4)
```

```
109     FORMAT(F8.4)
110     FORMAT(I5)
112     FORMAT(//,X,'STEP IS TOO LARGE FOR SCAN INTERVAL, START AGAIN',//)
113     FORMAT(X,'ENTER CHART SCALE (NM PER CM) IN NM (AS NNN.NN): ',$)
115     FORMAT(X,'SCAN FROM HIGH TO LOW WAVELENGTH, CORRECT? (Y,N): ',$)
116     FORMAT(X,'SCAN FROM LOW TO HIGH WAVELENGTH, CORRECT? (Y,N): ',$)
118     FORMAT(X,'SAME VALUE FOR START AND FINISH, TRY AGAIN',///)
120     FORMAT(X,'ENTER O.D. MAXIMUM (ANY REAL NUMBER) :',$)
121     FORMAT(F6.3)
122     FORMAT(X,'ENTER OFFSET FOR REAL TIME OUTPUT (IN O.D. UNITS) : ',$)
300     FORMAT(///////,X,'THERE WERE',I3,' FILE(S) JUST OBTAINED, STARTING
     1 WITH ',14A1)
301     FORMAT(X,'THE STARTING LAMBDA WAS ',F10.4,' NM')
302     FORMAT(X,'THE ENDING LAMBDA WAS ',F10.4,' NM')
303     FORMAT(X,'THE INTERVAL BETWEEN DATA POINTS WAS ',F6.4,' NM')
304     FORMAT(X,'THE CHART SCALE WAS ',F8.4,' NM/CM')
307     FORMAT(X,'THE O.D. SCALE WAS O.D. ',F6.3,' FULL SCALE')
308     FORMAT(X,'THE REAL TIME OFFSET WAS ',F6.3,' O.D. UNITS')
333     FORMAT(/////,X,'DO YOU WANT ANOTHER SPECTRUM? (Y,N): ',$)
334     FORMAT(/X,'THE INTEGRATOR PARAMETERS WERE :')
335     FORMAT(X,50A1)
        END
```

```
      SUBROUTINE CHART
C
C     CONTROLS THE CHART RECORDER SPEEDS, SENSITIVITY, PEN UP DOWN, ETC.
C     THROUGH THE VISUAL 102 VIDEO TERMINAL PRINTER PORT
C
      common/sub1/jans
      common/sub2/cntrl,ir,js,is,ispace
      LOGICAL *1 V(1),S(1)
      INTEGER CNTRL,SCALER,speeds
      V(1)=0                        !V(1) is the voltage scale setting
      S(1)=0                        !S(1) is the chart speed
      IF(CNTRL.EQ.2)GO TO 1000      !go there between multiple scans
      IF(CNTRL.EQ.3)GO TO 2000      !go there at end of program
      if(ispace.eq.1) go to 1       !branch if computer steps the recorder
2897  write(7,53)                   !ask for speed if external control
53    format(x,'enter chart speed (1 thru 10,12,15,20,30,40,50,60)',$)
      read(5,55) speeds
      IF(speeds.EQ.1) S(1)=33
      IF(speeds.EQ.2) S(1)=34
      IF(speeds.EQ.3) S(1)=35
      IF(speeds.EQ.4) S(1)=36
      IF(speeds.EQ.5) S(1)=37
      IF(speeds.EQ.6) S(1)=37
      IF(speeds.EQ.7) S(1)=39
      IF(speeds.EQ.8) S(1)=40
      IF(speeds.EQ.9) S(1)=41
      IF(speeds.EQ.10) S(1)=42
      IF(speeds.EQ.12) S(1)=43
      IF(speeds.EQ.15) S(1)=44
      IF(speeds.EQ.20) S(1)=45
      IF(speeds.EQ.30) S(1)=46
      IF(speeds.EQ.40) S(1)=47
      IF(speeds.EQ.50) S(1)=48
      IF(speeds.EQ.60) S(1)=49
      if(S(1).ne.0) go to 1
      WRITE(7,42)
42    FORMAT(X,'ILLEGAL SPEED, TRY AGAIN')
      GO TO 2897
1     write(7,54)
54    format(x,'ENTER O.D. SCALE FACTOR'/x,'(divide O.D. by this to get
     1 the full scale O.D. of the real time output)'/x,'(use values: 1,2
     2,5,10,20,50,100) :',$)
      READ(5,55)SCALER              !Scaler sets the chart sensitivity
55    FORMAT(I3)
      IF(SCALER.EQ.1)V(1)=101
      IF(SCALER.EQ.2)V(1)=102
      IF(SCALER.EQ.5)V(1)=103
      IF(SCALER.EQ.10)V(1)=104
      IF(SCALER.EQ.20)V(1)=105
      IF(SCALER.EQ.50)V(1)=106
      IF(SCALER.EQ.100)V(1)=107
```

```
      IF(V(1).NE.0)GO TO 2
      WRITE(7,32)
32    FORMAT(X,'ILLEGAL EXPANSION FACTOR, TRY AGAIN')
      GO TO 1
2     imode=1
      call onrec(imode)          !onrec sets the terminal(V 102) to
c     controller mode (F2 in printer control menu #5); thus anything sent
c     to the terminal is passed on out the terminal's aux. modem to which
c     the recorder is connected.
c
      write(7,98)V(1)            !set sensitivity
98    format(X,'333qs',1a1,$)    !stop chart(3 times), zero check on, pen down
      imode=0
      call onrec(imode)          !back to ordinary terminal mode
      PAUSE 'SET PEN TO A MAJOR DIVISION AND ADJUST ZERO'
      imode=1
      call onrec(imode)          !recorder control on
      write(7,500)
500   format(X,'trsw',$)         !pen up, zero check off, pen down, mark trace
      if(ispace.eq.0)write(7,501) S(1)    !set chart speed if necessary
501   format(x,1a1,'2')          !chart speed, chart motor on
      imode=0
      call onrec(imode)          !back to ordinary terminal
      RETURN
C
C
C
1000  if(ispace.eq.0)return      !if not computer stepping the chart, return
      IWAIT=5                    !set wait time to five seconds
1002  imode=1                    !recorder control on
      call onrec(imode)
      write(7,1005)
1005  format(X,'wtq412',$)       !mark trace,pen up,zero on,60 cm/min,chart on
      CALL GTIM(TIME1)                    !let
      CALL CVTTIM(TIME1,IH,IM,IS1,ITIC)   !chart
1699  CALL GTIM(TIME2)                    !run
      CALL CVTTIM(TIME2,IH,IM,IS2,ITIC)   !for
      IF(IS2.LT.IS1)IS2=IS2+60            !five
      IF(IS2.LT.(IS1+IWAIT))GO TO 1699    !seconds
      write(7,1700)
1700  format(X,'3333',$)         !stop chart(4 times)
      IF(CNTRL.EQ.3)GO TO 2009   !see below, line 2000
      write(7,1755)V(1)
1755  format(X,'rsw',1a1,$)      !zero off,pen down,mark trace,set sensitivity
      imode=0
      call onrec(imode)          !back to ordinary terminal
      RETURN
C
C
C
2000  IWAIT=6                    !set wait time to 6 seconds
      imode=1
      call onrec(imode)          !recorder control on
```

```
      write(7,2001)
2001  format(x,'33333')          !stop chart (5 times)
      imode=0
      call onrec(imode)          !back to ordinary terminal
      WRITE(7,9999)
9999  FORMAT(//,X,'DO YOU WANT A TEAR OFF SPACE (Y,N)? : ',$)
      CALL YORN
      IF(JANS.EQ.1)GO TO 1002    !if space is wanted, use above routine
2005  imode=1
      call onrec(imode)          !recorder control on
2009  write(7,2010)
2010  format(X,'wtq',$)          !mark trace, pen up, zero on, we're done
      imode=0
      call onrec(imode)          !ordinary terminal on
      RETURN
      END
```

```
      subroutine IBDAT
C
C     THIS ROUTINE TRIGGERS DATA READING BY THE INTEGRATOR, SCALES IT,
C     TAKES THE RATIO AND THE LOGARITHM AND WRITES TO THE OUTPUT FILE.
C
      COMMON NREC,ICOUNT,ISENSE/BLK1/IDATA(260)/BLK3/aGAIN,offset
      common/sub2/ic,irange
      common/gainer/updown
      logical*1 messag(50)
      integer updown
      REAL*8 DATA,adata,bdata,cdata,offset,again
      IF(IRANGE.EQ.0)GO TO 4
      icheck=icheck+1
      if(icheck.ne.10)go to 1
      updown=1
      ISTAT=IBSTS(1)
      ISTAT=IBSTS(1)
      IF((ISTAT.AND."1).EQ.1)call IBGAIN !channel A overload( make "A" ref.)
      call ibget(1)
      N=IBRECV(messag,50,1)
      decode (20,98,messag)adata,bdata
      if (adata.lt.0.9)updown=-1
      if (updown.eq.-1) call ibgain
      icheck=0
1     ICOUNT=ICOUNT+1
      CALL IBSDC(1)              !CLEARS THE 385-EO FOR NEXT READING
      CALL IBGET(1)              !TRIGGERS THE 385-EO TO TAKE A READING
      N=IBRECV(messag,50,1)      !GET DATA (samp,ref IN ASCII FORM)
      decode (20,98,messag)adata,bdata
98    format(2d19.10)
      cdata=adata/bdata
      IF(CDATA.GT.0.0D0)DATA = DLOG10(cdata)       !THIS IS THE ABSORBANCE
      IF(CDATA.LT.0.0D0)DATA = -DLOG10(DABS(cdata))
      IF(CDATA.EQ.0.0D0)TYPE *,'RATIO IS ZERO ---- SOMETHING IS WRONG'
      IF(CDATA.EQ.0.0D0)DATA = 0.0
C
      IDATA(ICOUNT) = DATA * aGAIN                 !4096=0.v  DAC OUTPUT
C                                                  !0000=10.v DAC OUTPUT
C                                                  ! F.S. OD | aGAIN
C                                                  !-------------------
C                                                  !    .25  | 16384
C                                                  !    .5   |  8192
C                                                  !     1.  |  4096
C                                                  !    1.5  |  2731
C                                                  !     2.  |  2048
C                                                  !     3.  |  1024
C
      IOUT = (4096 - IDATA(ICOUNT) + (OFFSET*aGAIN))
      CALL IPOKIO("170440,IOUT)!CHANGED 13-DEC-85!NEWEST VALUE OUTPUT TO DAC(1)
      IF(ICOUNT.EQ.256) GO TO 4
      RETURN
```

```
4       IF(ICOUNT.EQ.0) CLOSE(UNIT=1)
        IF(ICOUNT.EQ.0) RETURN
2000    WRITE(1'NREC)(IDATA(I),I=1,256)
        DO 2050 I=1,260
                IDATA(I)=0
2050    CONTINUE
        ICOUNT=0
        IF(IRANGE.EQ.0)GO TO 3000
        RETURN
3000    CLOSE(UNIT=1)
        ISENSE=-(ISENSE)
        RETURN
        END
```

```
      SUBROUTINE IBGAIN
c     This routine is entered if the Ithaco 385EO senses an overload or
c     if the reference lock-in output is < 0.09v.
c     It then determines what the 397EO LIA gain settings are and changes
c     them by a factor of ten. The routine then waits 10 seconds for the
c     time constants to settle on the new readings.
      integer updown
      common/gainer/updown
      logical*1 MESSAG(50),nessag(3)
      messag(1)=63              ! 63 = '?' gets 385EO to ready parameters
      message(2)=13             ! 13 = 'CR' end of message
      nessag(1)=71              ! 71 = 'G' character controlling LIA gain
      nessag(3)=13              ! 13 = 'CR' end of message
      CALL IBSEOI(messag,2,1)   ! send '?CR' to 385EO
      CALL IBRECV(MESSAG,50,1)  ! receive 385EO parameter string
      do 10 i=1,50                                  ! find the 'G'
            if(messag(i).eq."107)go to 20           ! in the
10    continue                                      ! parameter string
20    nessag(2)=(messag(i+1)+updown)      ! +/- 1 to the digit after the 'G'
      if(nessag(2).eq.0.or.nessag(2).eq.7)go to 30
      call ibseoi(nessag,3,1)             ! send modified gain code: 'Gn'
      call isleep(0,0,10,0)               ! wait 10 s for RC to settle
      return
30    type *,'computer attempt to set LIA gain past limits of operation'
      return
      END
```

```
      SUBROUTINE IBINIT
c     This routine sets up the parameters of the Ithaco 385EO integrator and
c     allows the user to change LIA gain settings and the number of inte-
c     grator time periods (1 period = 1/60 sec) to sample the signal for.
c
c     The initial set up is as follows:
c
c     A1 -> 10v full scale sensitivity
c     B0 -> 2 Hz bandwidth when Auto-Gain is x100
c     R1 -> Autorange delay 1/60 sec.
c     TB -> Trigger integration start from the computer bus
c     OC -> Continous output mode (read data right after trigger)
c     MA -> Send data in ASCII format
c     D3 -> (combined D1 and D2) integrator returns values for channel A and
c           channel B to the computer when asked for data
c     S0 -> disable service request (interrupts) operation
c
c
      common/sub1/jans
      LOGICAL *1 MESSAG(50)
      CALL IBIFC                          !THIS CLEARS THE INSTRUMENT BUS
      CALL IBSDC(1)                       !THIS CLEARS THE INTEGRATOR
      CALL IBSEND('A1B0R1TBOCMAD3S0',-1,1)        !send parameters (see above)
      MESSAG(1)=13
      CALL IBSEOI(MESSAG,1,1)
8     MESSAG(1)=63              ! ask
      MESSAG(2)=13              ! for
      CALL IBSEOI(MESSAG,2,1)   ! parameter string
      N=IBRECV(MESSAG,50,1)     ! receive parameter string
      WRITE(7,1000)
1000  FORMAT(/X,'THE INTEGRATOR PARAMETERS ARE : ')
      WRITE(7,1001) (MESSAG(I),I=1,N-1)   !write parameters
1001  FORMAT(X,50A1)
      WRITE(7,1002)
1002  FORMAT(X,'DO YOU WANT TO MAKE ANY CHANGES? (Y,N) : ',$)
      CALL YORN
      IF(JANS.EQ.0)RETURN
9     WRITE(7,1003)
1003  FORMAT(X,'ENTER PARAMETERS (DONT USE SPACES) :',$)
      READ(7,1004)NCHAR,MESSAG   !accept param. to send to 385EO
1004  FORMAT(Q,50A1)
      IF(NCHAR.GT.50)GO TO 10
      CALL IBSEND(MESSAG,NCHAR,1)         !send param.
      CALL IBSEOI(15,1,1)
      GO TO 8
10    WRITE(7,1005)
1005  FORMAT(X,'MESSAGE TOO LONG, 50 CHARACTERS TOTAL, TRY AGAIN!!!')
      GO TO 9
      END
```

```
      SUBROUTINE JYSCAN
C
C     THIS ROUTINE SENDS OUT SQUARE WAVE PULSES TO THE MONOCHROMATOR
C     SCAN MOTOR (0 TO +5 V) AND CONTROLS SCAN DIRECTION
C
C     BACKWARD SCANNING
      COMMON NREC,ICOUNT,ISENSE
      common/sub2/ic,ir,js,istep
      IF(ISENSE.LT.0)GO TO 1000
      IF(ISENSE.GT.0)GO TO 2000
1000  CALL IPOKIO("167772,"024207)
      DO 8 K = 1,ISTEP
               CALL IPOKIO("167772,"024206)
               DO 99 M = 1,2
               L=L+1
               L=L-1
99             CONTINUE
               CALL IPOKIO("167772,"024207)
8     CONTINUE
      RETURN
C
C
C
2000  CALL IPOKIO("167772,"024407)
      DO 18 K = 1,ISTEP
               CALL IPOKIO("167772,"024406)
               DO 199 M = 1,2
               L=L+1
               L=L-1
199            CONTINUE
               CALL IPOKIO("167772,"024407)
18    CONTINUE
      RETURN
      END
```

```
      SUBROUTINE NEWFIL
C
C     THIS ROUTINE OPENS OUTPUT FILES FOR DATA RECORDING
C
      COMMON NREC,ICOUNT/BLK1/IDATA(260)
      common/sub1/jans,IRPEAT,INUM,NAM
      LOGICAL*1 FILNAM(15),NAM(14),NUM(4)
      IF(IRPEAT.EQ.0)RETURN
      DO 100 J=1,260
              IDATA(J)=0
100   CONTINUE
      INUM=INUM+1
      if(inum.ne.1)go to 6
      DO 5 I=1,14
              IF(NAM(I).EQ.' ')GO TO 6
              FILNAM(I)=NAM(I)
5     CONTINUE
6     OPEN(UNIT=1,NAME=FILNAM,TYPE='NEW',FORM='UNFORMATTED',
     1INITIALSIZE=0,ACCESS='DIRECT',ASSOCIATEVARIABLE=NREC,
     2RECORDSIZE=128)
      NREC=1
      ICOUNT=0
      IRPEAT=IRPEAT-1
      IPOS=INDEX(FILNAM,'.')
      IPOS=IPOS+1
      CALL SUBSTR(FILNAM,NUM,IPOS)
      ilen=len(num)
      DECODE(ilen,10,NUM)JNUM
      JNUM=JNUM+1
      if(jnum.eq.10.or.jnum.eq.100)ilen=ilen+1
      ENCODE(ilen,10,NUM)JNUM
10    FORMAT(I3)
      CALL INSERT(NUM,FILNAM,IPOS)
19    format(x,14a1)
      RETURN
      END
```

```
      SUBROUTINE ONREC(IMODE)
C
C
      IF(IMODE.EQ.0)GO TO 1000
C
C
C     THE FIRST ROUTINE SETS THE VISUAL 102 TO PRINTER CONTROLLER MODE
C
      ib=27
      ic=91
      id=53
      ie=105
      write(7,101)ib,ic,id,ie
101   format(X,4a1,$)
      RETURN
C
C
C     THIS ROUTINE RESETS THE TERMINAL TO NORMAL STATUS
C
C
1000  id=52
      write(7,101)ib,ic,id,ie
      RETURN
      END
```

```
      SUBROUTINE PEN
C
C     SENDS SQUARE WAVE PULSES TO THE CHART DRIVE MOTOR (0 TO +5 V)
C
      common/sub2/ic,ir,jstep
C
C     USE DAC CHANNEL 0 (+5v)
C
      DO 500 L=1,JSTEP
             DO 1000 N=1,375
                    M=N+1
1000         CONTINUE
             CALL IPOKIO("170444,"4000)
             DO 700 J=1,375
                    K=J+1
700          CONTINUE
             CALL IPOKIO("170444,"2000)
500   CONTINUE
      RETURN
      END
```

```
C
C   SUBROUTINE YORN LOOKS FOR A CONSOLE RESPONSE
C   TO A YES-OR-NO QUESTION.  IF RESPONSE BEGINS
C   WITH 'Y' A VALUE OF 1 IS RETURNED IN JANSR;
C   IF WITH AN 'N,' A VALUE OF 0 IS RETURNED.
C
      SUBROUTINE YORN
      common/sub1/jansr
      LOGICAL*1 ANSWER(20)
      JANSR=0
10    READ (5,11) ANSWER
11    FORMAT (20A)
      IF (ANSWER(1).EQ.'Y')GO TO 13
      IF (ANSWER(1).EQ.'N')GO TO 14
      WRITE (7,12)
12    FORMAT (X,'GIVE YES OR NO RESPONSE: ',$)
      GO TO 10
13    JANSR=1
14    RETURN
      END
```